Australia's Wine Future

A CLIMATE ATLAS

Remenyi, T.A. [1,2]; Rollins, D.A. [1,2]; Love, P.T. [1,2]; Earl, N.O. [1,2]; Bindoff, N.L. [1,3]; Harris, R.M.B. [1,2]

[1] Climate Futures, Antarctic Climate & Ecosystems CRC, University of Tasmania, Hobart
[2] Discipline of Geography & Spacial Sciences, University of Tasmania, Hobart
[3] Institute for Marine and Antarctic Studies (IMAS), University of Tasmania, Hobart

This research was funded by the Wine Australia Project UT1504
'Australia's Wine Future: Adapting to short-term climate variability and long-term climate change'

Contact: Rebecca.Harris@utas.edu.au

Disclaimer

The material in this atlas is based on computer modelling projections for climate change scenarios and, as such, there are inherent uncertainties in the data. While every effort has been made to ensure the material in this atlas is accurate, Wine Australia and the University of Tasmania provide no warranty, guarantee or representation that the material will prove to be accurate, complete, up-to-date, non-infringing or fit for purpose. The use of the material is entirely at the risk of the user. The user must independently verify the suitability of the material for their own use.

To the maximum extent permitted by law, Wine Australia and the University of Tasmania, any other participating organisation and their officers, employees, contractors and agents exclude liability for any loss, damage, costs or expenses whether direct, indirect, consequential including loss of profits, opportunity and third party claims that may be caused through the use of, reliance upon, or interpretation of the material in this atlas.

Citation

Remenyi, T.A., Rollins, D.A., Love, P.T., Earl, N.O., Bindoff, N.L., Harris, R.M.B. (2019) *Australia's Wine Future — A Climate Atlas*, University of Tasmania, Hobart, Tasmania.

ISBN: 978-1-922352-06-4 (electronic); 978-1-922352-05-7 (print)

Acknowledgements

The authors would like to acknowledge Wine Australia and the Antarctic Climate & Ecosystems CRC (University of Tasmania) for their funding and support.

Our CSIRO colleagues, Dr Marcus Thatcher, Dr Tony Rafter, Dr Claire Trenham and Dr Matt Paget produced the underlying data and collaborated in the validation and analysis of the climate trends.

Our UTas, SARDI and AWRI colleagues, Dr Fiona Kerslake, Dr Peter Hayman, Dr Dane Thomas, Dr Paul Petrie and Dr Mark Kristic provided valuable connections, perspectives and insights into the wine industry. Their involvement enabled us to understand the true needs of growers and wine makers.

Many industry contributors hosted us during visits and generously gave us their time in interviews. Their constructive feedback was invaluable in making sure that the atlas is relevant and accessible.

This project used the R programming language and would therefore like to recognise the efforts of the *R-core team* and those of *RStudio* in providing the tools and interfaces that made data analysis and visualisation possible and innovative. This project also used the LaTeXtypesetting system. We would like to recognise the contributors to this system.

A special thanks to Dr Michael Sumner for all his efforts upskilling our team in programming, workflow management, geospatial data and a host of specific programming packages we used within this project.

Requests and enquiries

Requests and enquiries concerning reproduction rights should be addressed to:

Communications and Media Office
University of Tasmania
+61 3 6226 2124
Media.Office@utas.edu.au

Foreword

My interest in viticultural climatology goes back to the late 1970s when Richard Smart and I published a climatic classification of Australian wine regions by means of novel indices of temperature, rainfall, aridity, sunshine hours and relative humidity. This was the first time that this had been done in Australia and our aim was to aid vineyard site selection and to provide guidelines for varietal selection, at a time of major change in the Australian wine industry. In hindsight, our methods were relatively simplistic, but they did provide a good platform for inter-regional comparison and a better basis for the discussion of the impact of climate on wine style and quality.

Therefore, I was delighted to learn that a team of well-credentialed climate scientists from the University of Tasmania had been engaged to produce a climate atlas of Australian wine regions. This method of presentation of climatic information is well overdue and will prove to be a most valuable resource. The graphical presentation of climatic indices in a true atlas format allows for easy interpretation, while the details to describe the methodology and approaches that underpin the climate modelling, scenarios development and data analysis are there for those who are technically inclined.

The first part of the atlas is a comparison of the *current period* (1997 to 2017) with the *base period* (1961 to 1990). The authors have utilised well known climatic indices, such as *Growing Season Temperature*, *rainfall* and *aridity*, which clearly demonstrate the significant changes that have taken place in all regions over the past few decades. They have also created some novel indices, designed to better represent the physiological requirements of grapevines over the entire year. By doing so they have been able to capture the influence of heat units, for example, at the beginning of the season on the timing of key phenological events (as we are well aware, we have observed the earlier occurence of budburst and flowering in many regions over the past 20 years). Also, *Non-Growing Season Rainfall* change since the base period clearly shows the influence of the drying trend in most regions.

The second part of the atlas presents the projected climate across all Australian wine regions out to 2100. This includes detailed presentations for each individual wine region (or Geographic Indication), grouped for each State (WA, SA, NSW, Vic., Tas. and QLD). The evidence is clear. The industry faces many challenges in the future, not only in terms of diminished productivity and declining wine quality in a warming and drying climate but also in terms of increased likelihood of risk of heat stress of vineyard workers.

Congratulations to the authors and to Wine Australia on the production of this seminal work.

Dr Peter Dry AM
Adjunct Associate Professor, University of Adelaide
Emeritus Fellow, The Australian Wine Research Institute

Contents

AGCD	Australian Gridded Climate Data
AI	Aridity Index
AWAP	Australian Water Availability Project
BoM	The Australian Bureau of Meteorology
BARRA	The Australian Bureau of Meteorology Atmospheric high-resolution Regional Reanalysis for Australia
CCAM	CSIRO's Conformal Cubic Atmospheric Model
CFAP2019	Climate Futures Australasian Projections 2019
CFT	Climate Futures for Tasmania
CMIP	Coupled Model Intercomparison Project - Has three most common variations CMIP3 and followed by CMIP5 and the current CMIP6, which indicate the experimental configuration of the intercomparisons
CORDEX	Coordinated Regional Downscaling Experiment
CSIRO	Commonwealth Scientific and Industrial Research Organisation
EHF	Excess Heat Factor
Ensemble member	The output from one CCAM simulation driven by one of the six global models
ENSO	El Niño-Southern Oscillation
ERA	European Centre for Medium-Range Weather Forecasts re-analysis
GCM	Global Climate Model
GDD	Growing Degree Days
GI	Geographic Indication
GSR	Growing Season Rainfall
GST	Growing Season Temperature
IOD	Indian Ocean Dipole
IPCC	Intergovernmental Panel on Climate Change
IPCC-AR5	Intergovernmental Panel on Climate Change Fifth Assessment Report
MOST	Monin-Obukhov Similarity Theory
NRM	National Resource Management
PDO	Pacific Decadal Oscillation
RCM	Regional Climate Model
RCP	Representative Concentration Pathway - Comes in the flavours RCP2.6 (best case), RCP4.5, RCP6.5 and RCP8.5 (worst case, business as usual)
SAM	Southern Annular Mode
SRES	Special Report on Emissions Scenarios
SST	Sea Surface Temperature
UHI	Urban Heat Island
UTas	University of Tasmania
WCRP	World Climate Research Programme

Introduction

Over the last century, Australia's climate has warmed by 1°C, and few regions have been unaffected (CSIRO and Bureau of Meteorology, 2018). Hotter average temperatures, hotter summers, longer heatwaves, more frequent bushfires and changes to rainfall intensity and seasonality have already had impacts across the country, and these trends are expected to continue. Rapid and ongoing climate change has the potential to affect all aspects of the wine industry, including vineyard performance, pest and disease incidence, wine quality and market competitiveness. In recognition of these challenges, Wine Australia funded a collaborative research project to consider the impact of climate variability and longer-term trends in climate on the wine industry.

Australia's wine future (2016–2019) was a collaborative research project that brought together researchers from a range of disciplines, including climate scientists, viticulturalists and adaptation specialists. The project was led by the Antarctic Climate Ecosystems Cooperative Research Centre (ACE CRC, University of Tasmania) in partnership with the South Australian Research and Development Institute (SARDI), the Australian Wine Research Institute (AWRI), CSIRO Marine and Atmospheric Research and the Tasmanian Institute of Agriculture (TIA).

The Australian wine sector is likely to face challenges as the climate continues to warm, but, in general, grape growers are experienced in responding to short-term climate surprises. In the short- to medium-term, adaptation approaches may be learnt from the regions that are currently experiencing the climate conditions that Australia is predicted to see in the future. Fine-scaled climate information tailored for particular sector applications is vital for identifying such adaptation needs.

Australia's wine future generated the finest available climate projections for South-eastern Australia and provided detailed information about how the climate may change in the near, mid and long-term time horizons. In addition to providing climate information, the project focused on how climate information can be used to inform adaptation decisions and identify lessons that might be transferable across regions already managing a range of climate challenges.

The main legacy of the project is this atlas of climate information for all Australian wine regions, providing information to grape growers and wine makers about climate trends for the near, mid- and long-term horizons. The atlas showcases the most up-to-date climate information at the finest resolution available in Australia, based on the CSIRO's Conformal Cubic Atmospheric Model (CCAM). Viticultural indices are presented that describe temperature, heat accumulation, heatwaves, rainfall, and moisture indices. Future trends in mean climate conditions, variability and extremes are visualised with reference to the current and historical climate. High resolution maps and time series for each region are presented to show the projected change in climate indices over time, highlighting the variability within and across the wine regions of Australia. The new atlas will help to answer the question – What will my region's climate look like in the future? This is essential knowledge for making good management decisions and supporting strategic decisions over the longer term such as changing varieties or vineyard sites both within and between regions. The atlas is an important resource that will help the wine industry understand how climate change could affect grape yield, profitability and wine styles across Australia into the future.

Part I

Australia's Wine Future — A Climate Atlas

OBSERVED CLIMATE ACROSS AUSTRALIA'S WINE REGIONS

Wine Australia Geographical Indications

Figure 1: Wine Regions of Australia
Based on Wine Australia Geographical Indications

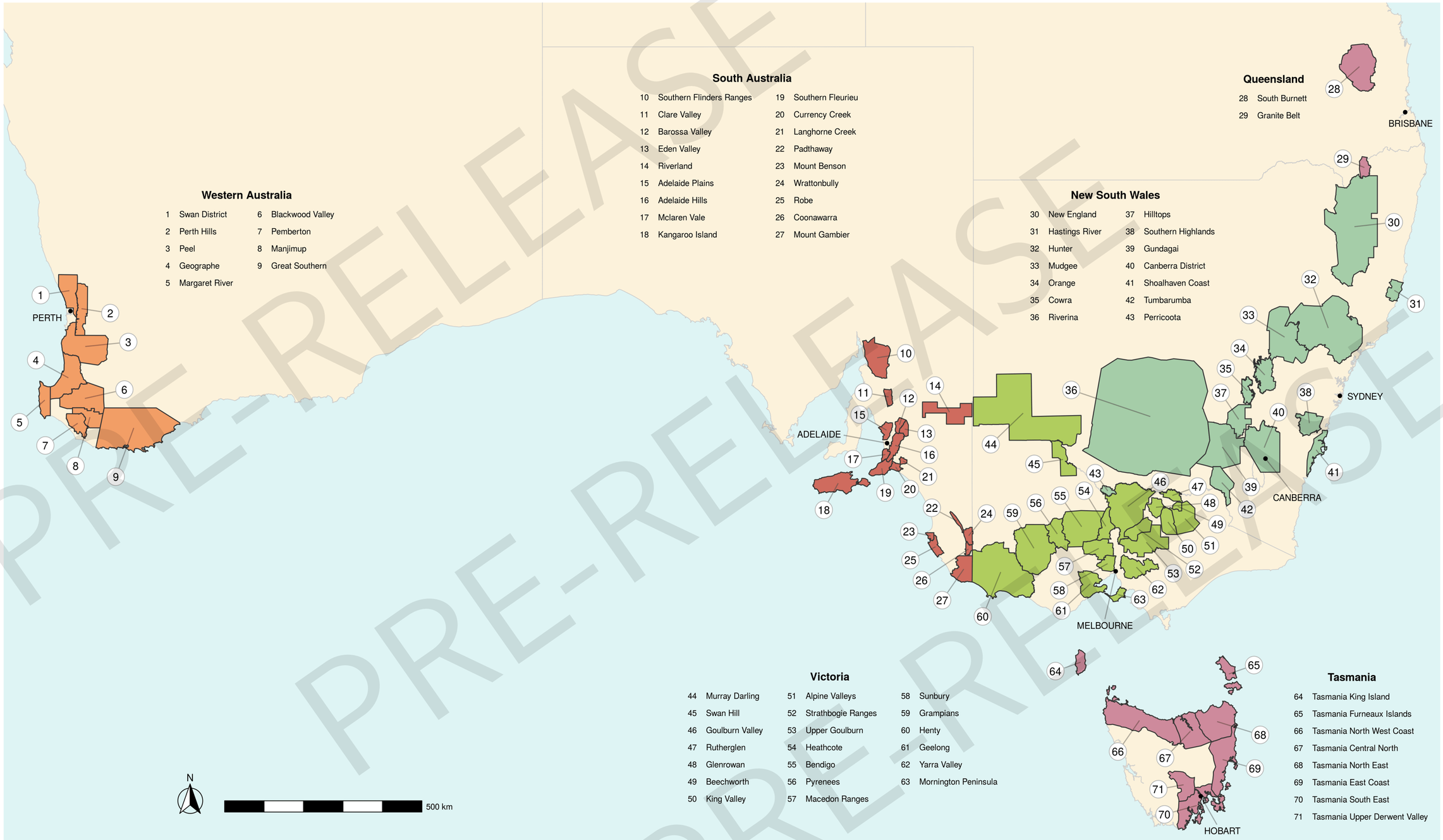

Figure 1: Spatial representation of the Australian wine regions used within this atlas. For mainland Australia these are the Wine Australia Geographical Indications (GI). The Tasmania GI was divided into 8 regions based on Australian Bureau of Meteorology forecast districts, in recognition of the different climatic zones across the state.

OBSERVED CLIMATE ACROSS AUSTRALIA'S WINE REGIONS

National Maps

Figure 2: Observed mean Growing Season Temperature across Australia's wine regions
Current period (1997–2017)

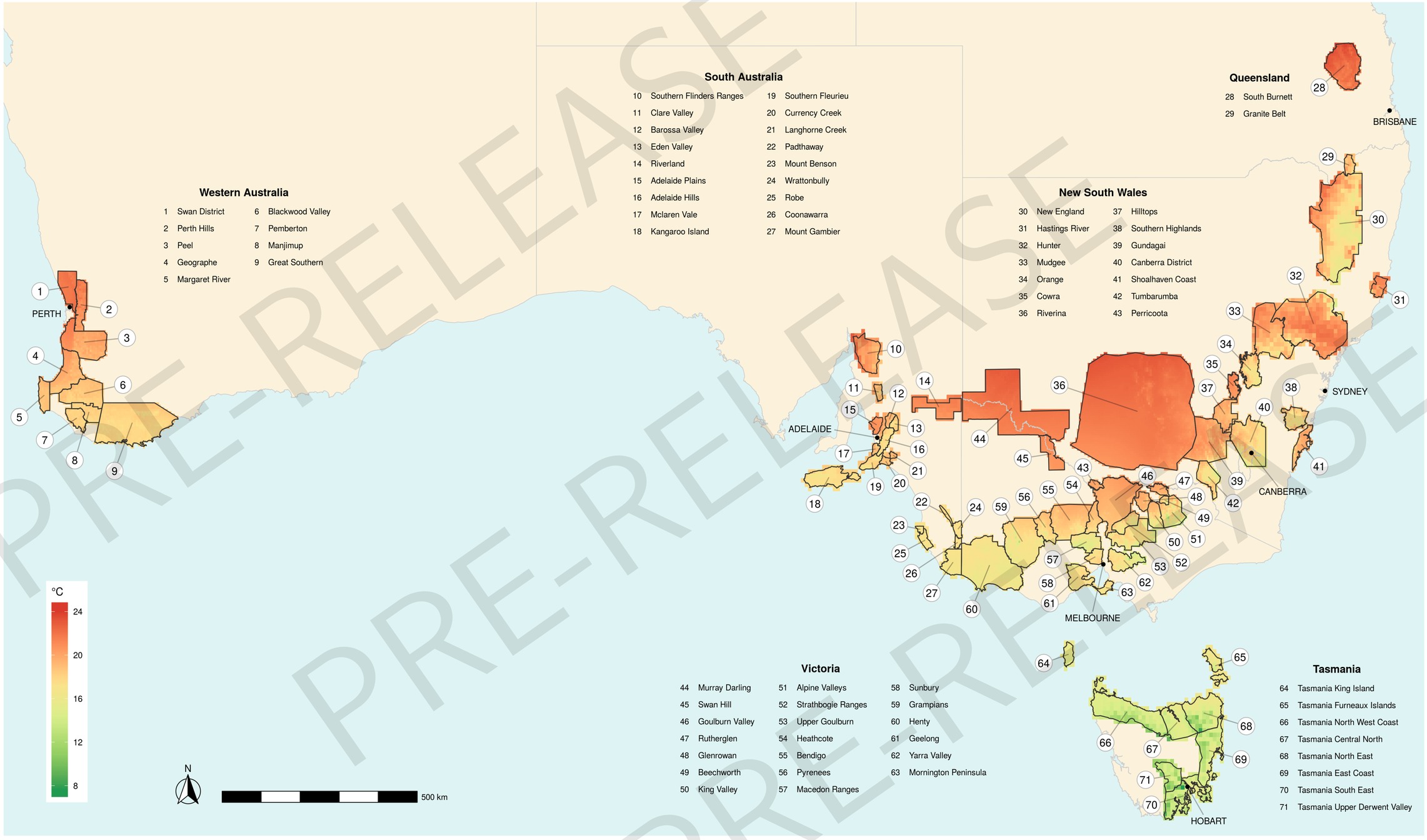

Figure 2: Observed mean *Growing Season Temperature* (Oct–Apr) across all growing years from 1997–2017.

OBSERVED CLIMATE ACROSS AUSTRALIA'S WINE REGIONS

National Maps

Figure 3: Observed change in mean Growing Season Temperature across Australia's wine regions
Current period (1997–2017) minus baseline period (1961–1990)

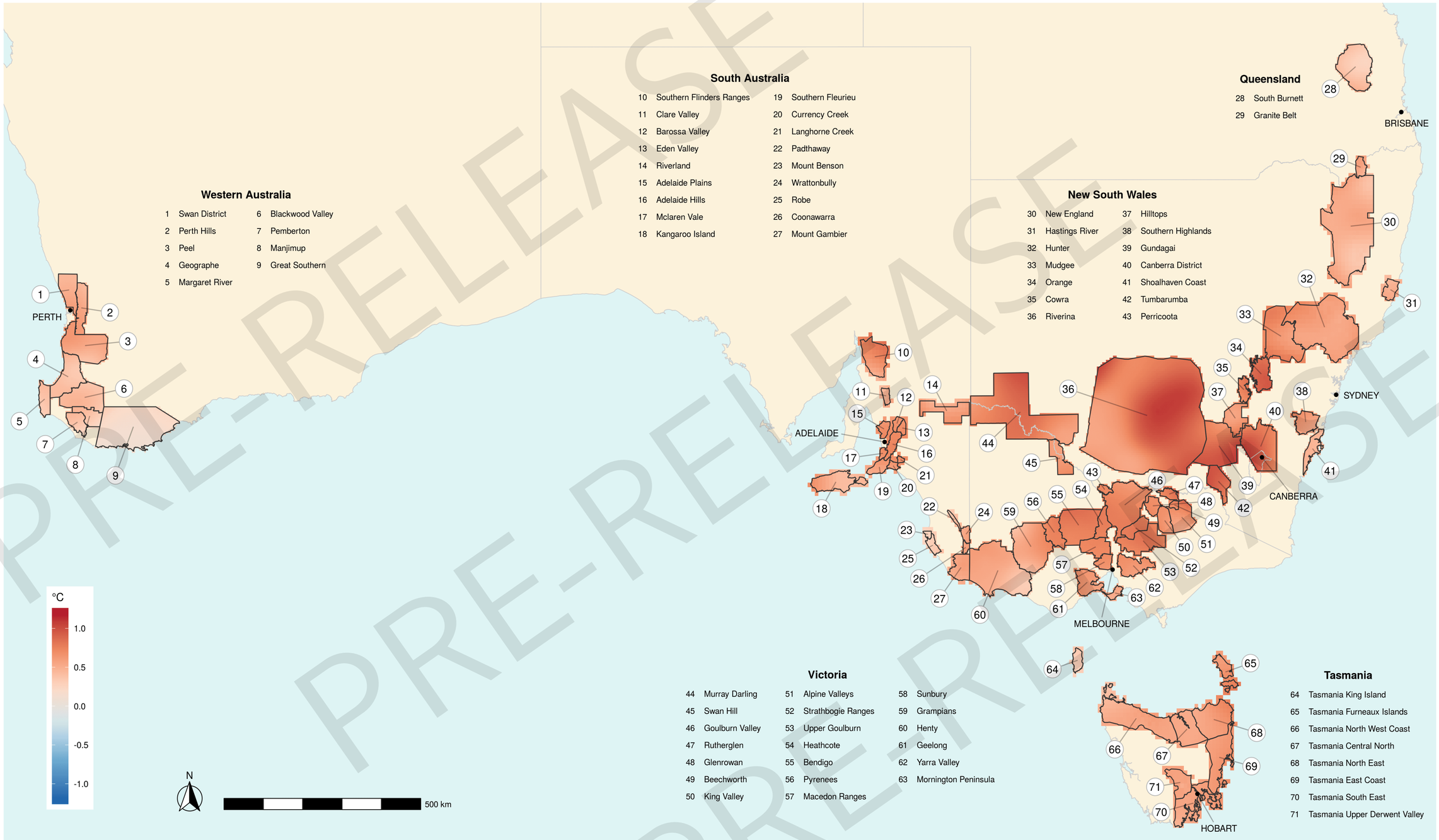

Figure 3: The change in *Growing Season Temperature* between the current (1997–2017) and historical (1961–1990) periods. *Growing Season Temperature* has increased across the region over recent decades.

OBSERVED CLIMATE ACROSS AUSTRALIA'S WINE REGIONS

National Maps

Figure 4: Observed mean Growing Season Rainfall across Australia's wine regions
Current period (1997–2017)

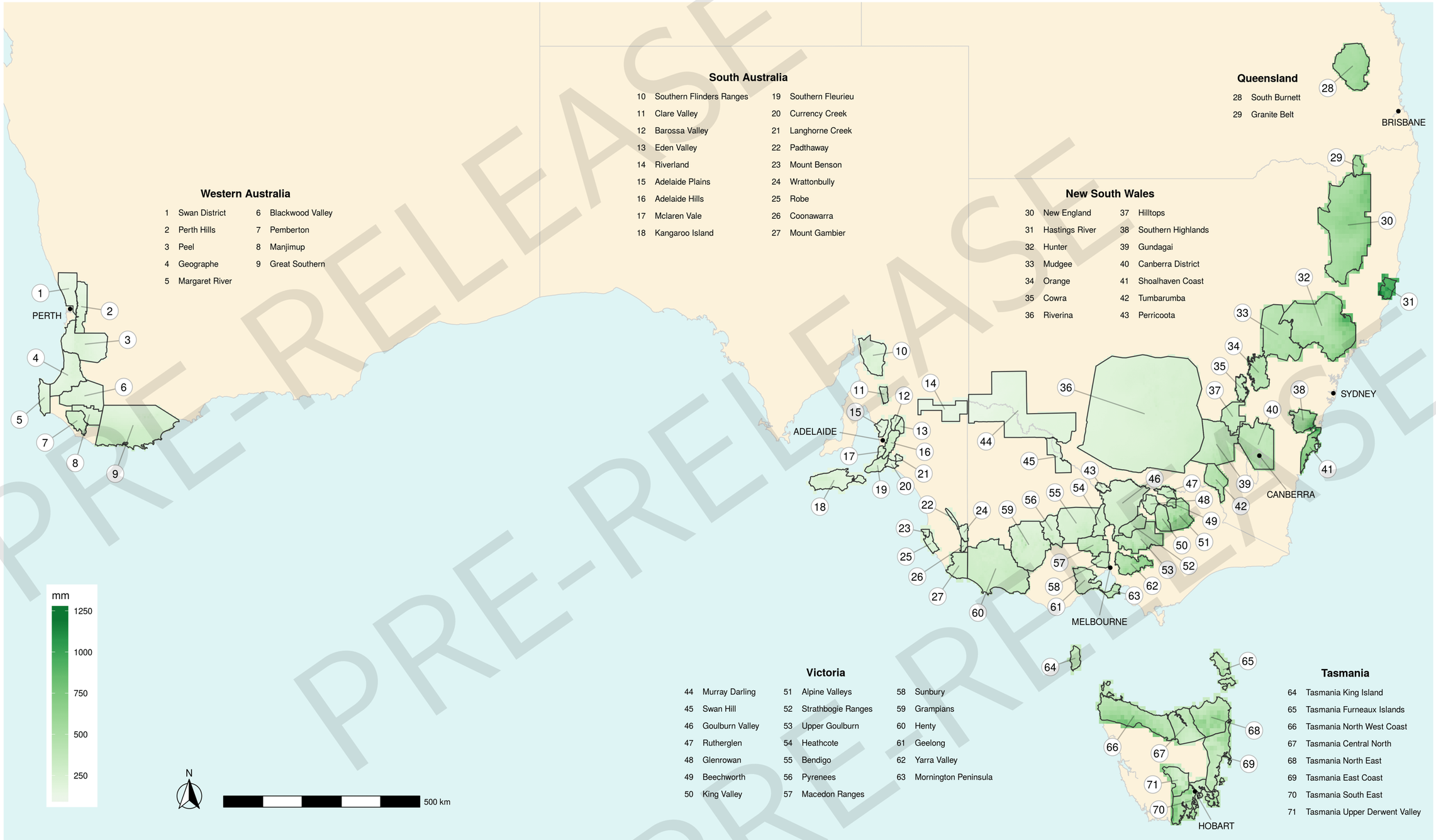

Figure 4: Observed mean *Growing Season Rainfall* (Oct–Apr) across all growing years from 1997–2017.

OBSERVED CLIMATE ACROSS AUSTRALIA'S WINE REGIONS

National Maps

Figure 5: Observed change in mean Growing Season Rainfall across Australia's wine regions
Current period (1997–2017) minus baseline period (1961–1990)

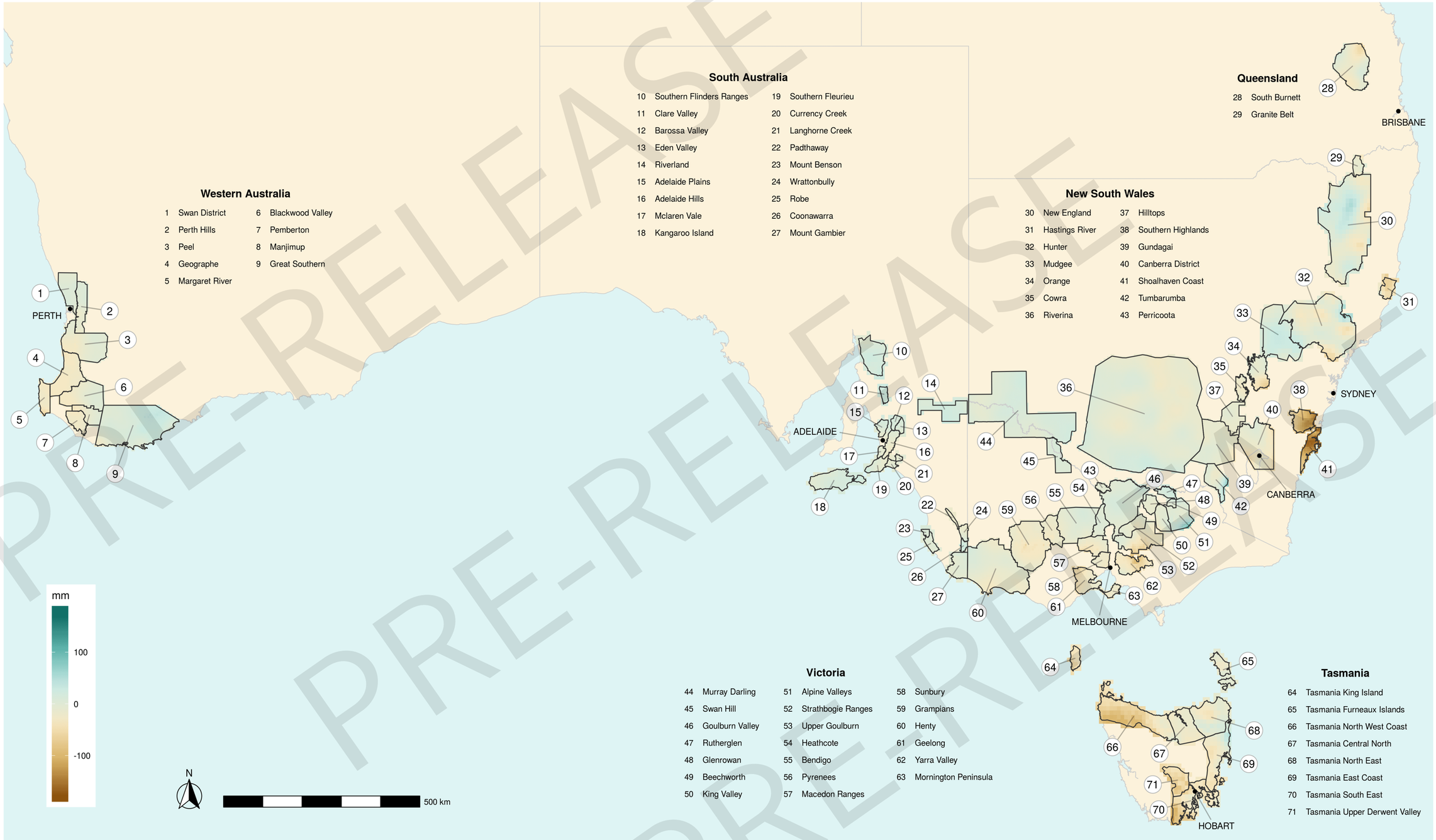

Figure 5: Change in *Growing Season Rainfall* (Oct–Apr) between the current (1997–2017) and historical (1961–1990) periods. Negative values indicate a trend towards drier conditions. Positive values indicate a trend towards wetter conditions.

OBSERVED CLIMATE ACROSS AUSTRALIA'S WINE REGIONS

National Maps

Figure 6: Observed mean Non-Growing Season Rainfall across Australia's wine regions
Current period (1997–2017)

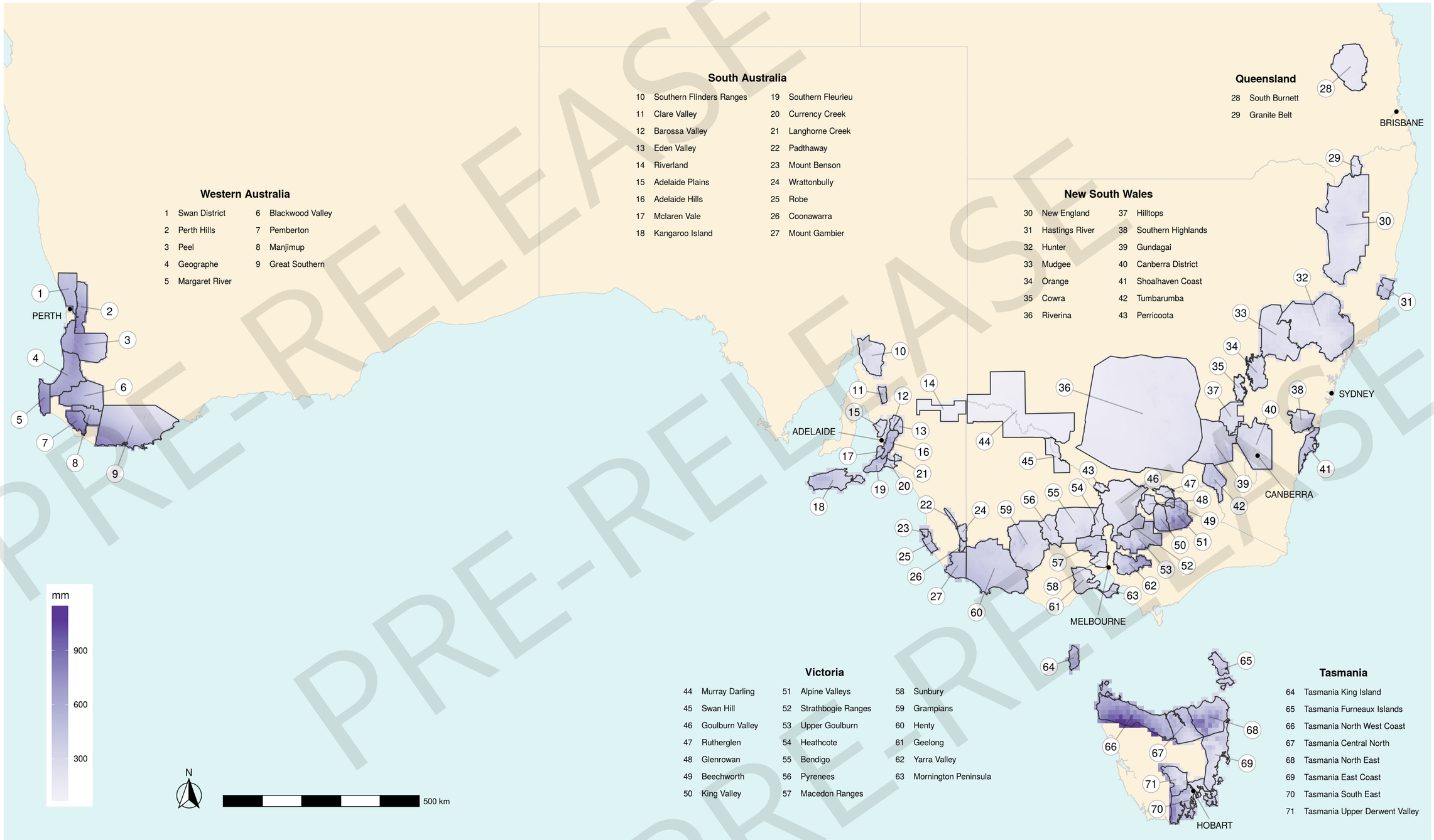

Figure 6: Observed mean *Non-Growing Season Rainfall* (May–Sep) across all growing years from 1997–2017.

Figure 7: Observed change in mean Non-Growing Season Rainfall across Australia's wine regions
Current period (1997–2017) minus baseline period (1961–1990)

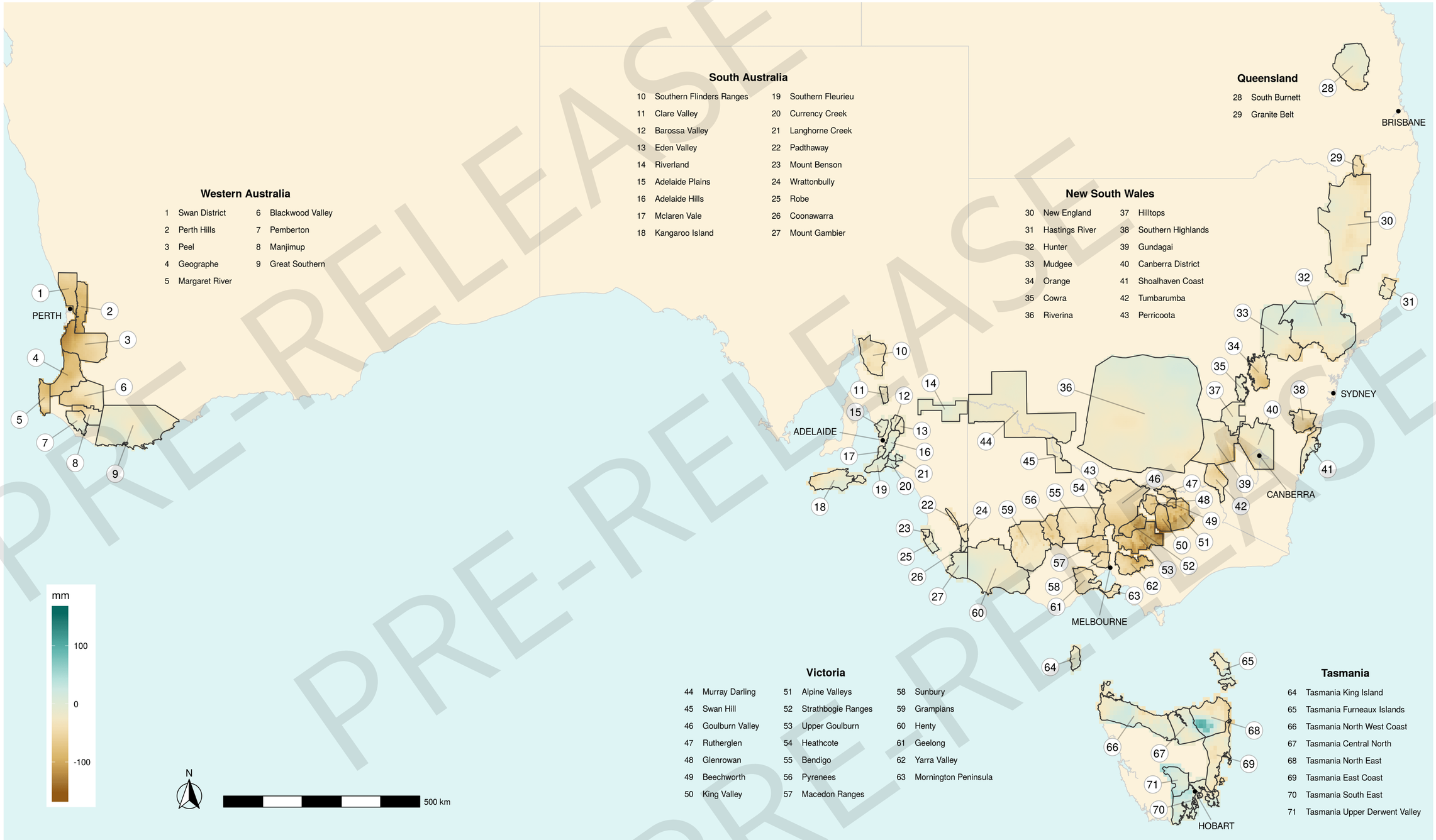

Figure 7: Change in *Non-Growing Season Rainfall* (May–Sep) between the current (1997–2017) and historical (1961–1990) periods. Negative values indicate a trend towards drier conditions. Positive values indicate a trend towards wetter conditions.

OBSERVED CLIMATE ACROSS AUSTRALIA'S WINE REGIONS

National Maps

Figure 8: Observed mean Growing Year Rainfall across Australia's wine regions
Current period (1997–2017)

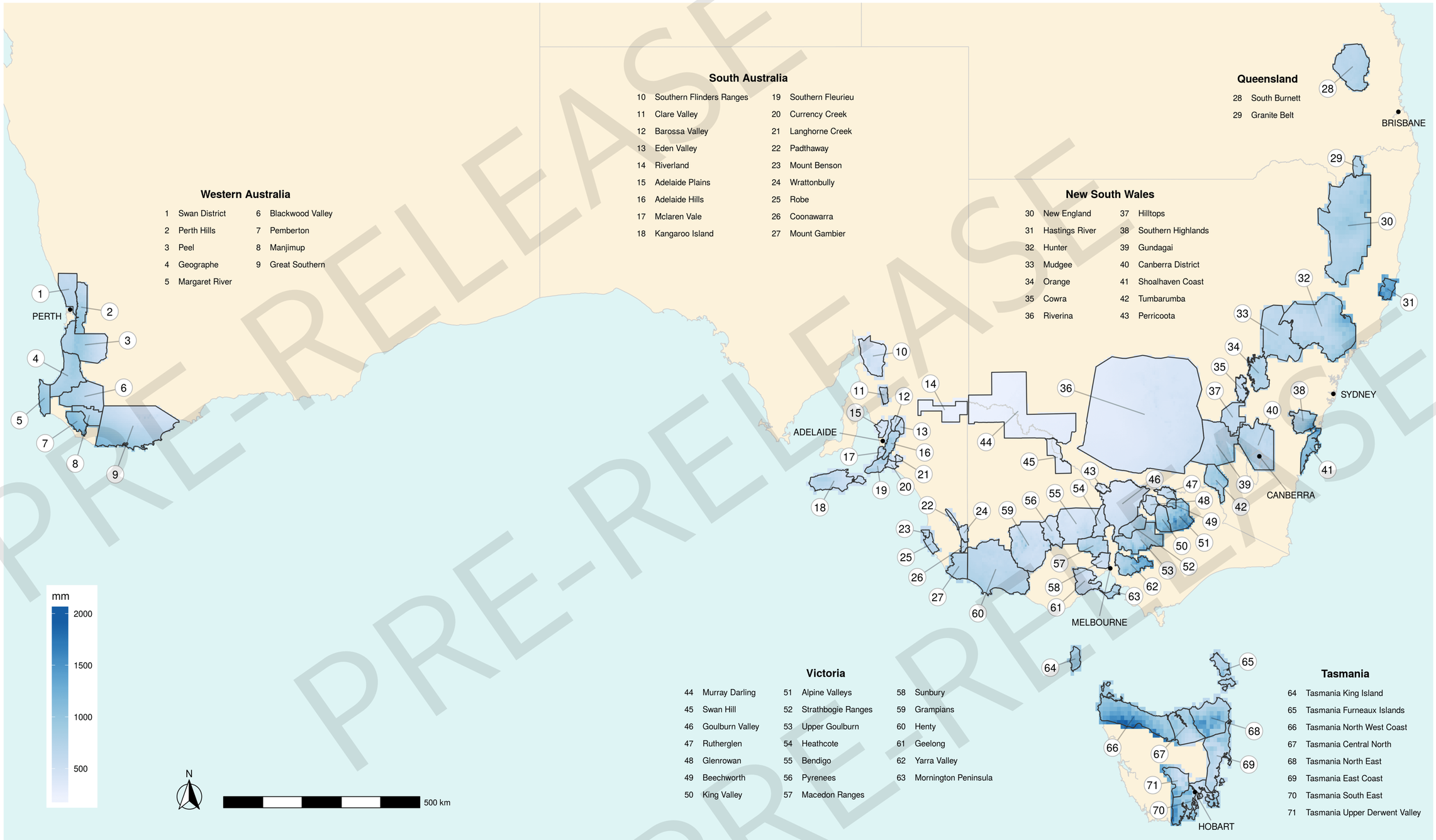

Figure 8: Observed mean *Annual Rainfall* (Jul–Jun) across all growing years from 1997–2017.

OBSERVED CLIMATE ACROSS AUSTRALIA'S WINE REGIONS

National Maps

Figure 9: Observed change in mean Growing Year Rainfall across Australia's wine regions
Current period (1997–2017) minus baseline period (1961–1990)

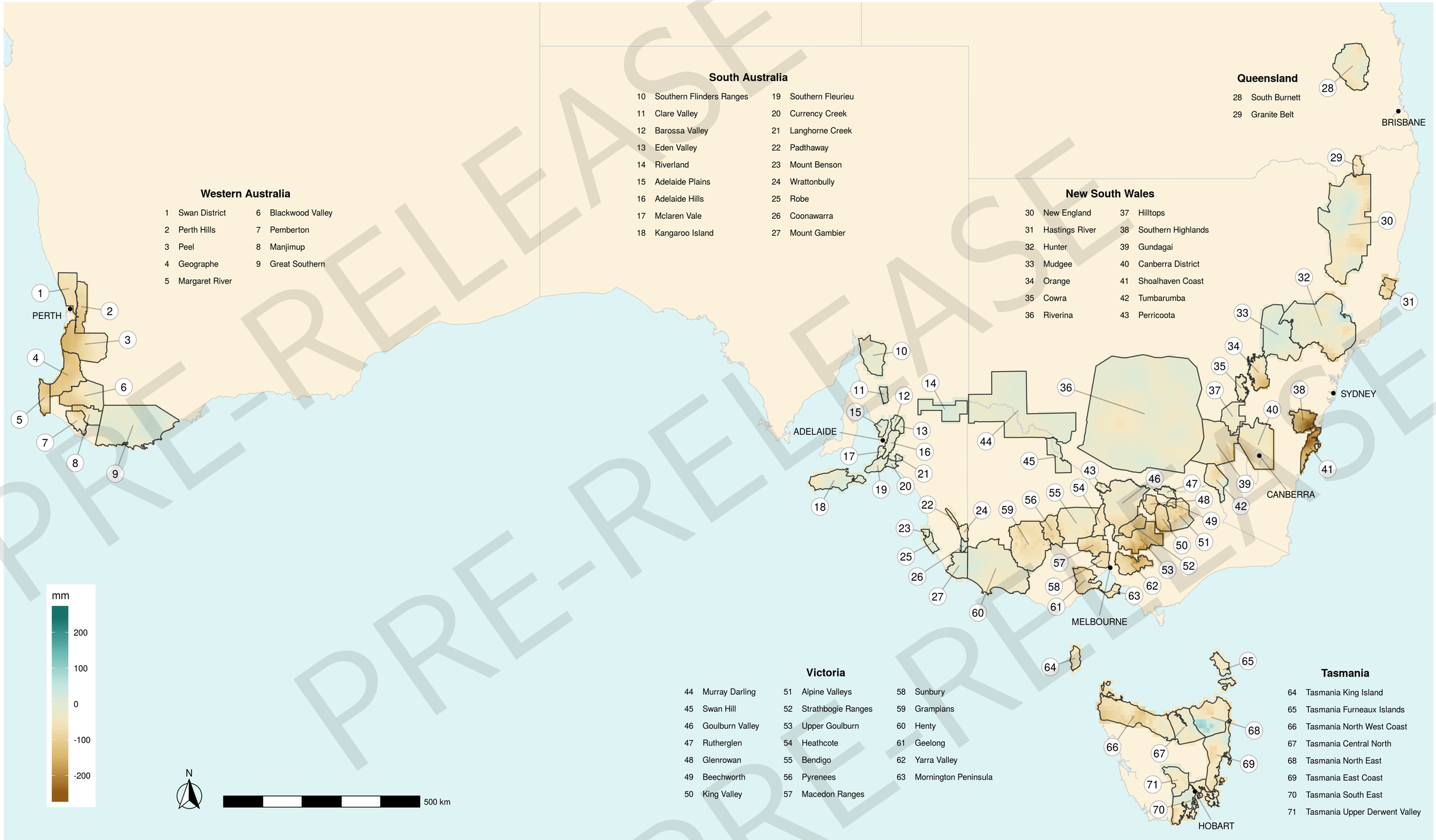

Figure 9: Change in *Annual Rainfall* (Jul–Jun) between the current (1997–2017) and historical (1961–1990) periods. Negative values indicate a trend towards drier conditions. Positive values indicate a trend towards wetter conditions.

OBSERVED CLIMATE ACROSS AUSTRALIA'S WINE REGIONS

National Maps

Figure 10: Observed mean Aridity Index across Australia's wine regions
Current period (1997–2017)

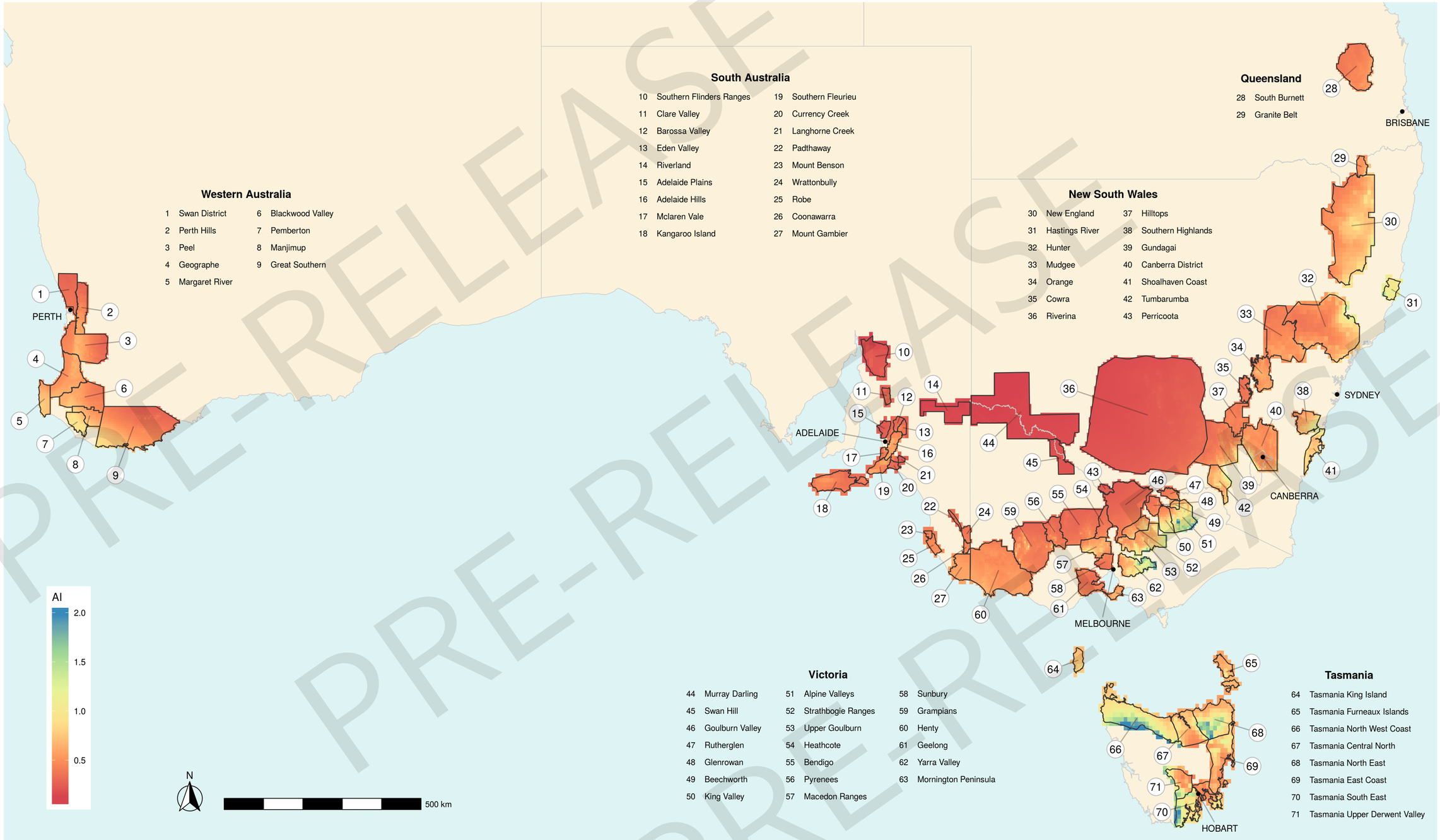

Figure 10: Observed mean annual Aridity Index across all growing years from 1997–2017. Aridity Index is a value that characterises the ratio between the mean annual rainfall and mean annual evaporation. Low values indicate drier conditions. High values indicate wetter conditions.

OBSERVED CLIMATE ACROSS AUSTRALIA'S WINE REGIONS

National Maps

Figure 11: Observed change in mean Aridity Index across Australia's wine regions
Current period (1997–2017) minus baseline period (1961–1990)

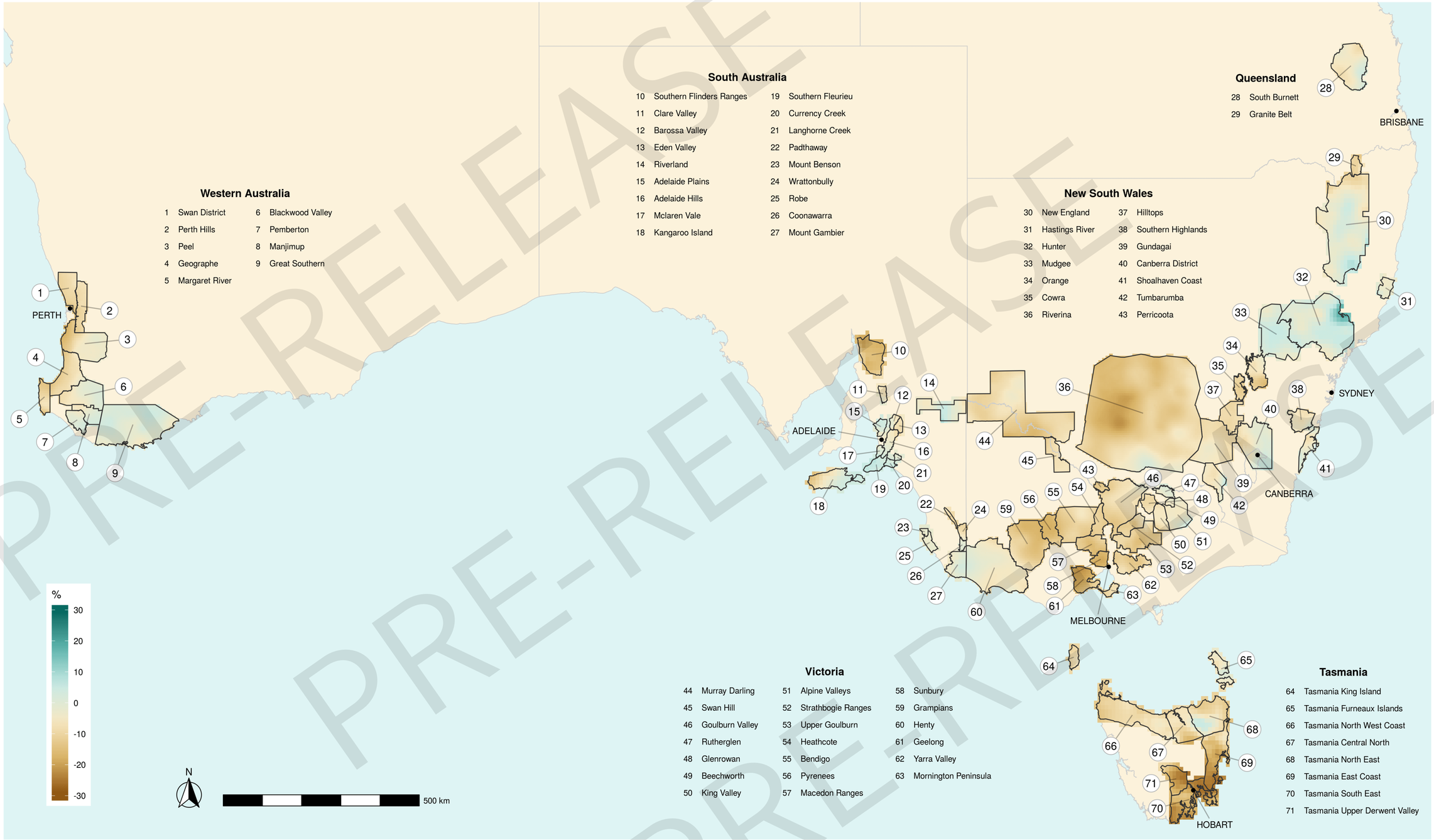

Figure 11: Observed percentage change in mean annual Aridity Index between the current (1997–2017) and historical (1961–1990) periods. This shows the change already experienced across the country. Negative values indicate a trend towards drier conditions. Positive values indicate a trend towards wetter conditions.

OBSERVED CLIMATE ACROSS AUSTRALIA'S WINE REGIONS

Reference Bar Charts

Figure 12: Mean Growing Season Temperature for current period (1997–2017)

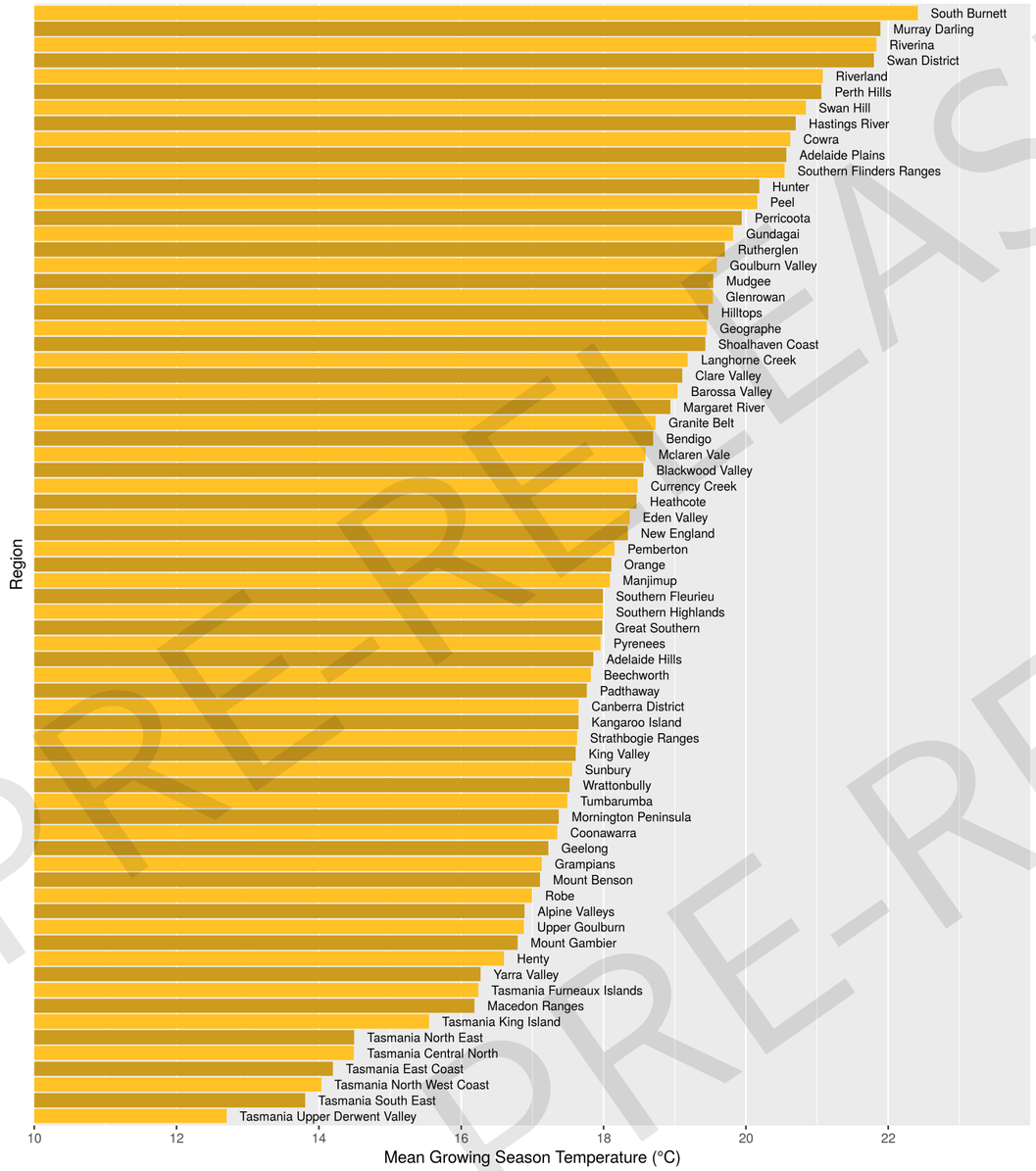

Figure 12: Wine regions of Australia ranked by observed mean *Growing Season Temperature* for the period 1997–2017. The growing season is defined to be October to April; e.g. the first growing season is October 1997 to April 1998, and the last growing season is October 2016 to April 2017.

Figure 13: Mean maximum growing year Growing Degree Days for current period (1997–2017)

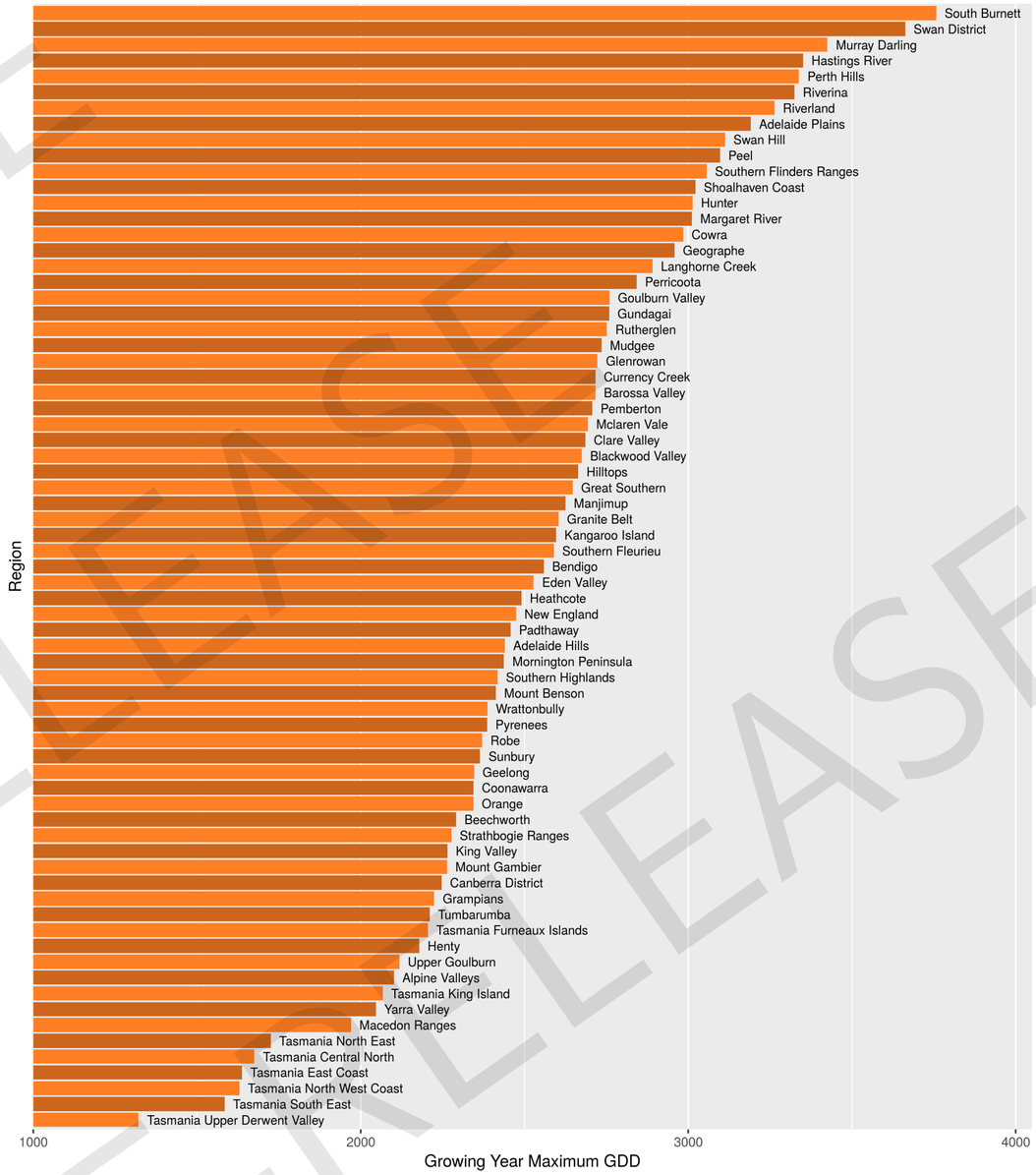

Figure 13: Wine regions of Australia ranked by observed growing year maximum *Growing Degree Days* for the period 1997–2017. The values are calculated for each *growing year* (July to June). The growing season is defined to be October to April; e.g. the first growing season is October 1997 to April 1998, and the last growing season is October 2016 to April 2017.

OBSERVED CLIMATE ACROSS AUSTRALIA'S WINE REGIONS

Reference Bar Charts

Figure 14: Mean Growing Season Rainfall for current period (1997–2017)

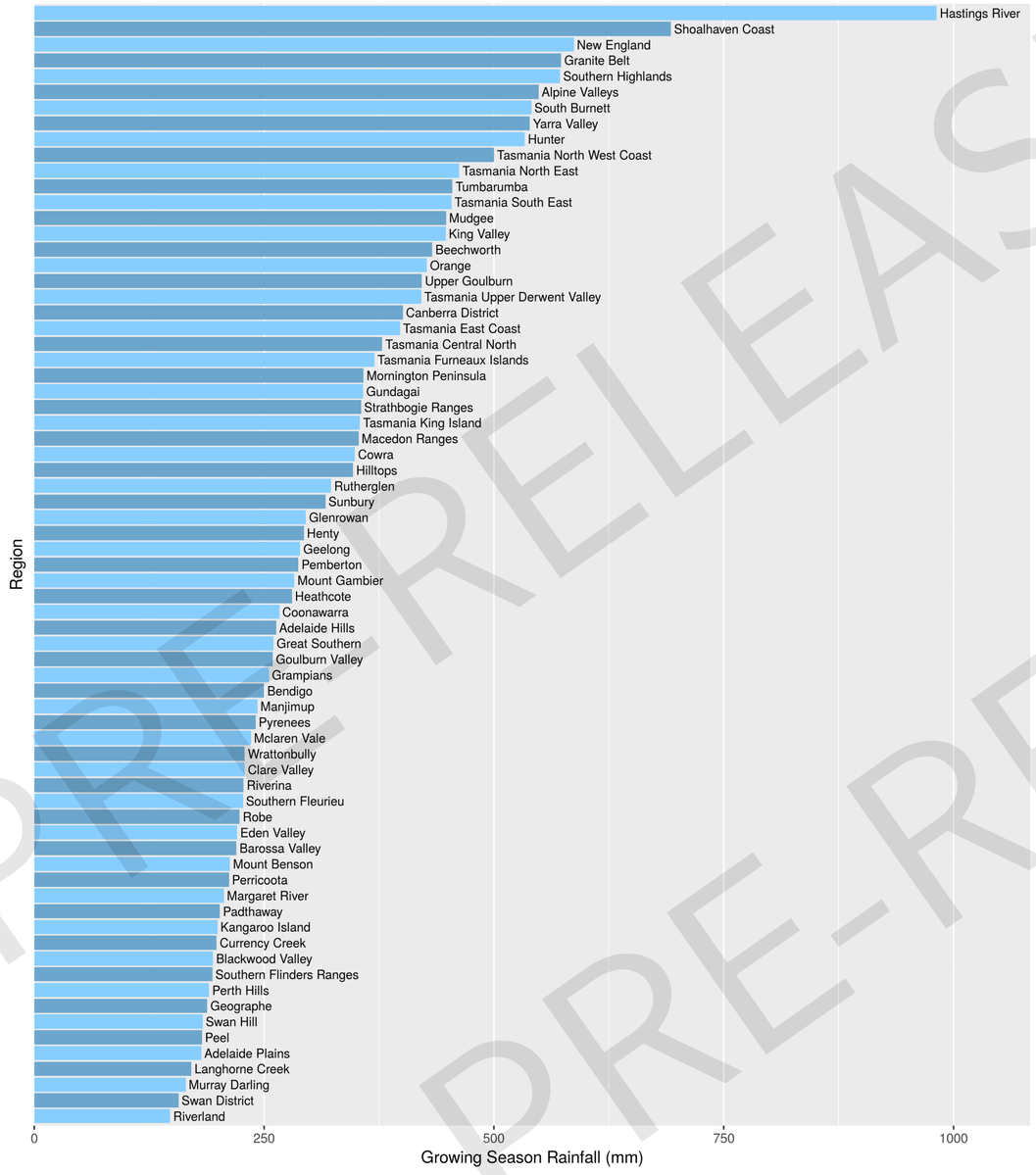

Figure 14: Wine regions of Australia ranked by total *Growing Season Rainfall* for the period 1997–2017. The growing season is defined to be October to April; e.g. the first growing season is October 1997 to April 1998, and the last growing season is October 2016 to April 2017.

Figure 15: Mean Non-Growing Season Rainfall for current period (1997–2017)

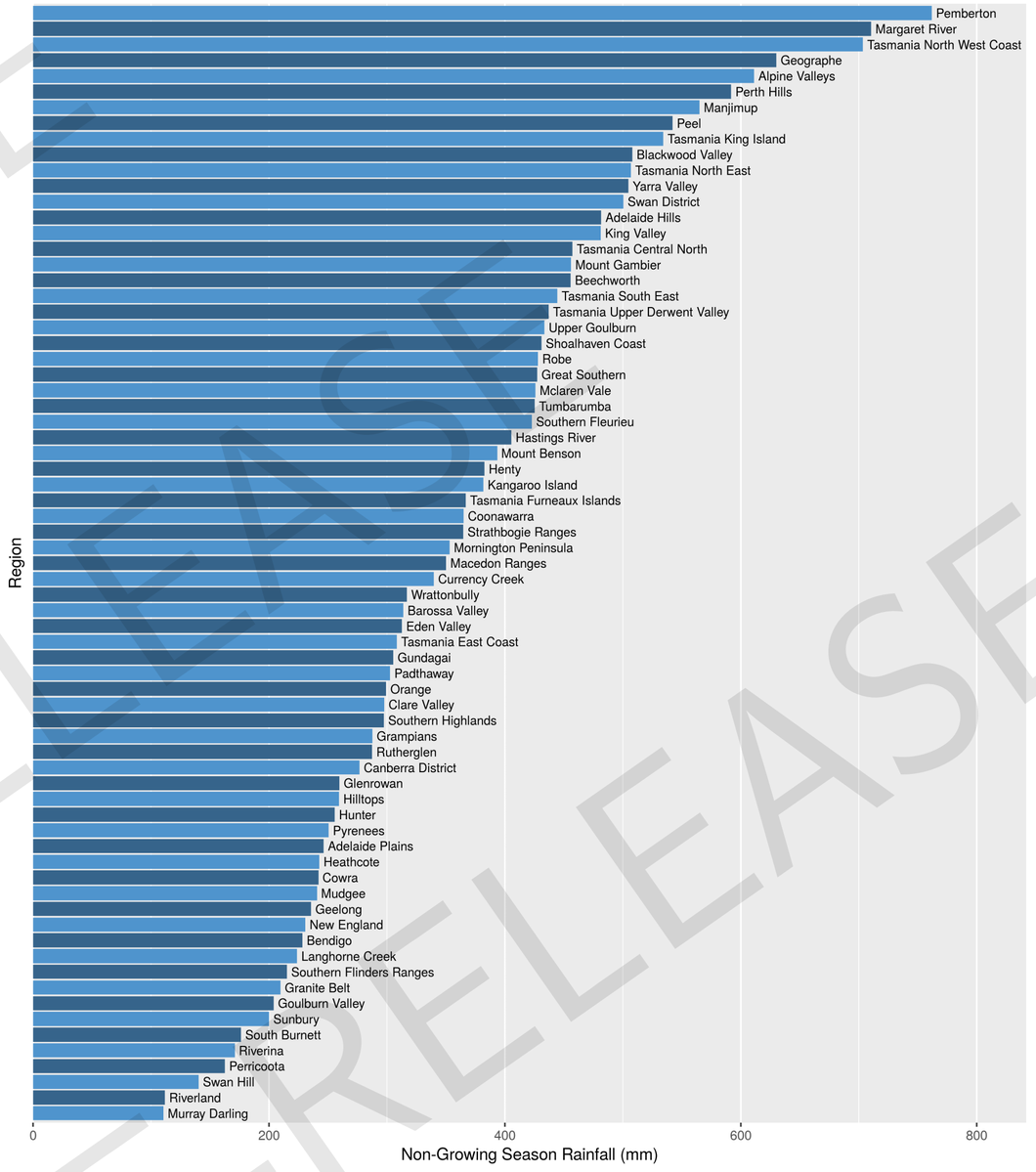

Figure 15: Wine regions of Australia ranked by total *Non-Growing Season Rainfall* for the period 1997–2017. The non-growing season is defined to be May to September; e.g. the first non-growing season is May 1997 to September 1997, and the last growing season is May 2016 to September 2016.

OBSERVED CLIMATE ACROSS AUSTRALIA'S WINE REGIONS

Reference Bar Charts

Figure 16: Mean Growing Year Rainfall for current period (1997–2017)

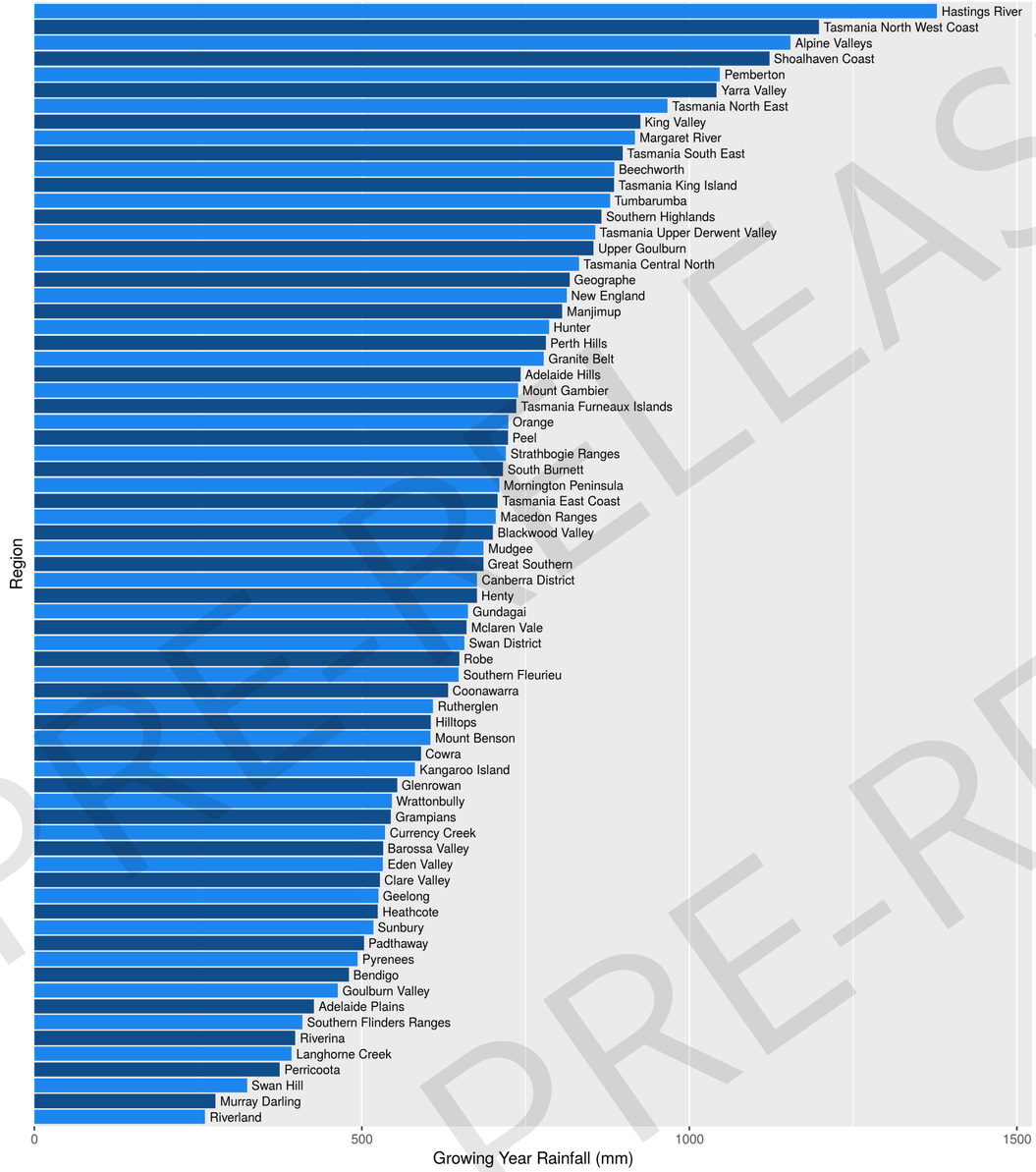

Figure 16: Wine regions of Australia ranked by total *Annual Rainfall* for the period 1997–2017. The annual periodis defined to be July to June; e.g. the first annual period is July 1997 to June 1998, and the last annual period is July 2016 to June 2017.

Figure 17: Mean growing year Aridity Index for current period (1997–2017)

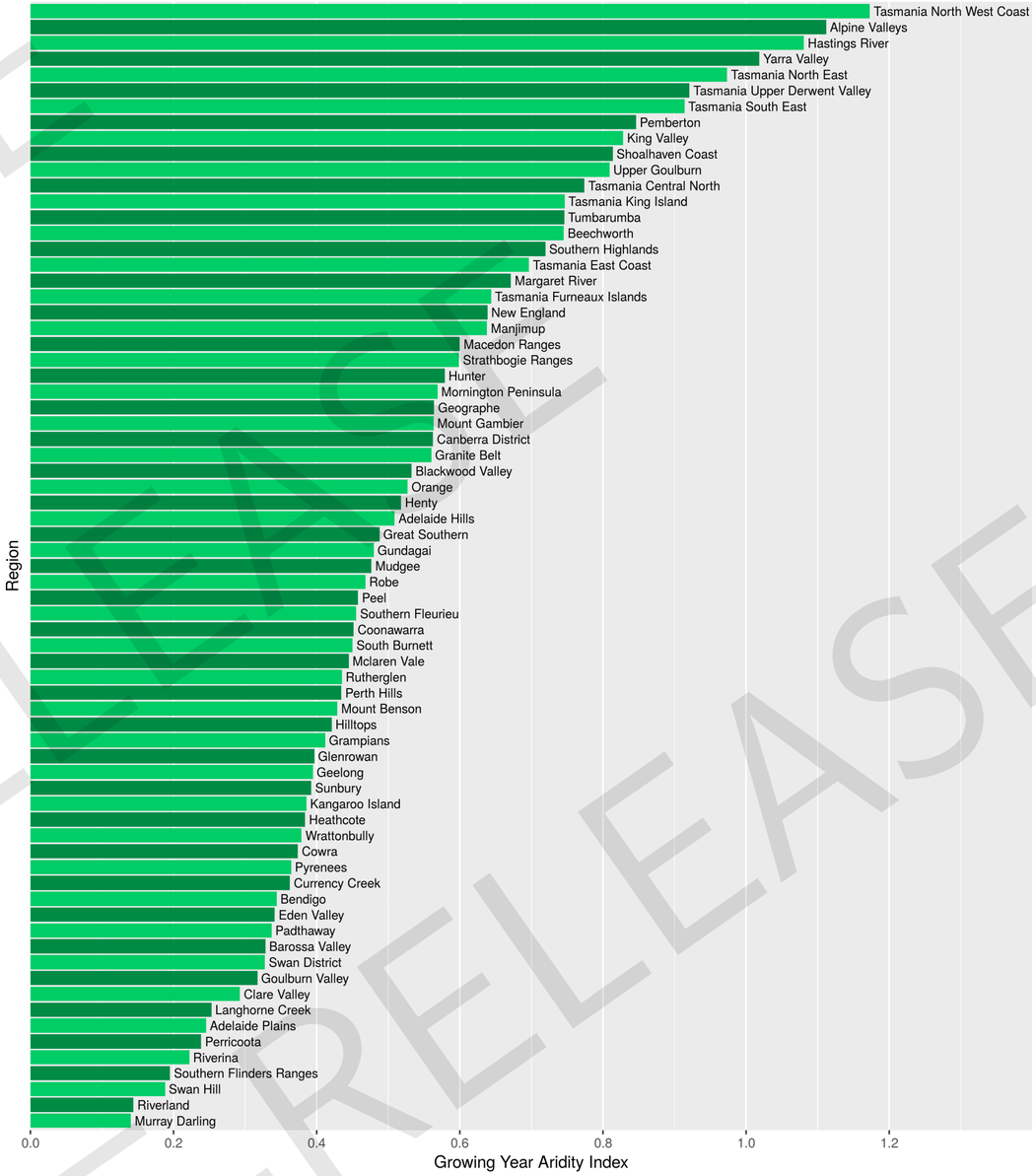

Figure 17: Wine regions of Australia ranked by mean growing year *Aridity Index* for the period 1997–2017. The growing season is defined to be October to April; e.g. the first growing season is October 1997 to April 1998, and the last growing season is October 2016 to April 2017.

Figure 18: Mean Growing Year Aridity Index vs mean Growing Season Temperature

Projected drift in climatic conditions for Australian wine regions across 20-year periods from 1997–2017 to 2081–2100

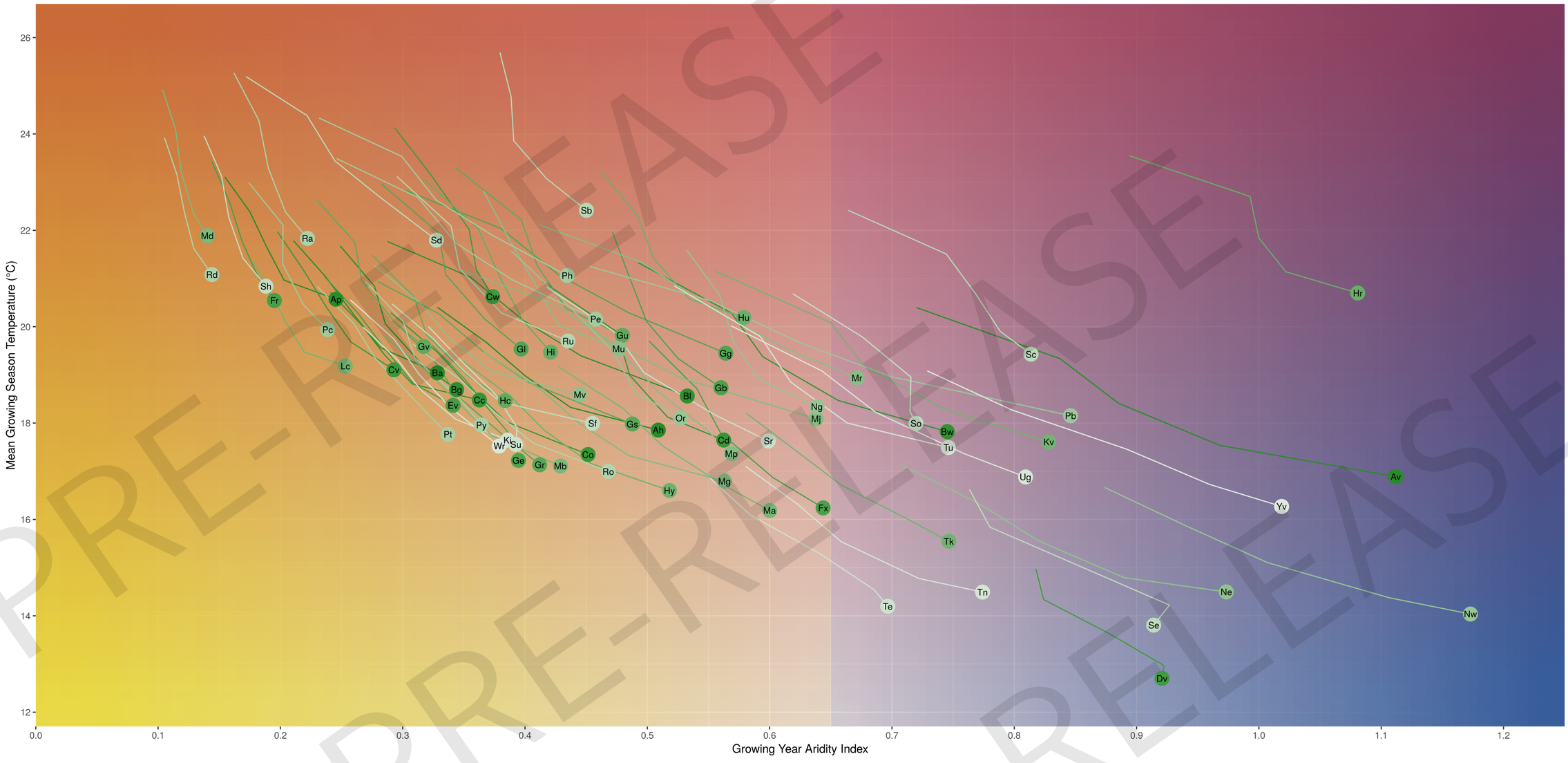

Region

Ah = Adelaide Hills	Bw = Beechworth	Dv = Tasmania Upper Derwent Valley	Gg = Geographe	Hc = Heathcote	Kv = King Valley	Mj = Manjimup	Ng = New England	Ph = Perth Hills	Ru = Rutherglen	Sh = Swan Hill	Tn = Tasmania Central North
Ap = Adelaide Plains	Cc = Currency Creek	Ev = Eden Valley	Gl = Glenrowan	Hi = Hilltops	Lc = Langhorne Creek	Mp = Mornington Peninsula	Nw = Tasmania North West Coast	Pt = Padthaway	Sb = South Burnett	So = Southern Highlands	Tu = Tumbarumba
Av = Alpine Valleys	Cd = Canberra District	Fr = Southern Flinders Ranges	Gr = Grampians	Hr = Hastings River	Ma = Macedon Ranges	Mr = Margaret River	Or = Orange	Py = Pyrenees	Sc = Shoalhaven Coast	Sr = Strathbogie Ranges	Ug = Upper Goulburn
Ba = Barossa Valley	Co = Coonawarra	Fx = Tasmania Furneaux Islands	Gs = Great Southern	Hu = Hunter	Mb = Mount Benson	Mu = Mudgee	Pb = Pemberton	Ra = Riverina	Sd = Swan District	Su = Sunbury	Wr = Wrattonbully
Bg = Bendigo	Cv = Clare Valley	Gb = Granite Belt	Gu = Gundagai	Hy = Henty	Md = Murray Darling	Mv = Mclaren Vale	Pc = Perricoota	Rd = Riverland	Se = Tasmania South East	Te = Tasmania East Coast	Yv = Yarra Valley
Bl = Blackwood Valley	Cw = Cowra	Ge = Geelong	Gv = Goulburn Valley	Ki = Kangaroo Island	Mg = Mount Gambier	Ne = Tasmania North East	Pe = Peel	Ro = Robe	Sf = Southern Fleurieu	Tk = Tasmania King Island	

Figure 1: Representation of mean *Growing Year Aridity Index* vs mean *Growing Season Temperature* for each Australian Geographic Indication, averaged within 20-year time periods (1997–2017, 2021–2040, 2041–2060, 2061–2080, and 2081–2100), following the RCP8.5 scenario. Points represent observed conditions during the *current period* (1997–2017). Lines indicate the general direction of change projected into the future (based on the CFAP2019 ensemble mean). Line segments represent the shorter-term direction of change projected between 20-year time periods. Values are regional and ensemble averages (i.e. a single value for each region, for each 20-year period). The plot shows a tendency of regions to move towards warmer and drier conditions (i.e. higher mean *Growing Season Temperature* and lower mean *Growing Year Aridity Index*). Regions that currently experience quite wet conditions (points on the right-hand side of the plot) are projected to have both drying and warming challenges to address into the future (pathways are diagonal). Regions that are already very arid (points on the left-hand side of plot) are projected to have challenges driven mostly by warming tempreatures (pathways are more vertical).

New South Wales

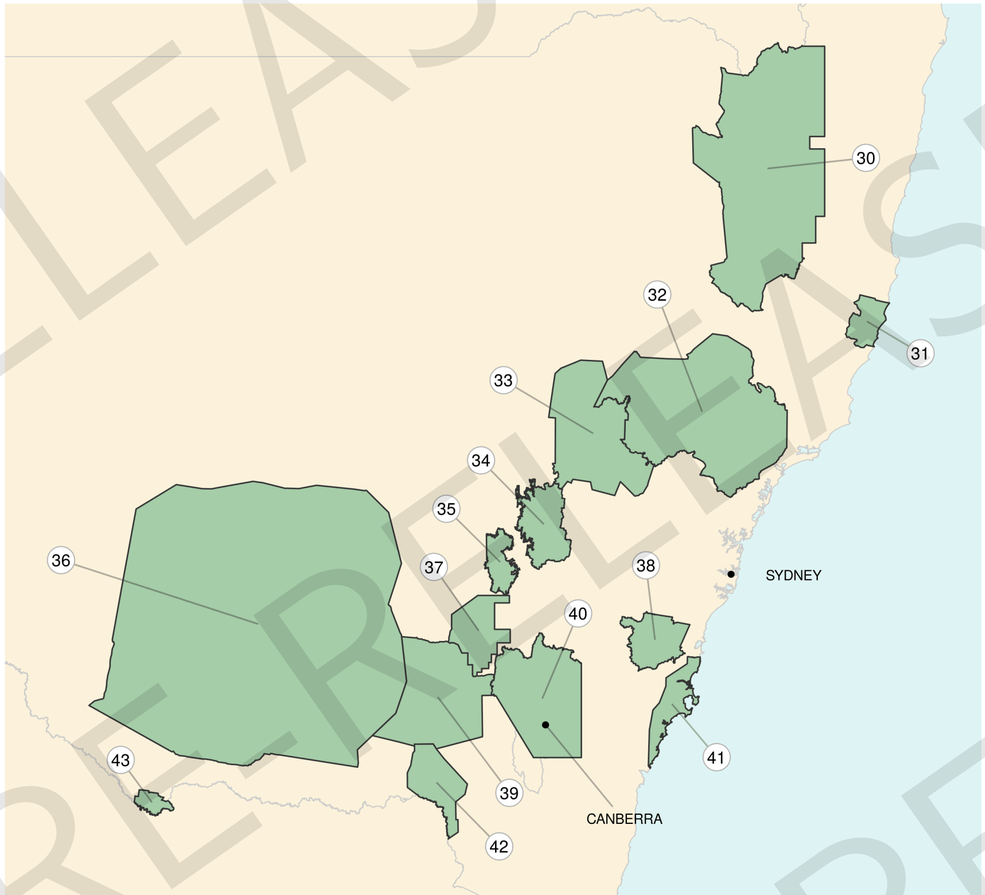

30	New England	37	Hilltops
31	Hastings River	38	Southern Highlands
32	Hunter	39	Gundagai
33	Mudgee	40	Canberra District
34	Orange	41	Shoalhaven Coast
35	Cowra	42	Tumbarumba
36	Riverina	43	Perricoota

AUSTRALIA'S WINE FUTURE
A CLIMATE ATLAS

HUNTER

RAINFALL

Projected Mean Growing Season Rainfall

534 mm 1997–2017

584 mm 2041–2060

589 mm 2081–2100

TEMPERATURE

Projected Mean Growing Season Temperature

20.2 °C 1997–2017

21.4 °C 2041–2060

23.2 °C 2081–2100

EXTREME HEAT

Projected Mean Excess Heat Factor

8.4 EHF 1997–2017

8.7 EHF 2041–2060

10.5 EHF 2081–2100

EXTREME COLD

Projected Mean Growing Season Frost Risk Days

0.7 days 1997–2017

0.3 days 2041–2060

0.1 days 2081–2100

ARIDITY

Projected Mean Annual Aridity Index

0.58 1997–2017

0.51 2041–2060

0.47 2081–2100

Wine Australia

ACE CRC ANTARCTIC CLIMATE & ECOSYSTEMS COOPERATIVE RESEARCH CENTRE

climatefutures

UNIVERSITY of TASMANIA

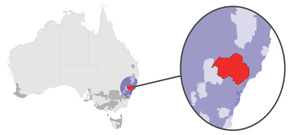

Figure 1: Observed mean Growing Season Temperature

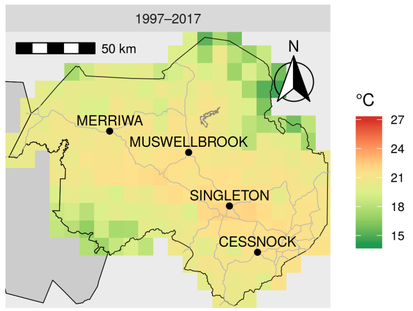

Figure 2: Observed change in mean Growing Season Temperature

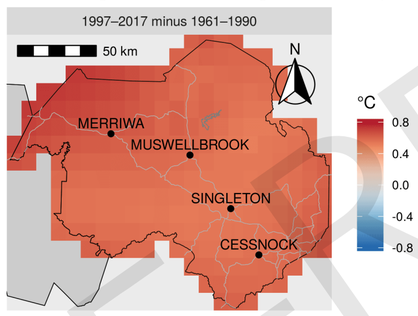

Figure 3: Projected mean Growing Season Temperature

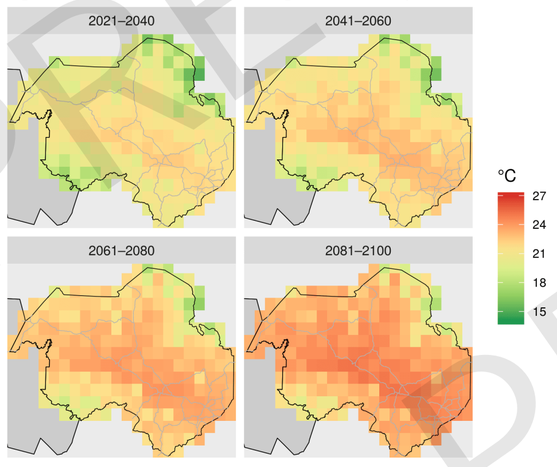

Figure 1: Observed mean *Growing Season Temperature* (Oct–Apr) across all growing years from 1997–2017.

Figure 2: The change in *Growing Season Temperature* between the current (1997–2017) and historical (1961–1990) periods. *Growing Season Temperature* has increased across the region over recent decades.

Figure 3: Projected mean *Growing Season Temperature* (Oct–Apr) for 20-year time periods from 2021 to 2100. *Growing Season Temperature* is expected to increase steadily into the future. Each grid cell is the mean of the 6 ensemble members.

Figure 4: Projected Growing Season Temperature (October to April)

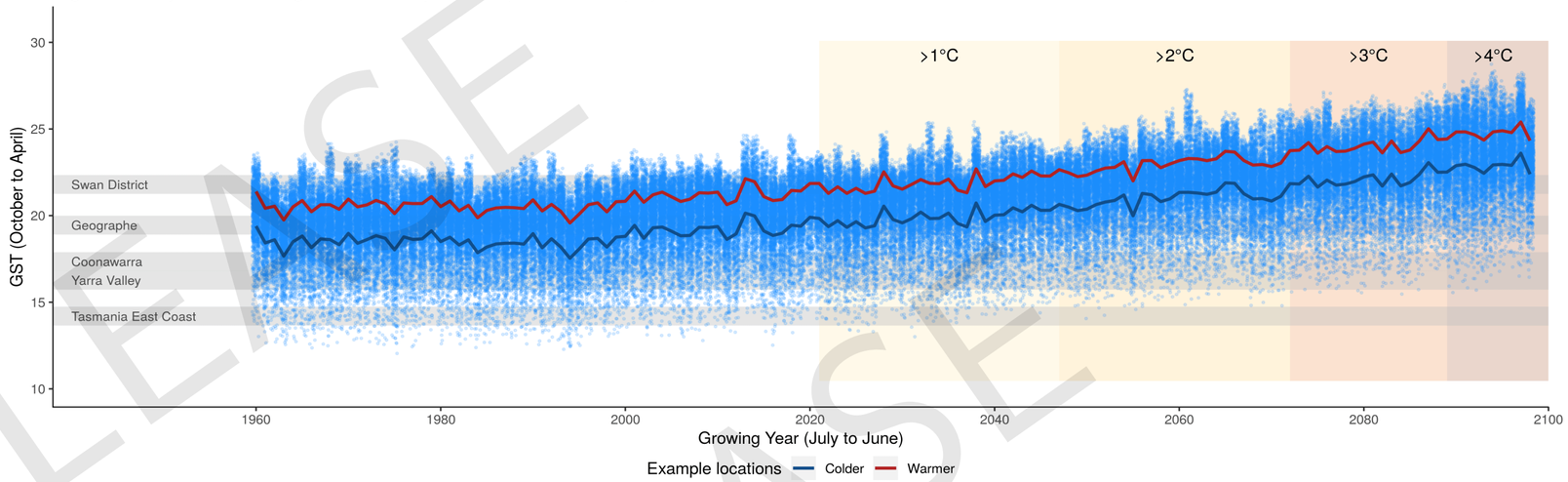

Figure 4: *Growing Season Temperature* (GST) over time. Blue points are the values for each grid cell, for each of the 6 ensemble members. Solid lines are timeseries representing grid cells for colder and warmer locations within the region based on current conditions (1997–2017). Horizontal grey bars represent the mean GST value during 1997–2017 in selected regions across Australia. These provide a comparison between current conditions elsewhere and future conditions in this region, helping to identify future analogue regions. Coloured bars represent the projected global temperature increase expected into the future (following the RCP 8.5 scenario). These can be used to make decisions based on *projected temperature change* rather than time (for example, if the rate of warming rapidly increases, useful information can still be extracted from these figures by using the shade boxes instead of the time-axis).

Figure 5: Distribution of Growing Season Temperature

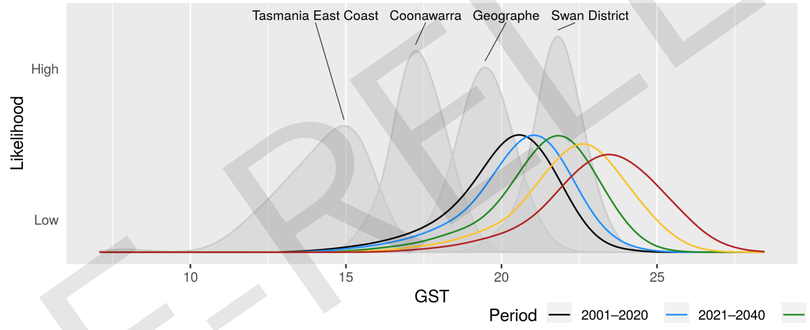

Figure 5: Probability distribution of GST for 20-year time periods from 2001 to 2100. Variability can occur spatially within the region, across years, or between ensemble members. Grey shapes represent the probability distribution of GST for contrasting regions during 1997–2017. A shift to the right (left) indicates warmer (cooler) conditions.

Figure 6: Distribution of Growing Degree Days

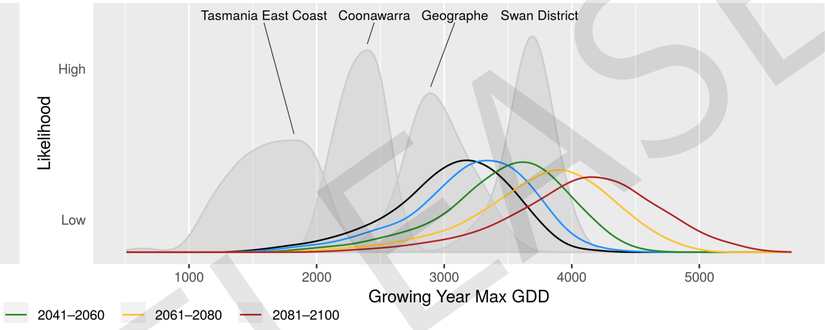

Figure 6: Probability distribution of growing year maximum GDD for 20-year time periods from 2001 to 2100. Variability can occur spatially within the region, across years, or between ensemble members. Grey shapes represent the probability distribution of growing year maximum GDD for contrasting regions during 1997–2017. A shift to the right (left) indicates warmer (cooler) conditions.

Figure 7: Projected cumulative Growing Degree Days

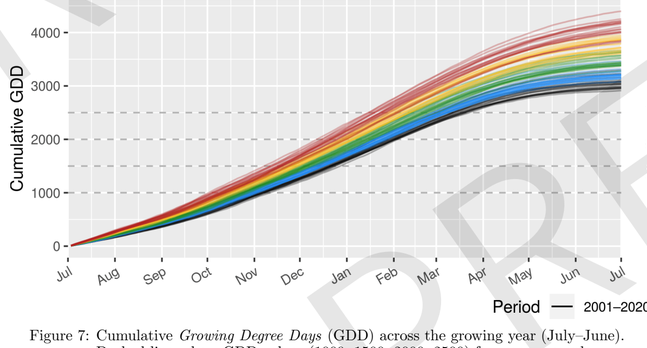

Figure 7: Cumulative *Growing Degree Days* (GDD) across the growing year (July–June). Dashed lines show GDD values (1000, 1500, 2000, 2500) for some example phenological thresholds. Each growing year is represented by a coloured line. In future time periods, heat accumulates faster, thresholds are reached earlier and maximum GDD reached is higher.

Figure 8: Distribution of date when Growing Degree Days reaches threshold

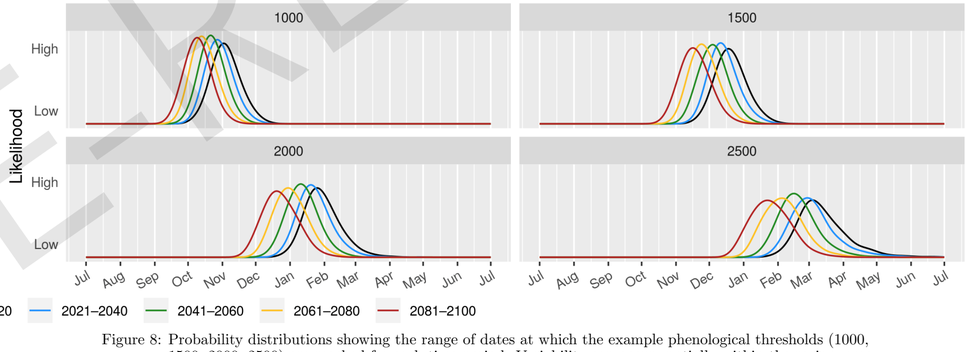

Figure 8: Probability distributions showing the range of dates at which the example phenological thresholds (1000, 1500, 2000, 2500) are reached for each time period. Variability can occur spatially within the region, across years, or between ensemble members. A shift to the left (right) indicates earlier (later) harvest dates. A wider (thinner) curve indicates a larger (smaller) range of harvest dates. A missing time period indicates that the specific phenological threshold was not reached within the growing year (July–June).

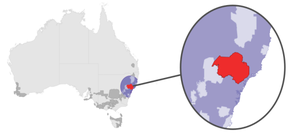

Figure 1: Observed mean Growing Season Rainfall

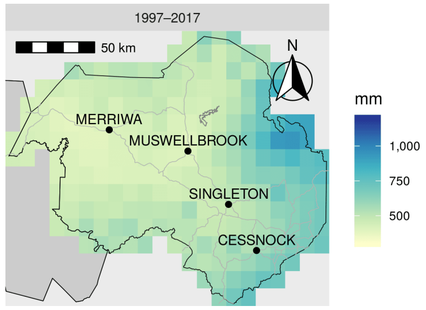

Figure 2: Observed change in mean Growing Season Rainfall

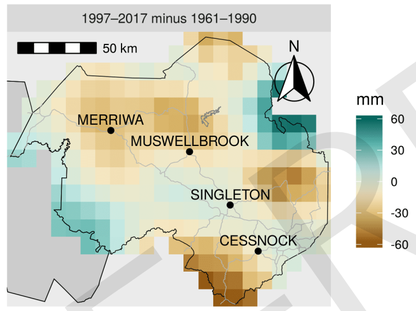

Figure 3: Projected mean Growing Season Rainfall

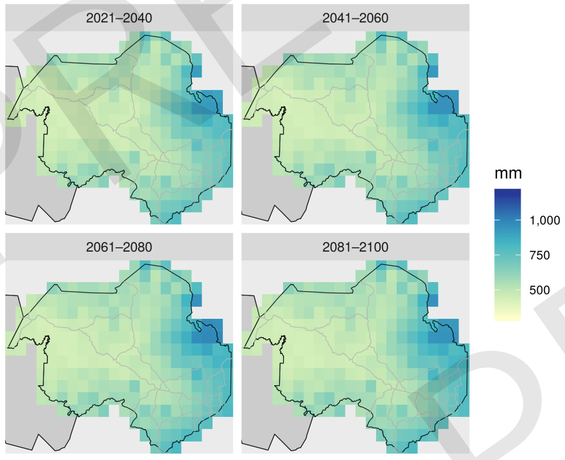

Figure 1: Observed mean *Growing Season Rainfall* (Oct–Apr) across all growing years from 1997–2017.

Figure 2: Change in *Growing Season Rainfall* (Oct–Apr) between the current (1997–2017) and historical (1961–1990) periods. Negative values indicate a trend towards drier conditions. Positive values indicate a trend towards wetter conditions.

Figure 3: Projected mean *Growing Season Rainfall* (Oct–Apr) for 20-year time periods from 2021 to 2100. Each grid cell is the mean of the 6 ensemble members.

Figure 4: Projected Growing Season Rainfall (October to April)

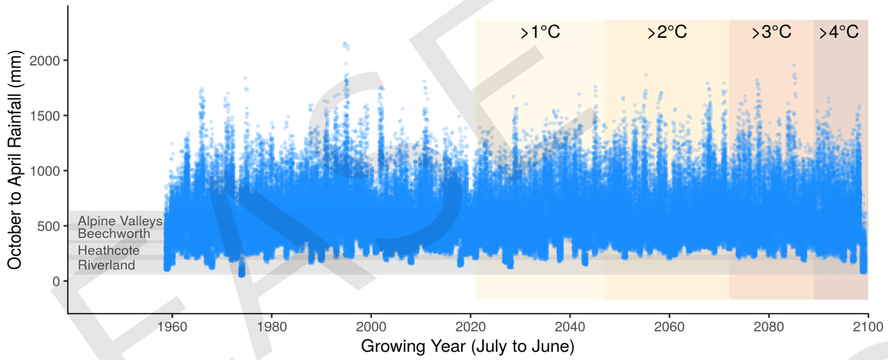

Figure 5: Projected Non-Growing Season Rainfall (May to September)

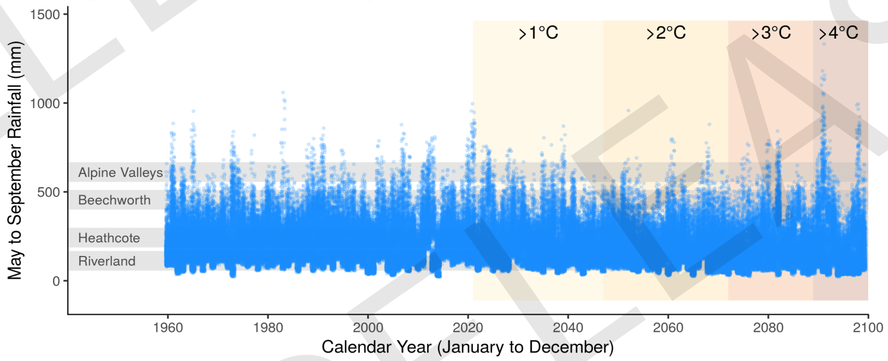

Figure 4: Time series of *Growing Season Rainfall* (mm). Blue points are the annual values for each grid cell, for each of the 6 ensemble members. Horizontal grey bars represent the mean *Growing Season Rainfall* value during 1997–2017 in selected regions across Australia. These provide a comparison between current conditions (1997–2017) elsewhere and future conditions in this region and help identify future analogue regions. Coloured bars represent the projected mean global temperature increase into the future (following the RCP 8.5 scenario). These can be used to make decisions based on *projected temperature change* rather than time.

Figure 5: As with Figure 4, but for *Non-Growing Season Rainfall* (mm). Horizontal grey bars represent the mean *Non-Growing Season Rainfall* value during 1997–2017 in selected regions across Australia.

Figure 6: Projected monthly rainfall

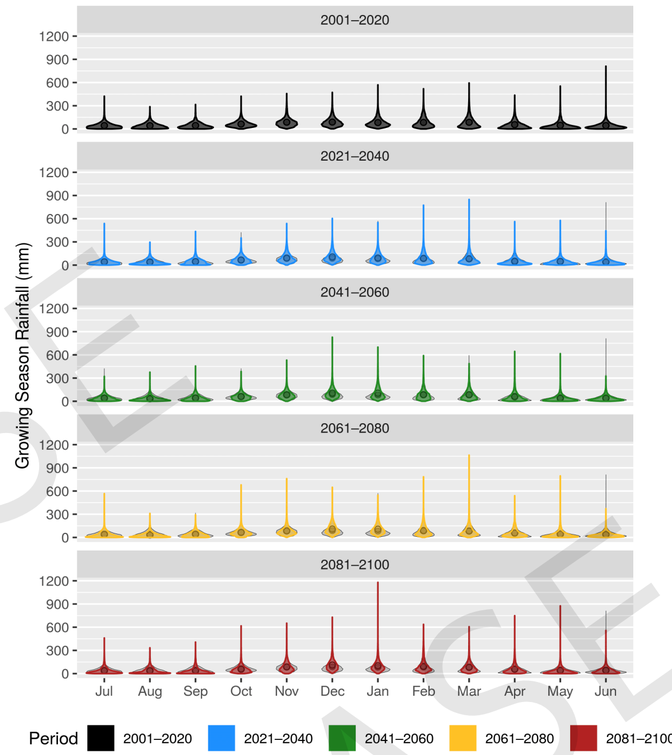

Figure 6: *Violin plots* of monthly rainfall (mm) for 20-year time periods from 2001 to 2100. Each violin represents monthly totals for each grid cell, for each of the 6 ensemble members, and for each growing year within the time period. In each panel the monthly violins indicate the expected probability distribution of rainfall across the growing year. The current period (2001–2020) is shadowed underneath the future time periods to highlight any differences expected into the future. Dots represent the mean monthly rainfall for each violin. If the violin shifts lower (higher) this indicates a change towards drier (wetter) conditions.

Figure 7: Distribution of seasonal rainfall

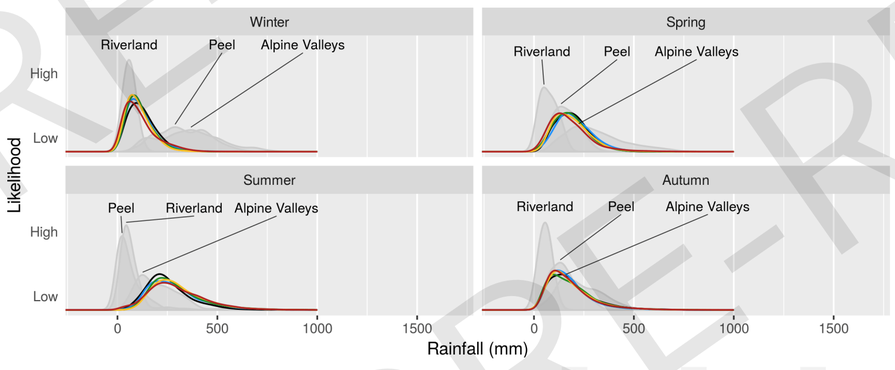

Figure 8: Distribution of number of rainy days during harvest

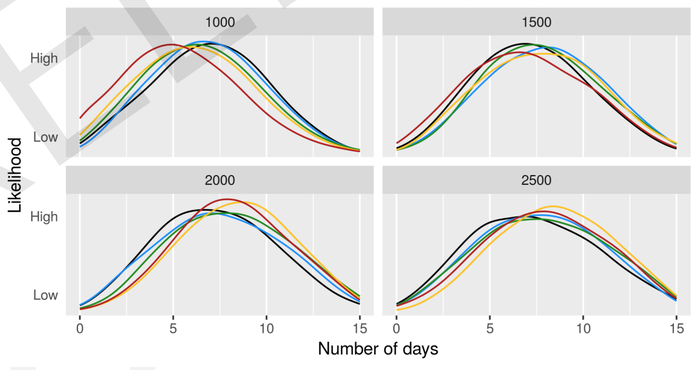

Figure 7: Seasonal rainfall (Winter, Spring, Summer, Autumn) (mm), presented as a probability distribution for each 20-year period. The shape of the curve is driven by the level of variability experienced within each 20-year period. Variability can occur spatially within the region, across years, or between ensemble members. Grey shapes represent the probability distribution of seasonal rainfall for contrasting regions during 1997–2017. Differences in the shape of curves between the current and future periods indicate a change in the typical conditions. A shift to the left (right) indicates an increase in drier (wetter) conditions.

Figure 8: Number of rainy days during harvest for each 20-year period. *Harvest* refers to the date when *Growing Degree Days* (GDD) reach example phenological thresholds (1000, 1500, 2000, 2500) which were chosen to reflect development time of different grape styles and varieties. Rainy days during harvest were defined as days with >10mm of rain from 7 days before to 7 days after the date each GDD threshold was reached. Variability can occur spatially within the region, across years, or between ensemble members. A shift in the curve to the left (right) indicates fewer (more) rainy days during harvest. A missing time period indicates that the specific phenological threshold was not reached within the growing year (July–June).

HUNTER

Aridity

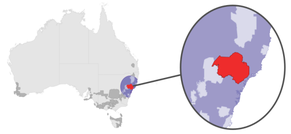

Figure 1: Observed mean annual Aridity Index

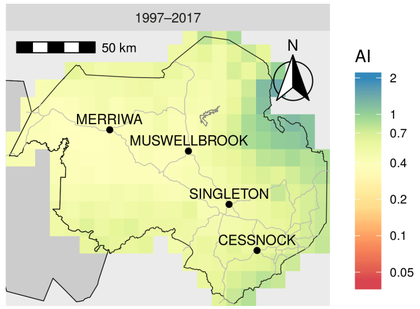

Figure 2: Obseved change in mean annual Aridity Index

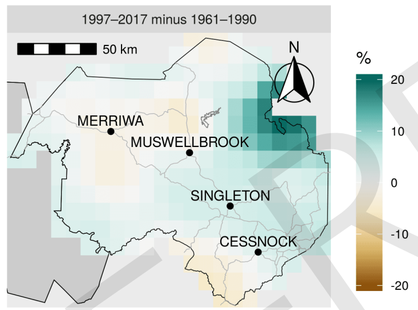

Figure 3: Projected mean annual Aridity Index

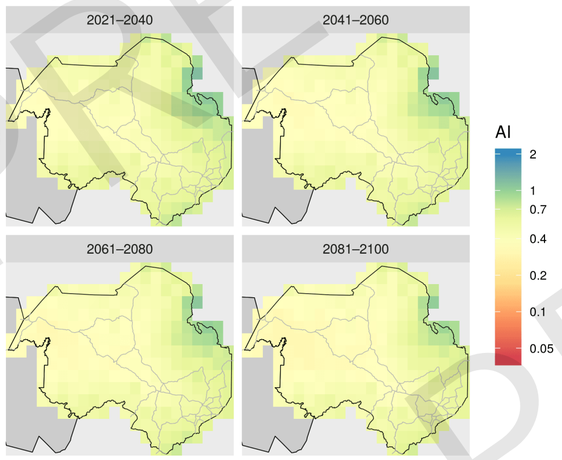

Figure 1: Observed mean annual Aridity Index across all growing years from 1997–2017. Aridity Index is a value that characterises the ratio between the mean annual rainfall and mean annual evaporation. Low (high) values indicate drier (wetter) conditions.

Figure 2: Observed percentage change in mean annual Aridity Index between the current (1997–2017) and historical (1961–1990) periods. This shows the change already experienced across the region. Negative (positive) values indicate a trend towards drier (wetter) conditions.

Figure 3: Projected mean annual Aridity Index for 20-year time periods from 2021 to 2100. Each grid cell is the mean of the 6 ensemble members. Decreasing (increasing) values indicate a trend towards drier (wetter) conditions.

Figure 4: Projected Aridity Index

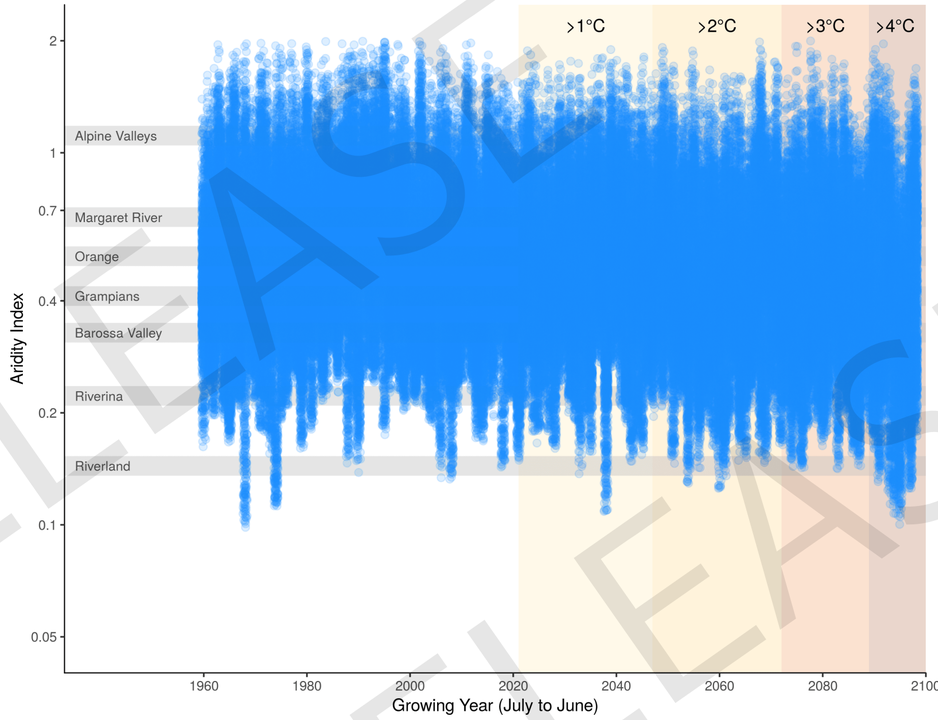

Figure 4: Time series of annual Aridity Index. Points are the annual means for each grid cell in the region, for each of the 6 ensemble members. Aridity Index values >2 all indicate very wet conditions. There is no meaningful difference past this value, so higher values were not presented. Horizontal grey bars represent the mean annual Aridity Index from selected regions across Australia — these provide an example of conditions this region may transition towards in the future. Coloured bars represent the projected global temperature increase expected in the future (following the RCP 8.5 scenario) which can be used to make decisions based on *projected temperature change* rather than *time* (for example, if the rate of warming rapidly increases, where temperature changes are experienced earlier, useful information can still be extracted from these figures by using the coloured boxes instead of the time-axis).

Figure 5: Projected monthly Aridity Index

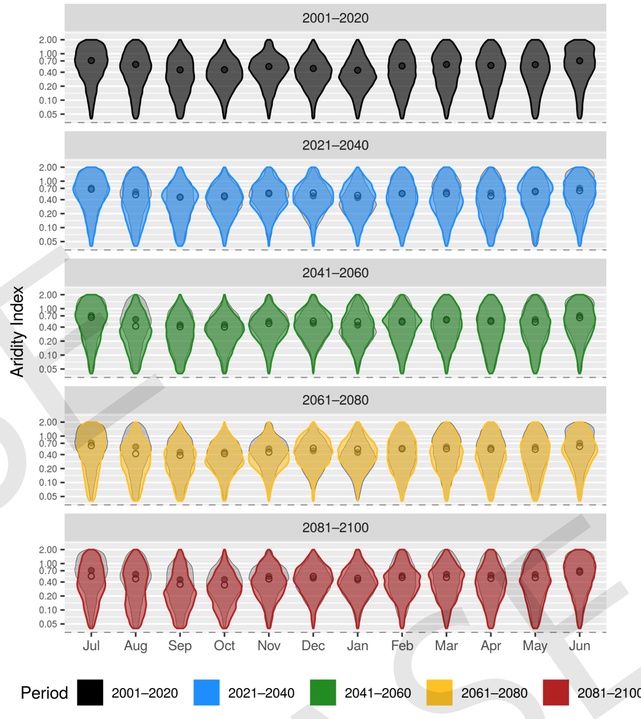

Figure 5: *Violin plots* of monthly Aridity Index for 20-year time periods from 2001 to 2100. Each violin represents monthly averages for each grid cell, for each of the 6 ensemble members, and for each growing year within the time period. In each 20-year panel the violins indicate the expected probability distribution of Aridity Index within each month across the growing year. The current period (2001–2020) is shadowed underneath the future time periods to highlight any differences expected into the future. Dots represent the mean monthly Aridity Index for each violin. If the violin shifts lower (higher) this indicates a change towards drier (wetter) conditions.

Figure 6: Distribution of seasonal Aridity Index

Figure 6: Seasonal Aridity Index (Winter, Spring, Summer, Autumn), presented as a probability distribution for each 20-year period. The shape of the curve is driven by the level of variability experienced within each 20-year period. Variability can occur spatially within the region, across years, or between ensemble members. Grey shapes represent the probability distribution of seasonal aridity for contrasting regions during 1997–2017. Differences in the shape of curves between the current and future periods indicate a change in the typical conditions. A shift to the left (right) indicates an increase in drier (wetter) conditions. Aridity Index values >2 all indicate very wet conditions.

Figure 7: Distribution of mean Aridity Index from July until harvest

Figure 7: Mean annual Aridity Index accumulated from start of the growing season (July) to *date of harvest*, presented as a probability distribution for each 20-year period. *Date of harvest* refers to the date at which *Growing Degree Days* reach some example phenological thresholds (1000, 1500, 2000, 2500), chosen to reflect development time of different grape styles and varieties. Variability can occur spatially within the region, across years, or between ensemble members. A shift to the left (right) indicates drier (wetter) conditions. A missing time period indicates that the specific phenological threshold was not reached within the growing year (July–June).

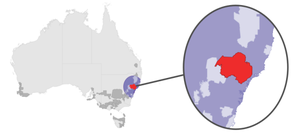

Figure 1: Observed mean Excess Heat Factor

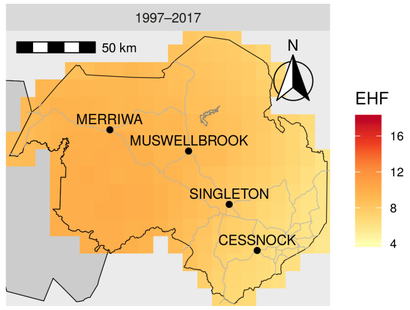

Figure 2: Observed change in mean Excess Heat Factor

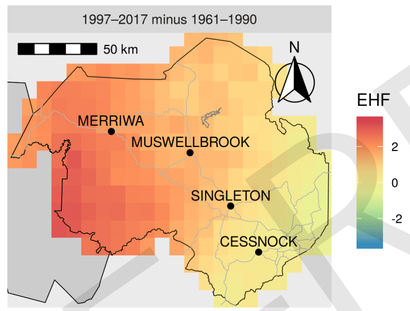

Figure 3: Projected mean Excess Heat Factor

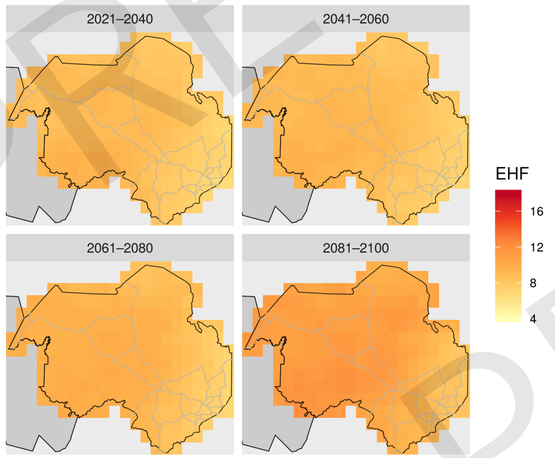

Figure 1: Observed mean *excess heat factor* (EHF) during heatwaves (as per Nairn and Fawcett (2013)), across all growing years from 1997–2017. EHF is an index that characterises heatwaves, high values indicate more intense heatwaves. The mean EHF is the mean value from all heatwaves that occurred from 1997–2017.

Figure 2: Change in mean EHF during heatwaves between the current (1997–2017) and historical (1961–1990) periods. Positive (negative) values indicate a trend towards more (less) intense heatwaves.

Figure 3: Projected mean EHF during heatwaves for 20-year time periods from 2021 to 2100. Each grid cell is the mean of the 6 ensemble members. Increasing (decreasing) values indicate a trend towards more (less) intense heatwaves.

Figure 4: Projected mean number of extreme heat days

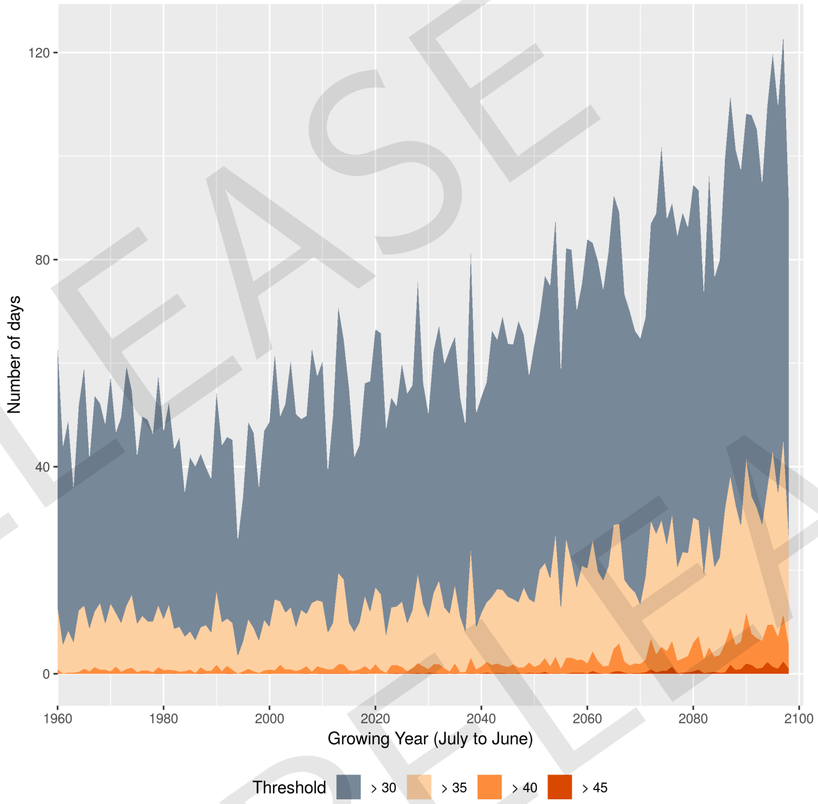

Figure 5: Projected number of days with severe risk to humans working outside

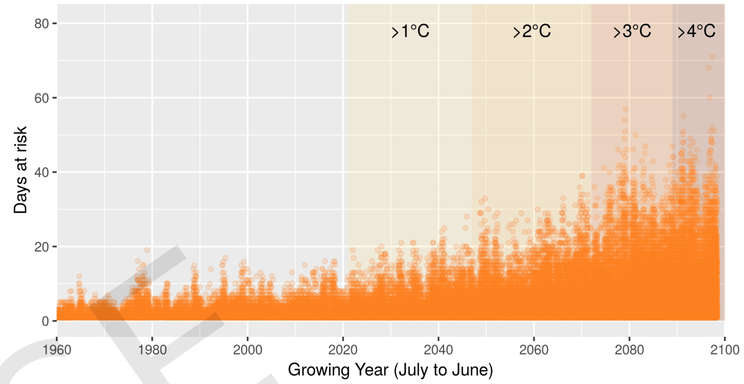

Figure 6: Projected range of hot summer days

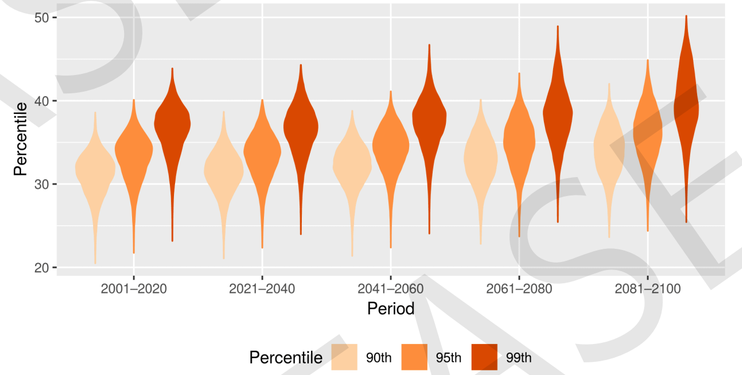

Figure 4: Time series of the number of days per growing year with temperatures greater than 30°C, 35°C, 40°C and 45°C. Areas indicate the number of days each threshold is exceeded per growing year. Values are averaged across all grid cells and the 6 ensemble members. Colours indicate each of the extreme threshold values. Generally increasing frequencies reflect a warming climate.

Figure 5: Time series of the number of days per growing year of *High human heat stress*. This is defined as days when daily maximum temperatures are >30°C and daily minimum humidity is >60%. These conditions cause severe risk of heat stress to humans (and potentially low productivity) to those working in exposed areas. Humans cannot work in high temperature, high humidity environments without appropriate adaptive behaviours and equipment. Points are for each grid cell from each of the 6 ensemble members. Coloured bars represent the projected global temperature increase expected into the future (following the RCP 8.5 scenario) which can be used to make decisions based on *projected temperature change* rather than *time*.

Figure 6: *Violins plots* of high temperatures (°C) per growing year for 20-year time periods from 2001 to 2100. Colours indicate extreme threshold values (90^{th}, 95^{th} and 99^{th} percentile) of temperature during each growing year. The 99^{th} percentile value reflects the 4^{th} hottest day each growing year; the 95^{th} percentile is the 18^{th} hottest day each growing year; and the 90^{th} percentile is the 36^{th} hottest day each growing 1year. Generally increasing values reflect a warming climate.

Figure 7: Distribution of daily minimum and maximum temperature during a heatwave

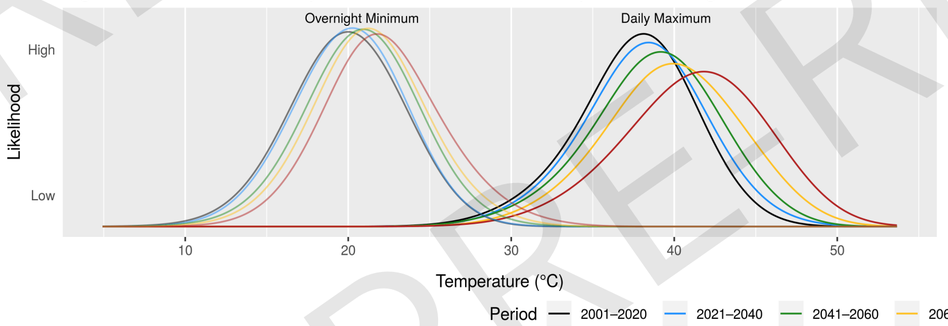

Figure 8: Distribution of date of heatwave days

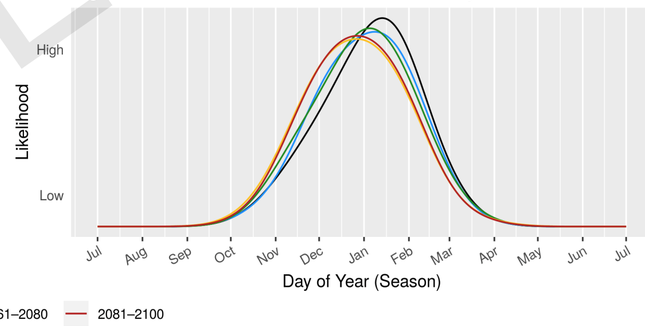

Figure 7: Probability distributions of daily maximum temperatures and minimum overnight temperatures during heatwaves. Colour of each curve indicates different 20-year periods. The shape of the curve is driven by the level of variability experienced within each 20-year period. Variability can occur spatially within the region, across years, or between ensemble members. A shift to the right (left) indicates higher (lower) temperature heatwaves.

Figure 8: Probability distribution of the date when heatwaves occur. The shape of the curve is driven by the level of variability experienced within each 20-year period. Variability can occur spatially within the region, across years, or between ensemble members. A shift to the left (right) indicates heatwaves occurring earlier (later).

HUNTER

Extremes — Cold

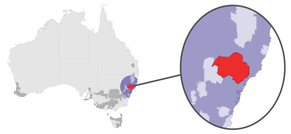

Figure 1: Observed mean frost risk days

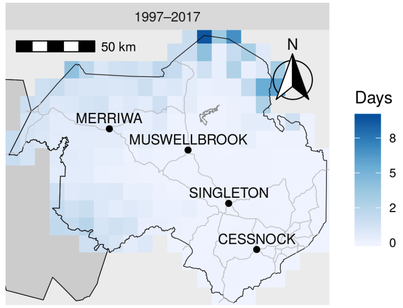

Figure 2: Observed change in mean frost risk days

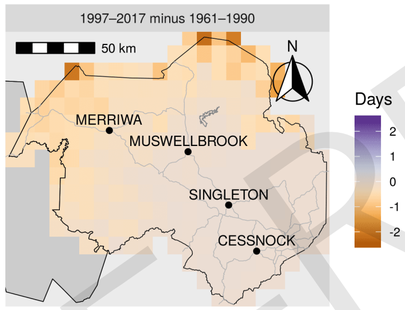

Figure 3: Projected mean frost risk days

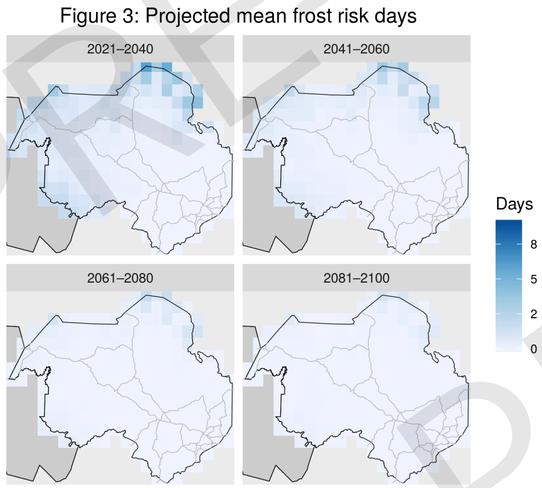

Figure 1: Observed mean number of days at risk of frost during the growing season (October to April) over the period 1997–2017. Days at risk of frost are those with a daily minimum temperature <2°C. High (low) values indicate high (low) frost risk.

Figure 2: Change in the mean number of days at risk of frost during the growing season (October to April) between the current (1997–2017) and historical (1961–1990) periods. Days at risk of frost are days with a minimum temperature <2°C. High (low) values indicate increased (decreased) frost risk.

Figure 3: Projected mean number of days at risk of frost during the growing season (October to April) for 20-year time periods from 2021 to 2100. Each grid cell is the mean of the 6 ensemble members. Increasing (decreasing) values indicate a trend towards higher (lower) frost risk.

Figure 4: Projected monthly minimum temperature

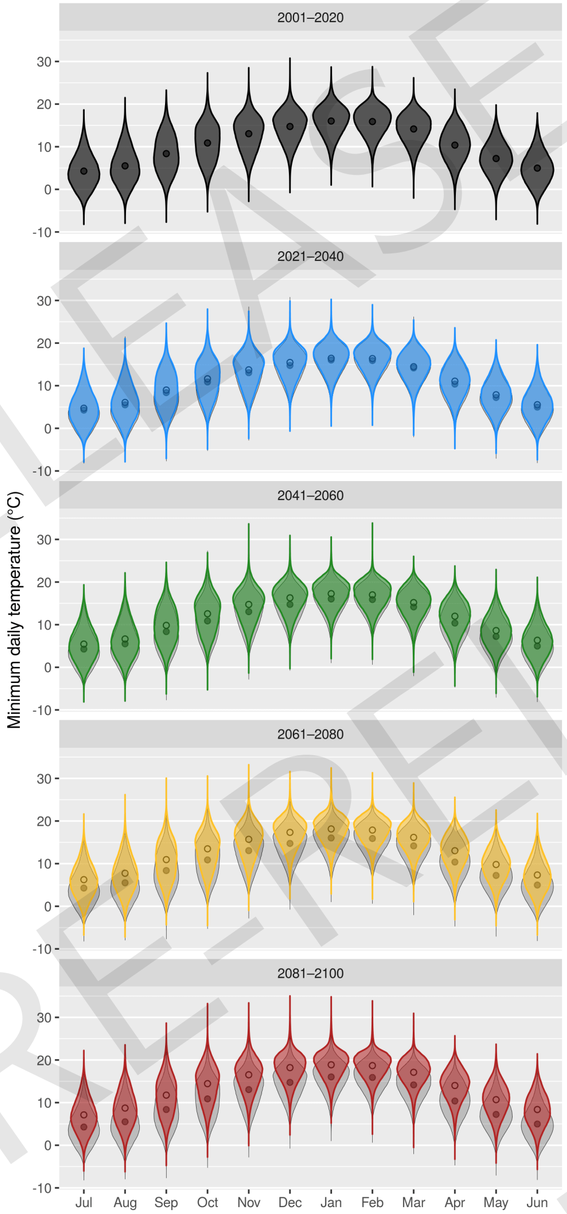

Figure 4: *Violin plots* of daily minimum temperature (°C) for each month for 20-year periods from 2001 to 2100. Each violin represents daily data for each grid cell, for each of the 6 ensemble members, and for each growing year within the time period; e.g. the top-left most violin represents the daily minimum temperature for every January day in the period 2001–2020, for each grid cell in the region, for each of the 6 ensemble members. The current period (2001-2020) has been shadowed underneath future time periods to highlight any differences expected into the future. Dots represent the means for each violin. If the violin shifts lower (higher) this indicates a change towards colder (warmer) conditions.

Figure 5: Projected monthly frost risk days

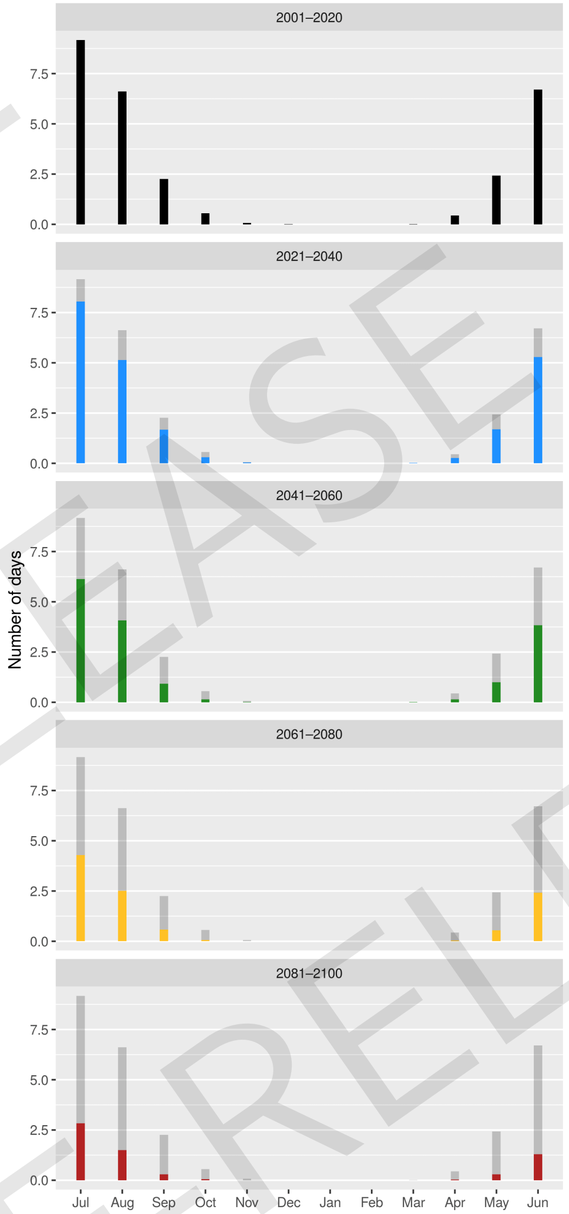

Figure 5: Monthly average cumulative frost days for 20-year periods from 2001 to 2100. Values are a summary across all grid cells, for all years with each 20-year period, for each of the 6 ensemble members. This reflects how frost risk varies across the year within each 20-year period. The current period (2001–2020) has been shadowed underneath future time periods to highlight any differences expected into the future.

Figure 6: Projected accumulated frost intensity

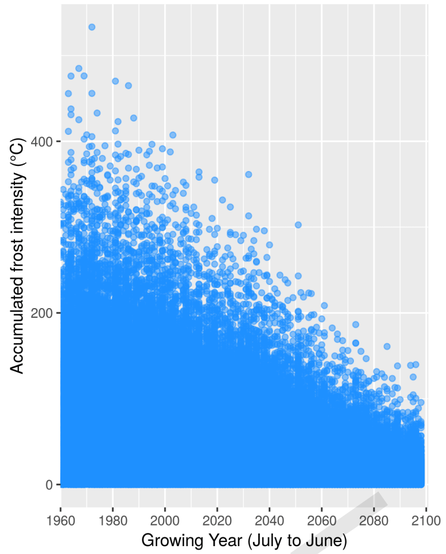

Figure 7: Projected mean number of extreme cold days

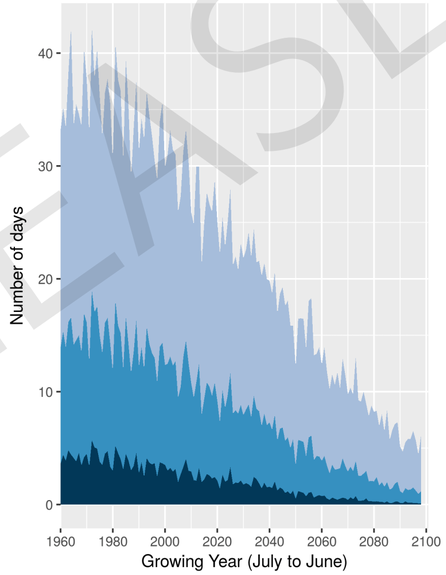

Figure 6: Timeseries of accumulated frost intensity, which is the cumulative total of temperatures less than 2°C over a growing season. This index characterises exposure to cold conditions. High values indicate cold winters/springs. Points are for each grid cell, averaged across the 6 ensemble members.

Figure 7: Time series of the number of days per growing year when temperature falls below selected thresholds (<2°C, <0°C, <-2°C). Areas indicate the number of days temperatures fall below each threshold per growing year. Values are averaged across all grid cells and the 6 ensemble members. Fewer instances reflect a warming climate.

AUSTRALIA'S WINE FUTURE
A CLIMATE ATLAS

RIVERINA

RAINFALL

Projected Mean Growing Season Rainfall

1997–2017	2041–2060	2081–2100
228 mm	233 mm	223 mm

TEMPERATURE

Projected Mean Growing Season Temperature

1997–2017	2041–2060	2081–2100
21.8 °C	23.3 °C	25.3 °C

EXTREME COLD

Projected Mean Growing Season Frost Risk Days

1997–2017	2041–2060	2081–2100
0.7 days	0.1 days	0.0 days

EXTREME HEAT

Projected Mean Excess Heat Factor

1997–2017	2041–2060	2081–2100
14.4 EHF	15.3 EHF	15.2 EHF

ARIDITY

Projected Mean Annual Aridity Index

1997–2017	2041–2060	2081–2100
0.22	0.19	0.16

Wine Australia

ACE CRC ANTARCTIC CLIMATE & ECOSYSTEMS COOPERATIVE RESEARCH CENTRE

climatefutures

UNIVERSITY of TASMANIA

RIVERINA

Heat

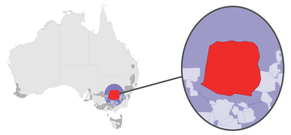

Figure 1: Observed mean Growing Season Temperature

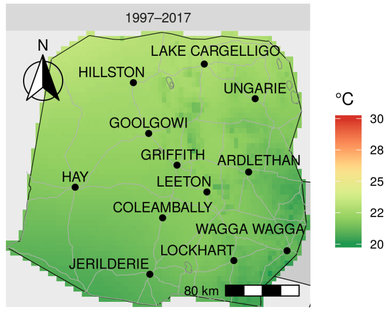

Figure 2: Observed change in mean Growing Season Temperature

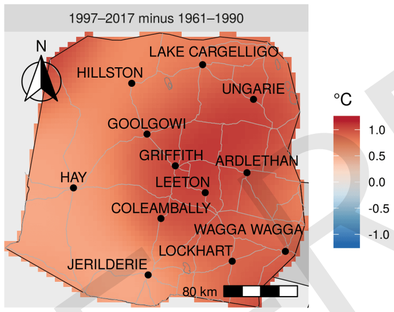

Figure 3: Projected mean Growing Season Temperature

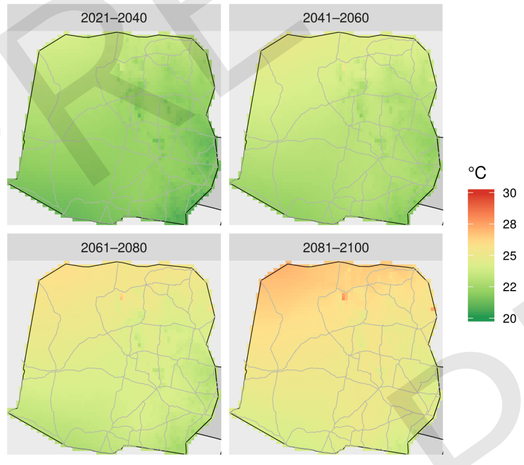

Figure 1: Observed mean *Growing Season Temperature* (Oct–Apr) across all growing years from 1997–2017.

Figure 2: The change in *Growing Season Temperature* between the current (1997–2017) and historical (1961–1990) periods. *Growing Season Temperature* has increased across the region over recent decades.

Figure 3: Projected mean *Growing Season Temperature* (Oct–Apr) for 20-year time periods from 2021 to 2100. *Growing Season Temperature* is expected to increase steadily into the future. Each grid cell is the mean of the 6 ensemble members.

Figure 4: Projected Growing Season Temperature (October to April)

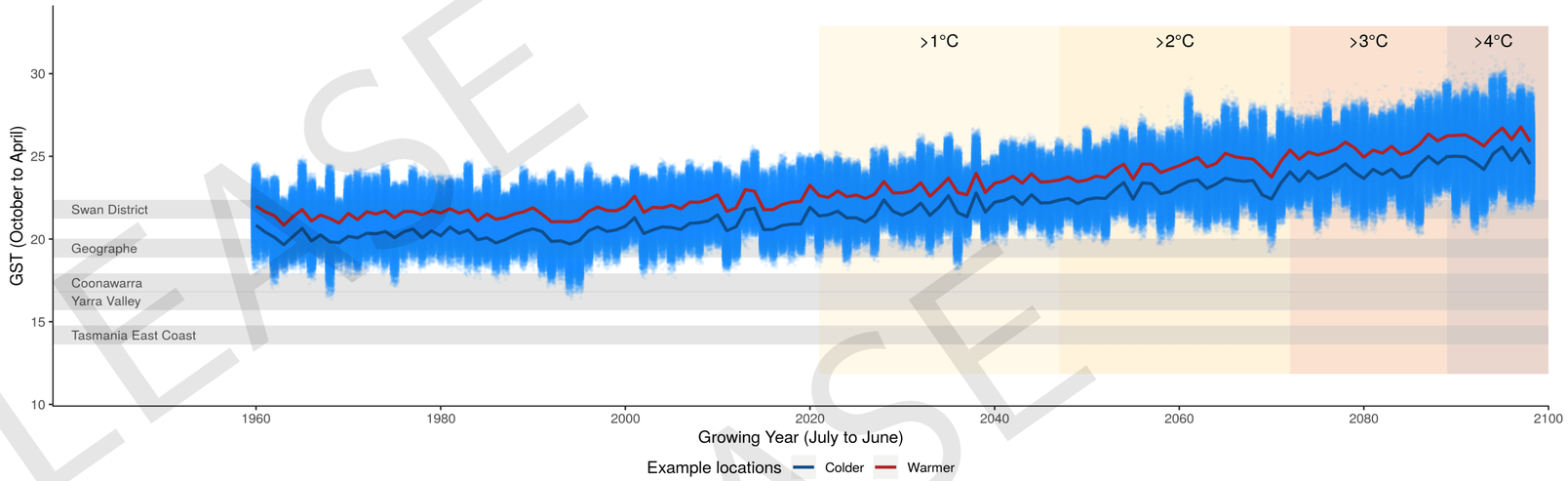

Figure 4: *Growing Season Temperature* (GST) over time. Blue points are the values for each grid cell, for each of the 6 ensemble members. Solid lines are timeseries representing grid cells for colder and warmer locations within the region based on current conditions (1997–2017). Horizontal grey bars represent the mean GST value during 1997–2017 in selected regions across Australia. These provide a comparison between current conditions elsewhere and future conditions in this region, helping to identify future analogue regions. Coloured bars represent the projected global temperature increase expected into the future (following the RCP 8.5 scenario). These can be used to make decisions based on *projected temperature change* rather than time (for example, if the rate of warming rapidly increases, useful information can still be extracted from these figures by using the shade boxes instead of the time-axis).

Figure 5: Distribution of Growing Season Temperature

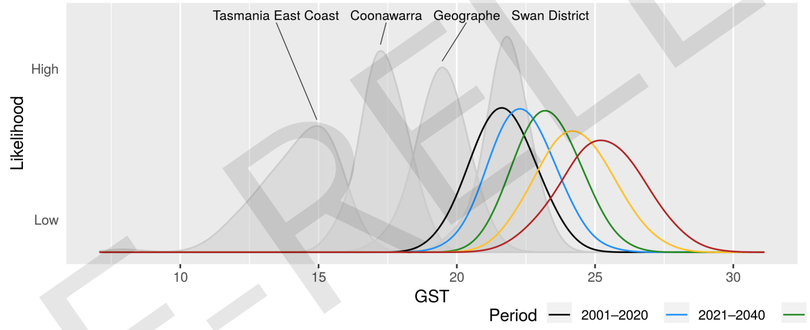

Figure 5: Probability distribution of GST for 20-year time periods from 2001 to 2100. Variability can occur spatially within the region, across years, or between ensemble members. Grey shapes represent the probability distribution of GST for contrasting regions during 1997–2017. A shift to the right (left) indicates warmer (cooler) conditions.

Figure 6: Distribution of Growing Degree Days

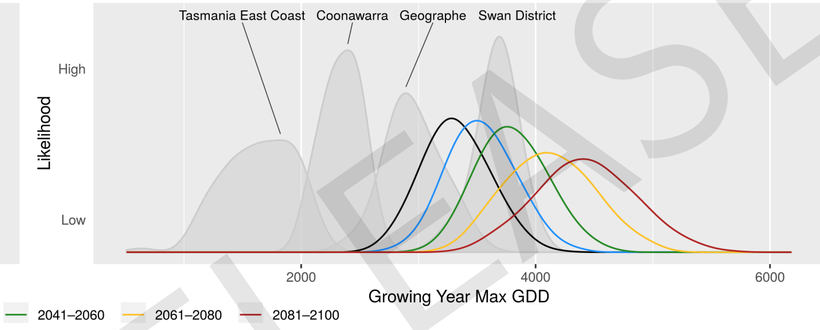

Figure 6: Probability distribution of growing year maximum GDD for 20-year time periods from 2001 to 2100. Variability can occur spatially within the region, across years, or between ensemble members. Grey shapes represent the probability distribution of growing year maximum GDD for contrasting regions during 1997–2017. A shift to the right (left) indicates warmer (cooler) conditions.

Figure 7: Projected cumulative Growing Degree Days

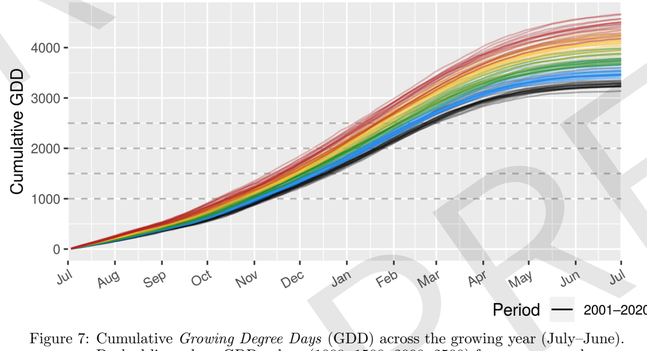

Figure 7: Cumulative *Growing Degree Days* (GDD) across the growing year (July–June). Dashed lines show GDD values (1000, 1500, 2000, 2500) for some example phenological thresholds. Each growing year is represented by a coloured line. In future time periods, heat accumulates faster, thresholds are reached earlier and maximum GDD reached is higher.

Figure 8: Distribution of date when Growing Degree Days reaches threshold

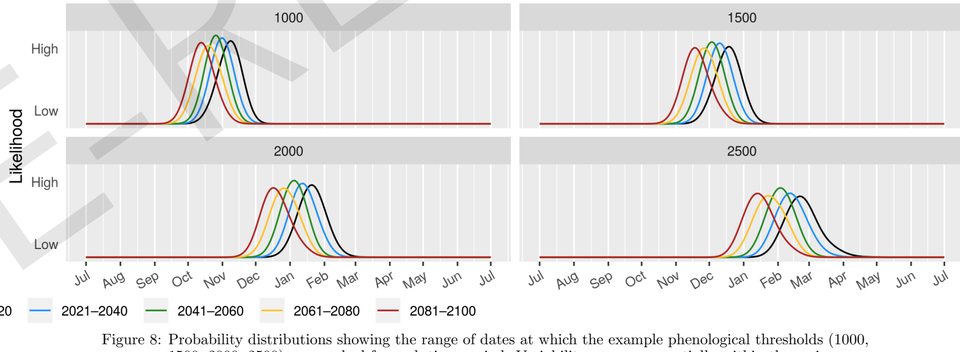

Figure 8: Probability distributions showing the range of dates at which the example phenological thresholds (1000, 1500, 2000, 2500) are reached for each time period. Variability can occur spatially within the region, across years, or between ensemble members. A shift to the left (right) indicates earlier (later) harvest dates. A wider (thinner) curve indicates a larger (smaller) range of harvest dates. A missing time period indicates that the specific phenological threshold was not reached within the growing year (July–June).

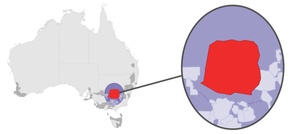

Figure 1: Observed mean Growing Season Rainfall

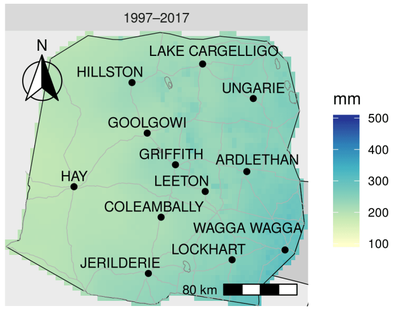

Figure 2: Observed change in mean Growing Season Rainfall

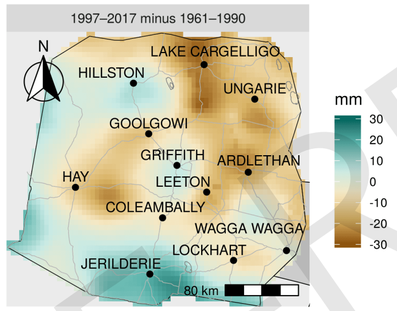

Figure 3: Projected mean Growing Season Rainfall

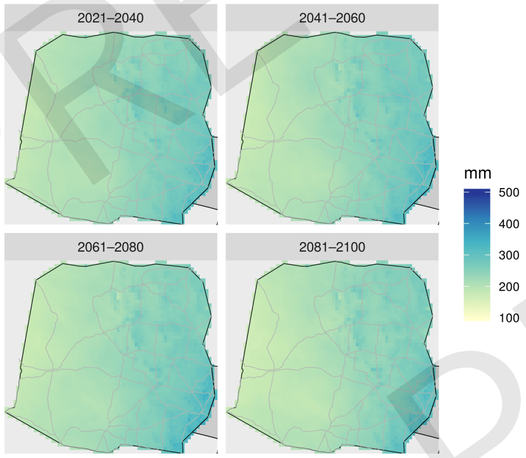

Figure 1: Observed mean *Growing Season Rainfall* (Oct–Apr) across all growing years from 1997–2017.

Figure 2: Change in *Growing Season Rainfall* (Oct–Apr) between the current (1997–2017) and historical (1961–1990) periods. Negative values indicate a trend towards drier conditions. Positive values indicate a trend towards wetter conditions.

Figure 3: Projected mean *Growing Season Rainfall* (Oct–Apr) for 20-year time periods from 2021 to 2100. Each grid cell is the mean of the 6 ensemble members.

Figure 4: Projected Growing Season Rainfall (October to April)

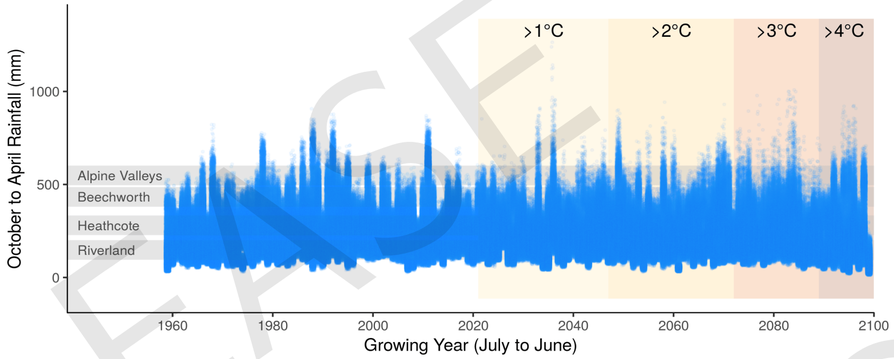

Figure 5: Projected Non-Growing Season Rainfall (May to September)

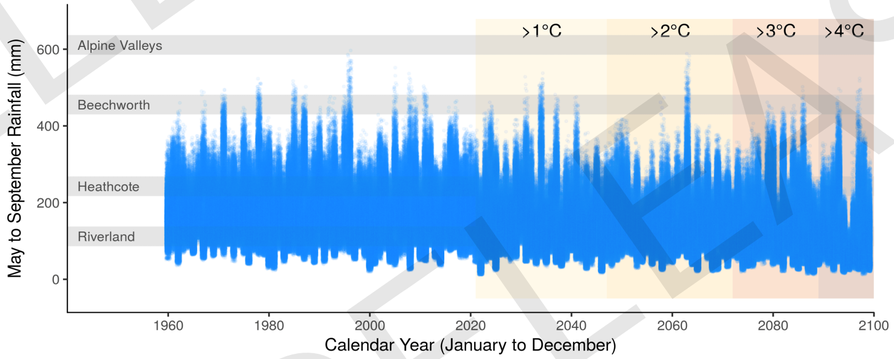

Figure 4: Time series of *Growing Season Rainfall* (mm). Blue points are the annual values for each grid cell, for each of the 6 ensemble members. Horizontal grey bars represent the mean *Growing Season Rainfall* value during 1997–2017 in selected regions across Australia. These provide a comparison between current conditions (1997–2017) elsewhere and future conditions in this region and help identify future analogue regions. Coloured bars represent the projected mean global temperature increase into the future (following the RCP 8.5 scenario). These can be used to make decisions based on *projected temperature change* rather than time.

Figure 5: As with Figure 4, but for *Non-Growing Season Rainfall* (mm). Horizontal grey bars represent the mean *Non-Growing Season Rainfall* value during 1997–2017 in selected regions across Australia.

Figure 6: Projected monthly rainfall

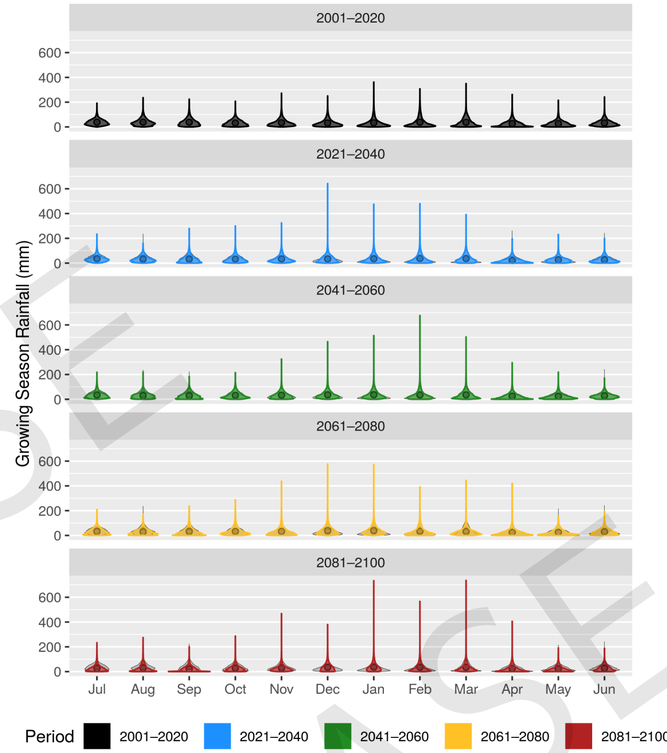

Figure 6: *Violin plots* of monthly rainfall (mm) for 20-year time periods from 2001 to 2100. Each violin represents monthly totals for each grid cell, for each of the 6 ensemble members, and for each growing year within the time period. In each panel the monthly violins indicate the expected probability distribution of rainfall across the growing year. The current period (2001–2020) is shadowed underneath the future time periods to highlight any differences expected into the future. Dots represent the mean monthly rainfall for each violin. If the violin shifts lower (higher) this indicates a change towards drier (wetter) conditions.

Figure 7: Distribution of seasonal rainfall

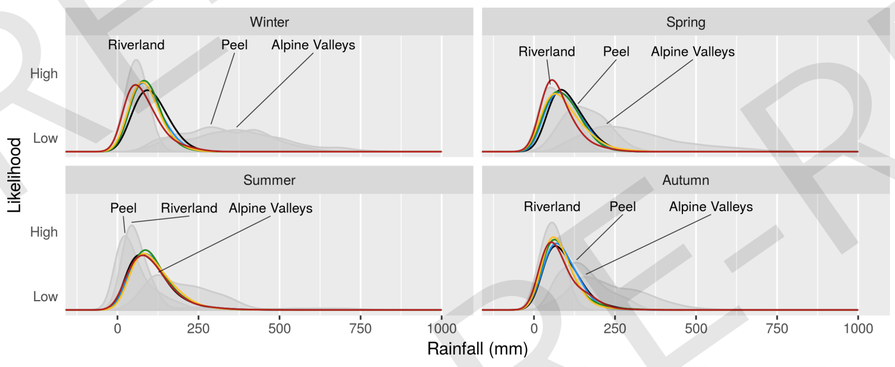

Figure 8: Distribution of number of rainy days during harvest

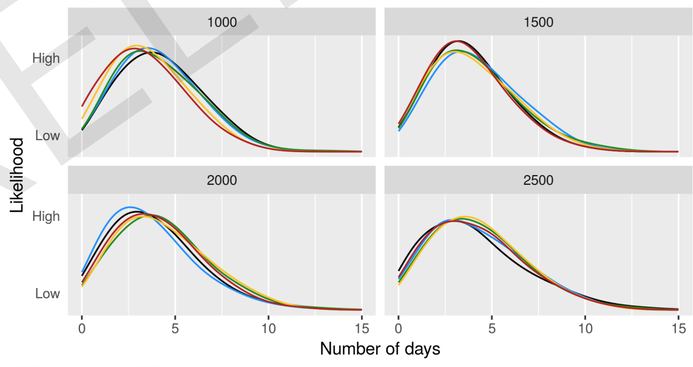

Figure 7: Seasonal rainfall (Winter, Spring, Summer, Autumn) (mm), presented as a probability distribution for each 20-year period. The shape of the curve is driven by the level of variability experienced within each 20-year period. Variability can occur spatially within the region, across years, or between ensemble members. Grey shapes represent the probability distribution of seasonal rainfall for contrasting regions during 1997–2017. Differences in the shape of curves between the current and future periods indicate a change in the typical conditions. A shift to the left (right) indicates an increase in drier (wetter) conditions.

Figure 8: Number of rainy days during harvest for each 20-year period. *Harvest* refers to the date when *Growing Degree Days* (GDD) reach example phenological thresholds (1000, 1500, 2000, 2500) which were chosen to reflect development time of different grape styles and varieties. Rainy days during harvest were defined as days with >10mm of rain from 7 days before to 7 days after the date each GDD threshold was reached. Variability can occur spatially within the region, across years, or between ensemble members. A shift in the curve to the left (right) indicates fewer (more) rainy days during harvest. A missing time period indicates that the specific phenological threshold was not reached within the growing year (July–June).

RIVERINA

Aridity

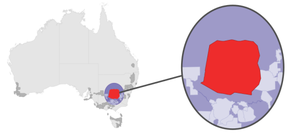

Figure 1: Observed mean annual Aridity Index

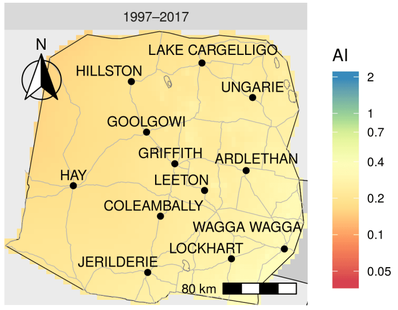

Figure 2: Obseved change in mean annual Aridity Index

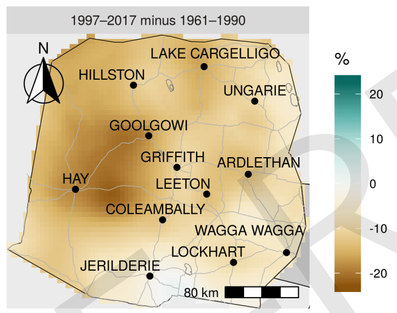

Figure 3: Projected mean annual Aridity Index

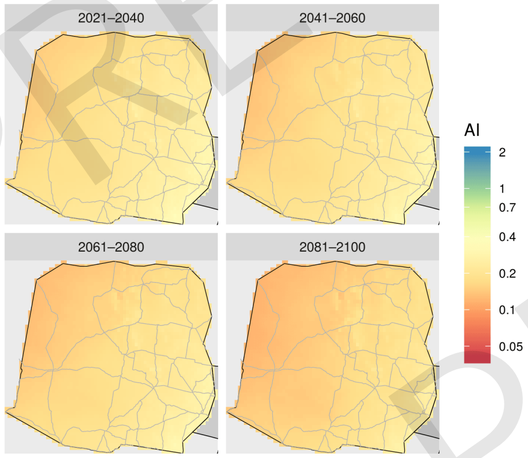

Figure 1: Observed mean annual Aridity Index across all growing years from 1997–2017. Aridity Index is a value that characterises the ratio between the mean annual rainfall and mean annual evaporation. Low (high) values indicate drier (wetter) conditions.

Figure 2: Observed percentage change in mean annual Aridity Index between the current (1997–2017) and historical (1961–1990) periods. This shows the change already experienced across the region. Negative (positive) values indicate a trend towards drier (wetter) conditions.

Figure 3: Projected mean annual Aridity Index for 20-year time periods from 2021 to 2100. Each grid cell is the mean of the 6 ensemble members. Decreasing (increasing) values indicate a trend towards drier (wetter) conditions.

Figure 4: Projected Aridity Index

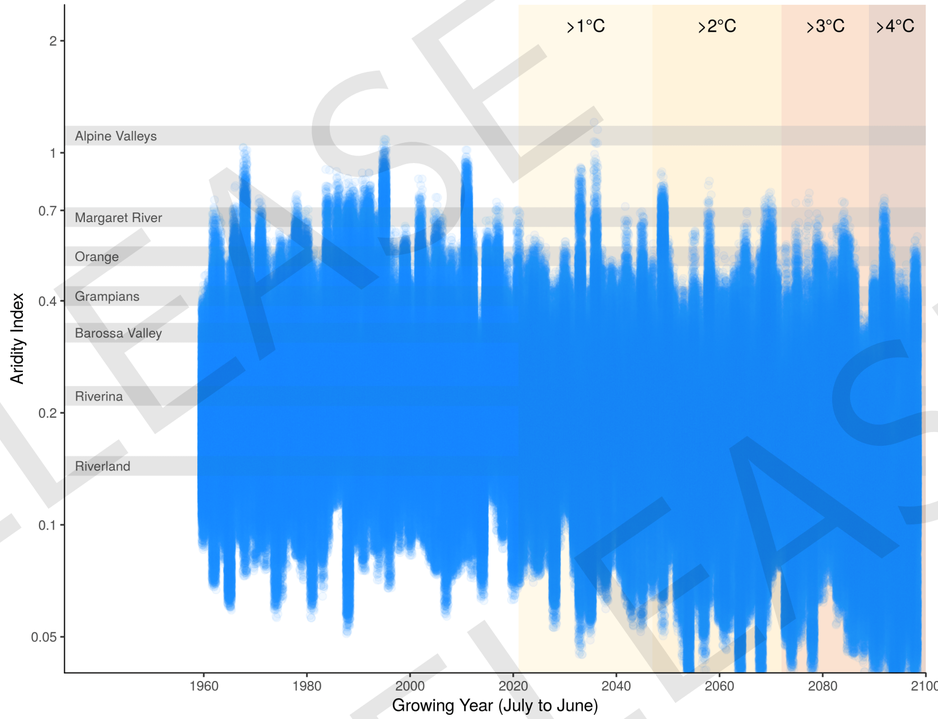

Figure 4: Time series of annual Aridity Index. Points are the annual means for each grid cell in the region, for each of the 6 ensemble members. Aridity Index values >2 all indicate very wet conditions. There is no meaningful difference past this value, so higher values were not presented. Horizontal grey bars represent the mean annual Aridity Index from selected regions across Australia — these provide an example of conditions this region may transition towards in the future. Coloured bars represent the projected global temperature increase expected in the future (following the RCP 8.5 scenario) which can be used to make decisions based on *projected temperature change* rather than *time* (for example, if the rate of warming rapidly increases, where temperature changes are experienced earlier, useful information can still be extracted from these figures by using the coloured boxes instead of the time-axis).

Figure 5: Projected monthly Aridity Index

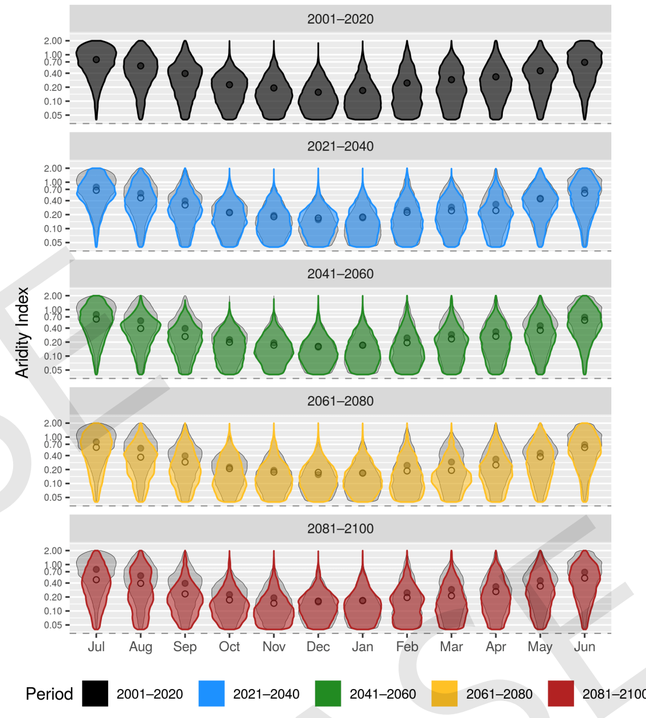

Figure 5: *Violin plots* of monthly Aridity Index for 20-year time periods from 2001 to 2100. Each violin represents monthly averages for each grid cell, for each of the 6 ensemble members, and for each growing year within the time period. In each 20-year panel the violins indicate the expected probability distribution of Aridity Index within each month across the growing year. The current period (2001–2020) is shadowed underneath the future time periods to highlight any differences expected into the future. Dots represent the mean monthly Aridity Index for each violin. If the violin shifts lower (higher) this indicates a change towards drier (wetter) conditions.

Figure 6: Distribution of seasonal Aridity Index

Figure 6: Seasonal Aridity Index (Winter, Spring, Summer, Autumn), presented as a probability distribution for each 20-year period. The shape of the curve is driven by the level of variability experienced within each 20-year period. Variability can occur spatially within the region, across years, or between ensemble members. Grey shapes represent the probability distribution of seasonal aridity for contrasting regions during 1997–2017. Differences in the shape of curves between the current and future periods indicate a change in the typical conditions. A shift to the left (right) indicates an increase in drier (wetter) conditions. Aridity Index values >2 all indicate very wet conditions.

Figure 7: Distribution of mean Aridity Index from July until harvest

Figure 7: Mean annual Aridity Index accumulated from start of the growing season (July) to *date of harvest*, presented as a probability distribution for each 20-year period. *Date of harvest* refers to the date at which *Growing Degree Days* reach some example phenological thresholds (1000, 1500, 2000, 2500), chosen to reflect development time of different grape styles and varieties. Variability can occur spatially within the region, across years, or between ensemble members. A shift to the left (right) indicates drier (wetter) conditions. A missing time period indicates that the specific phenological threshold was not reached within the growing year (July–June).

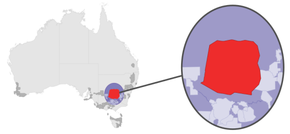

Figure 1: Observed mean Excess Heat Factor

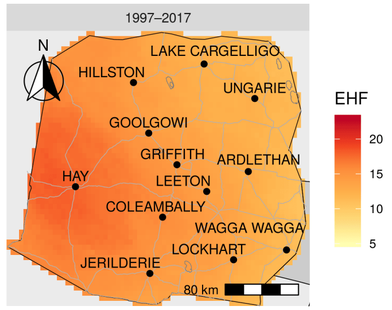

Figure 2: Observed change in mean Excess Heat Factor

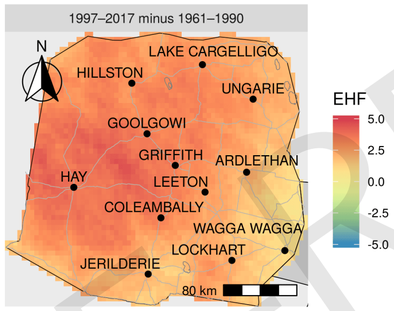

Figure 3: Projected mean EHF during heatwaves for 20-year time periods from 2021 to 2100. Each grid cell is the mean of the 6 ensemble members. Increasing (decreasing) values indicate a trend towards more (less) intense heatwaves.

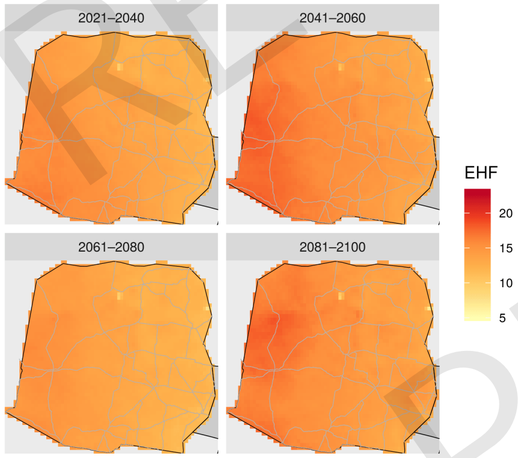

Figure 1: Observed mean *excess heat factor* (EHF) during heatwaves (as per Nairn and Fawcett (2013)), across all growing years from 1997–2017. EHF is an index that characterises heatwaves, high values indicate more intense heatwaves. The mean EHF is the mean value from all heatwaves that occurred from 1997–2017.

Figure 2: Change in mean EHF during heatwaves between the current (1997–2017) and historical (1961–1990) periods. Positive (negative) values indicate a trend towards more (less) intense heatwaves.

Figure 4: Projected mean number of extreme heat days

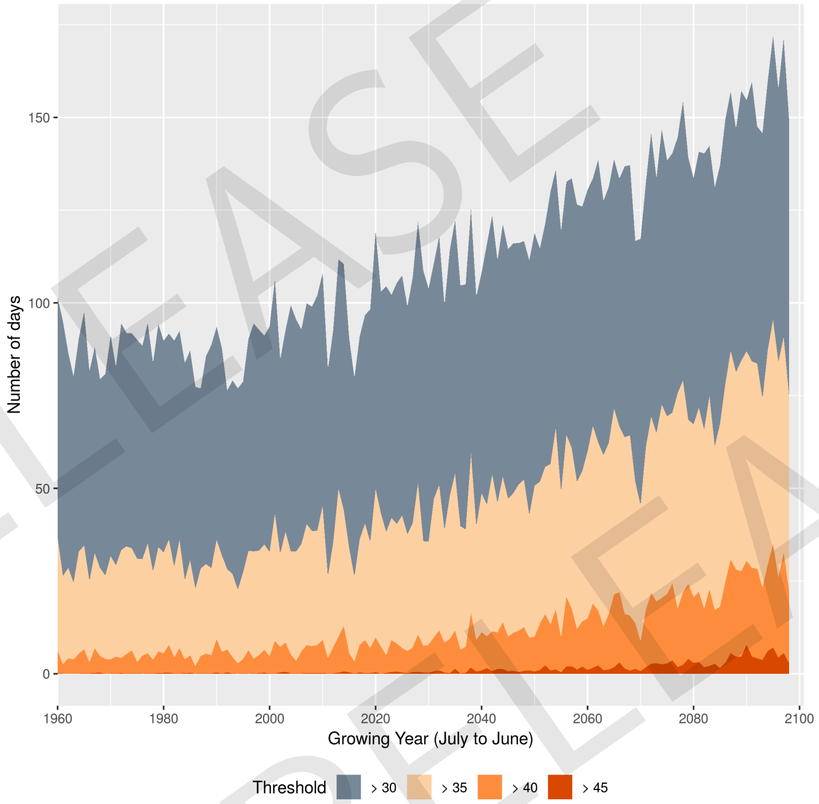

Figure 5: Projected number of days with severe risk to humans working outsid

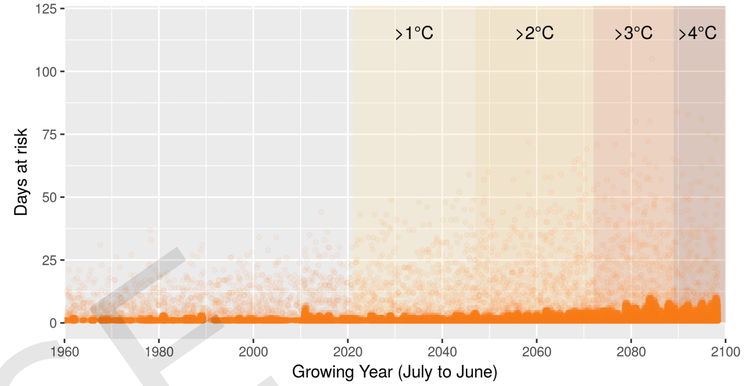

Figure 6: Projected range of hot summer days

Figure 4: Time series of the number of days per growing year with temperatures greater than 30°C, 35°C, 40°C and 45°C. Areas indicate the number of days each threshold is exceeded per growing year. Values are averaged across all grid cells and the 6 ensemble members. Colours indicate each of the extreme threshold values. Generally increasing frequencies reflect a warming climate.

Figure 5: Time series of the number of days per growing year of *High human heat stress*. This is defined as days when daily maximum temperatures are >30°C and daily minimum humidity is >60%. These conditions cause severe risk of heat stress to humans (and potentially low productivity) to those working in exposed areas. Humans cannot work in high temperature, high humidity environments without appropriate adaptive behaviours and equipment. Points are for each grid cell from each of the 6 ensemble members. Coloured bars represent the projected global temperature increase expected into the future (following the RCP 8.5 scenario) which can be used to make decisions based on *projected temperature change* rather than *time*.

Figure 6: *Violins plots* of high temperatures (°C) per growing year for 20-year time periods from 2001 to 2100. Colours indicate extreme threshold values (90^{th}, 95^{th} and 99^{th} percentile) of temperature during each growing year. The 99^{th} percentile value reflects the 4^{th} hottest day each growing year; the 95^{th} percentile is the 18^{th} hottest day each growing year; and the 90^{th} percentile is the 36^{th} hottest day each growing 1year. Generally increasing values reflect a warming climate.

Figure 7: Distribution of daily minimum and maximum temperature during a heatwave

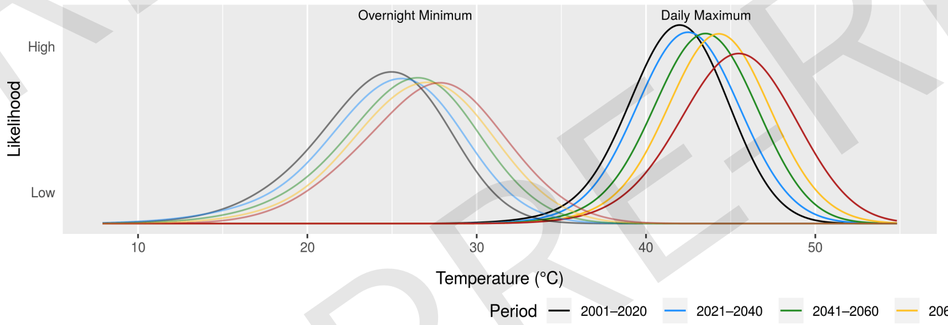

Figure 8: Distribution of date of heatwave days

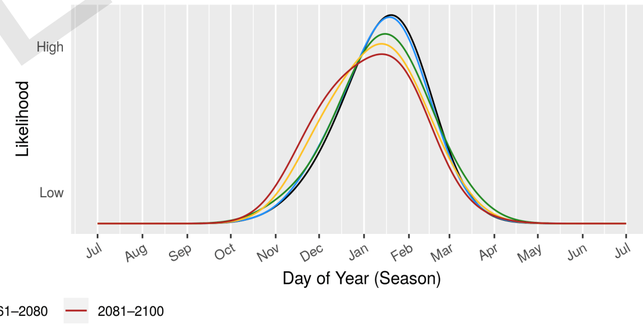

Figure 7: Probability distributions of daily maximum temperatures and minimum overnight temperatures during heatwaves. Colour of each curve indicates different 20-year periods. The shape of the curve is driven by the level of variability experienced within each 20-year period. Variability can occur spatially within the region, across years, or between ensemble members. A shift to the right (left) indicates higher (lower) temperature heatwaves.

Figure 8: Probability distribution of the date when heatwaves occur. The shape of the curve is driven by the level of variability experienced within each 20-year period. Variability can occur spatially within the region, across years, or between ensemble members. A shift to the left (right) indicates heatwaves occurring earlier (later).

RIVERINA

Extremes — Cold

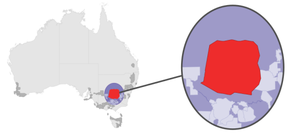

Figure 1: Observed mean frost risk days

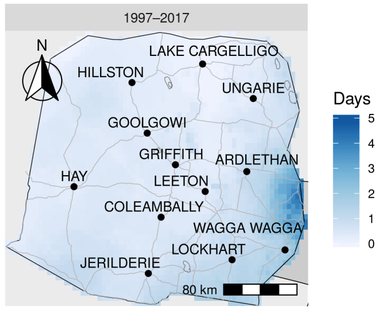

Figure 2: Observed change in mean frost risk days

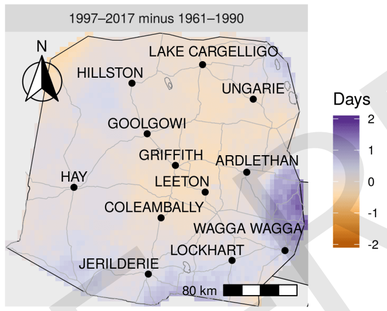

Figure 3: Projected mean frost risk days

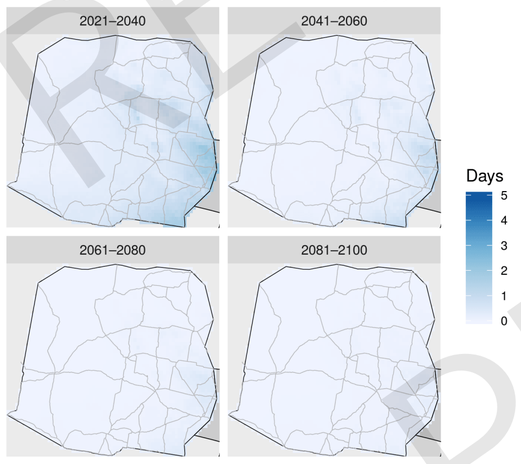

Figure 1: Observed mean number of days at risk of frost during the growing season (October to April) over the period 1997–2017. Days at risk of frost are those with a daily minimum temperature <2°C. High (low) values indicate high (low) frost risk.

Figure 2: Change in the mean number of days at risk of frost during the growing season (October to April) between the current (1997–2017) and historical (1961–1990) periods. Days at risk of frost are days with a minimum temperature <2°C. High (low) values indicate increased (decreased) frost risk.

Figure 3: Projected mean number of days at risk of frost during the growing season (October to April) for 20-year time periods from 2021 to 2100. Each grid cell is the mean of the 6 ensemble members. Increasing (decreasing) values indicate a trend towards higher (lower) frost risk.

Figure 4: Projected monthly minimum temperature

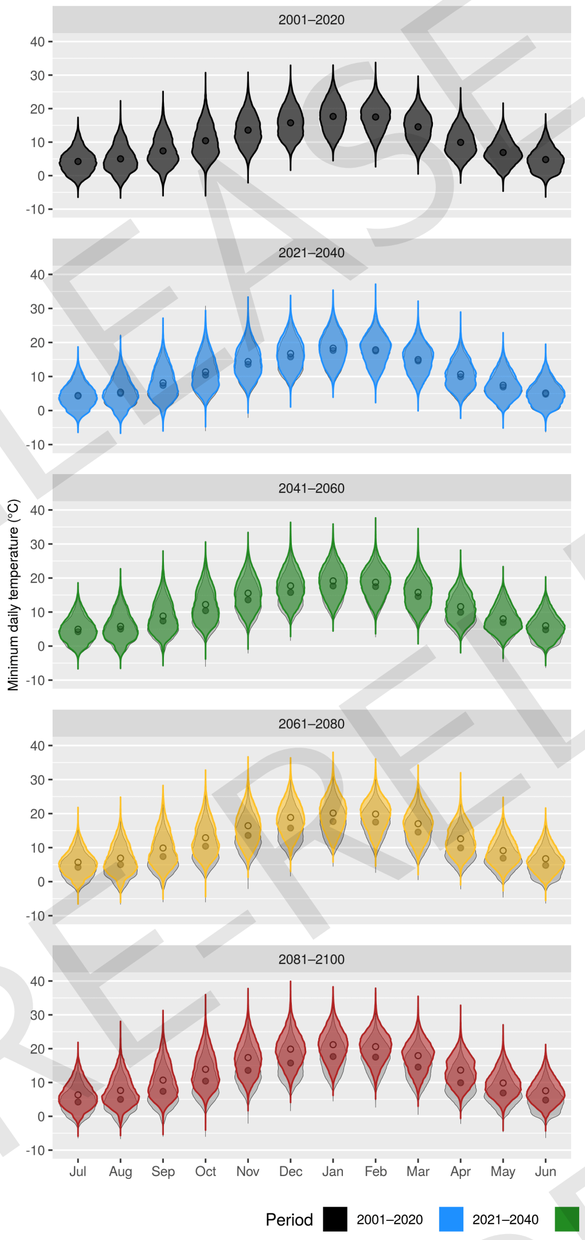

Figure 5: Projected monthly frost risk days

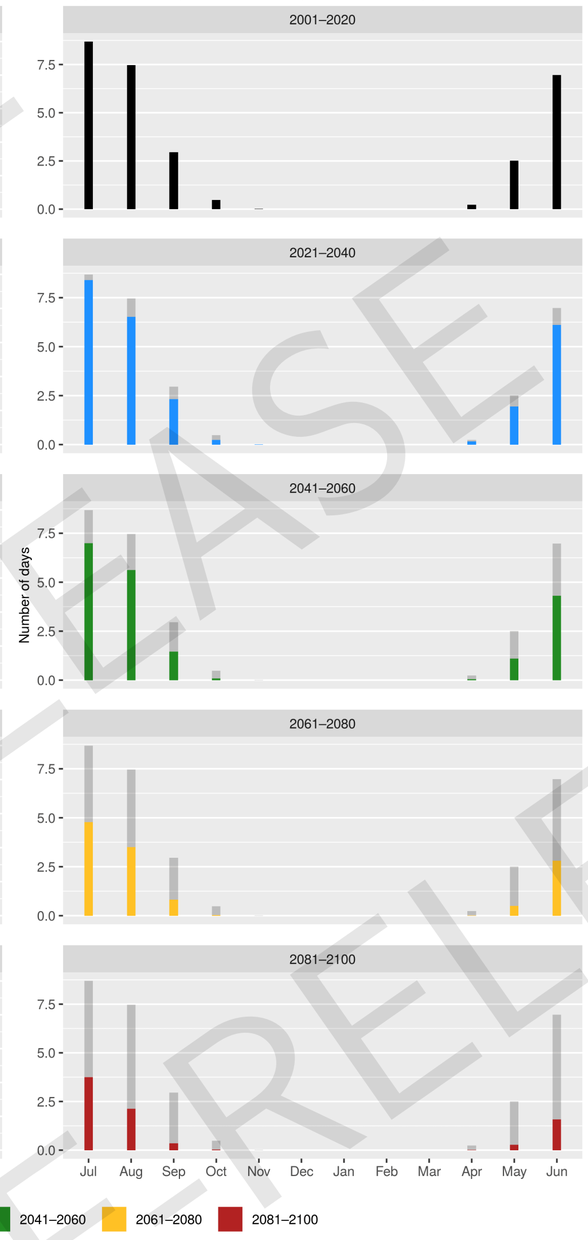

Figure 6: Projected accumulated frost intensity

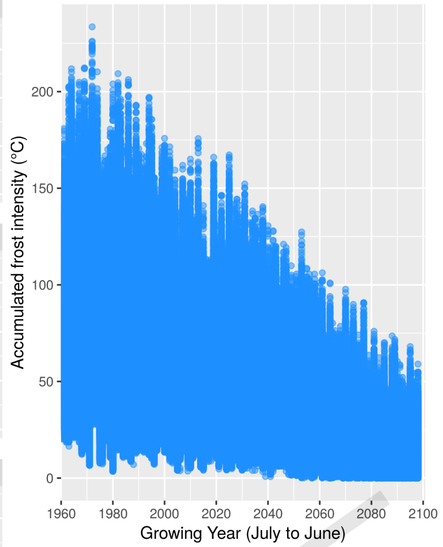

Figure 7: Projected mean number of extreme cold days

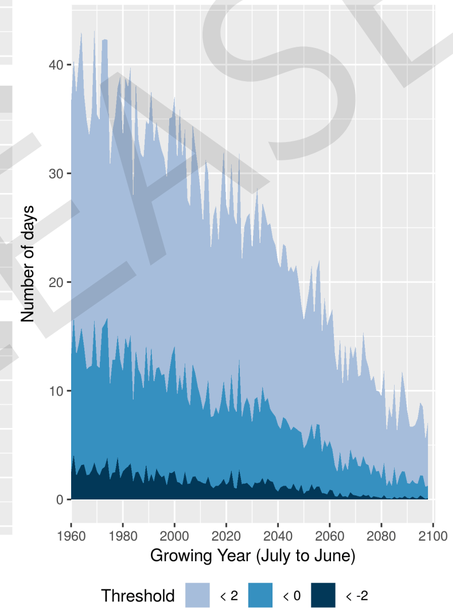

Figure 4: *Violin plots* of daily minimum temperature (°C) for each month for 20-year periods from 2001 to 2100. Each violin represents daily data for each grid cell, for each of the 6 ensemble members, and for each growing year within the time period; e.g. the top-left most violin represents the daily minimum temperature for every January day in the period 2001–2020, for each grid cell in the region, for each of the 6 ensemble members. The current period (2001-2020) has been shadowed underneath future time periods to highlight any differences expected into the future. Dots represent the means for each violin. If the violin shifts lower (higher) this indicates a change towards colder (warmer) conditions.

Figure 5: Monthly average cumulative frost days for 20-year periods from 2001 to 2100. Values are a summary across all grid cells, for all years with each 20-year period, for each of the 6 ensemble members. This reflects how frost risk varies across the year within each 20-year period. The current period (2001–2020) has been shadowed underneath future time periods to highlight any differences expected into the future.

Figure 6: Timeseries of accumulated frost intensity, which is the cumulative total of temperatures less than 2°C over a growing season. This index characterises exposure to cold conditions. High values indicate cold winters/springs. Points are for each grid cell, averaged across the 6 ensemble members.

Figure 7: Time series of the number of days per growing year when temperature falls below selected thresholds (<2°C, <0°C, <-2°C). Areas indicate the number of days temperatures fall below each threshold per growing year. Values are averaged across all grid cells and the 6 ensemble members. Fewer instances reflect a warming climate.

Part II

Methods and Interpretation

General background information

The difference between weather and climate

Weather describes what is happening in the atmosphere on a day-to-day basis or at a specific time, while climate describes the chance of experiencing particular kinds of weather at a specific location within a set period of time (typically >10 years).

The climate of a location is affected by latitude, topography, altitude and proximity to large water bodies and their associated currents and can only be assessed over long time periods in order to incorporate the natural variability that occurs over several years.

Climate change

Natural Greenhouse effect

Greenhouse gases such as carbon dioxide keep the earth warm by allowing radiation from the sun to enter the atmosphere, while trapping a greater portion of outgoing radiation within the climate system. This maintains an average global temperature at ~15°C. Without greenhouse gases, the average temperature on Earth would be ~-18°C, too cold to sustain life as we know it.

The amount of energy that the Earth receives from the sun changes over time naturally in response to variations in Earth's orientation and orbit relative to the sun and the internal radiation cycles occurring within the sun itself. Additionally, the distribution of tectonic plates influences the capacity of heat to be transported around the planet by the atmosphere and the oceans. For example, when the land areas are concentrated towards the poles (equator), there is more (less) snow and ice on Earth, which means more (less) energy is reflected straight back out to space, resulting in cooler (warmer) global average temperatures. The concentration of greenhouse gases also varies naturally over millions of years depending on volcanic activity, global vegetation types, interacting with biological inputs and outputs, controlled by long-term biogeochemical cycles. The complex interplay of these processes (and others) determines the Earth's climate at any point in geological time.

Enhanced Greenhouse effect

Since the industrial revolution, humans have been increasing the concentration and composition of greenhouse gases in the atmosphere. These changes have occurred extremely rapidly, becoming the dominant influence on global climate, overshadowing the influence of any natural cycles (IPCC, 2014). Before the industrial revolution, CO_2 levels were 280 ppm. In 2013, CO_2 levels surpassed 400ppm for the first time in recorded history. This level is higher than it has been in at least 800,000 years.

The more greenhouse gases humans put into the atmosphere by burning fossil fuels (oil/coal), the more heat is trapped in the Earth's system and the warmer the globe becomes. This affects atmospheric and ocean circulation patterns, fundamentally changing the way the climate system behaves. This changes the characteristics of climate experienced at any one location, both in terms of average conditions and the magnitude and intensity of extreme events (e.g., droughts, floods, heatwaves, cyclones etc.).

What are climate projections?

Climate projections are outputs from computer models used to represent the Earth's mean climate state and variability. They are not intended to predict the weather on particular dates in the future and their initial conditions are not based on observations.

The advantage of climate models is they can be nudged in different ways to determine the influence of particular variables on the climate system, or even test the impact of different future scenarios on the climate system over long timescales into the future. This allows climate projections to establish the range in future climates that could plausibly occur. These model-derived descriptions of possible future climates are dependent on what humans do regarding the greenhouse gas (mainly CO_2) emissions, under a set of plausible scenarios.

Climate projections are generally described in 20 or 30 year periods, to incorporate natural variability in the climate system. This reduces the effect of annual to decadal events (e.g., droughts, cool/ hot seasons or ENSO cycles) on the average.

What are climate predictions/forecasts?

Climate forecasts aim to accurately and precisely predict the weather that will be experienced at a precise place and time in the future. In order to achieve this, climate forecasts use observations to configure the atmosphere within a climate model so it represents the configuration of the actual atmosphere as accurately as possible (at a particular time, usually *today* or *now*). The more accurately the atmosphere is configured, the more likely it is that a forecasting model can accurately predict the future. Forecasting has improved such that the accuracy and precision of a 5 day forecast in 2017 is more reliable than a 2 day forecast in the 1980s. These improvements have been driven by advances such as higher resolution observational data archives (due to satellite and surface ocean measurements), increased computer processing power and improved understanding and representation of atmospheric dynamics within climate models.

What are weather reanalysis products?

Weather reanalysis products (such as the *ERA-Iterim* mentioned within the methods) are climate model outputs explicitly designed to provide estimates of atmospheric variables at locations or times between observations. A climate model is configured using observations and then is run forward in time until the next set of observations can be incorporated. Reanalysis data products provide data archives that are consistent (use the same assumptions and equations), have full spatial coverage across the target domain (no missing data points), are continuous through time and estimate atmospheric variables that either were not measured or cannot be measured. Reanalysis products aim to provide a *better estimate of the observed atmosphere*. They can be more accurate than observations (due to site specific interferences such as shading, or protection from winds).

Global Climate Models (GCMs)

Global Climate Models (GCMs) are used to simulate the Earth's climate and are important tools to understand how the global climate may change due to the warming influence of increased greenhouse gas concentrations. Global Climate Models simulate the different components of the Earth system, including the atmosphere, ocean, land-surface, sea-ice, aerosols and the carbon cycle.

The foundation of climate modelling is just a few mathematical equations that describe the four-dimensional (horizontal, vertical and temporal) motion of air and its thermodynamic (heat and energetic) state. These equations, in conjunction with the idea that mass and energy must be conserved, are used to estimate the change in the state of the atmosphere at each gridbox in a model. All gridboxes pass information between each other to best represent the atmosphere from one time step to another, giving a numerical representation of the atmosphere and oceans.

As far as possible, climate models are based on physical theory, and processes are explicitly resolved using physical equations. However, there are some processes that cannot be described by fundamental equations, either because they occur at a scale that is smaller than the size of the gridboxes (e.g., atmospheric phenomena such as small clouds or thermal updrafts), or because they are experimentally derived. These mechanisms have to be given a descriptive or simplified representation to be incorporated into the model.

The higher resolution (in both space and time), the smaller the gridboxes or timesteps, giving more information about the state of the atmosphere. This includes more detailed information about the land surface characteristics and topography, which greatly affect the weather. Very high resolution models are very computationally intensive as all of the equations have to be calculated for each pixel, and run for many decades. (In comparison, weather forecasting models can be run at far higher resolution because they only need to represent the atmosphere for a few days). GCMs are therefore generally run at coarse resolution (~50km–250km horizontal resolution, 10–20 vertical layers in the atmosphere, and up to 30 layers in the oceans, at 6 hourly timesteps).

Regional Climate Models (RCMs)

The complexity of GCMs results in them being configured for coarse resolutions (spatial resolution of 50 to 200km, temporal resolutions of 6 hourly timesteps), due to the limitations of current supercomputers. As a result, certain features in the regional climate are often poorly represented by GCMs including mountain ranges, coastlines, urban areas and other atmospheric phenomena such as storms and rainfall processes. Downscaling methods are sometimes employed to address this limitation of the GCMs, providing higher spatial and temporal resolution climate simulations for a region (typically improved resolutions of between 1 to 50km resolution, and temporal resolutions of 1 minute to 1 hourly timesteps). Two popular downscaling methods are statistical downscaling and dynamical downscaling. Statistical downscaling relies on historical statistical relationships between observations and large-scale behaviour of the atmosphere. Dynamical downscaling employs Regional Climate Models (RCMs) that are based on modelling techniques that are like those used by GCMs, but with the computing resources focused over a region and with a focus on the atmosphere and land-surface components (i.e., a trade-off is made where there is less space covered/included, but higher resolution representation of the climate system). In both cases, the downscaling process has key inputs from (i.e., they are informed by) coarse resolution GCM projections, often referred to as a *host* or *parent* climate model.

How well do climate models replicate the climate at different scales?

Scale is a key component of understanding the climate and fundamental to detecting climate change signals. GCMs are run at low resolution, so do not perform well when compared with observations from specific locations, as the gridpoint is representing the average of a vast area rather than a single point, which is affected by local microclimatic characteristics. This means that the subgrid scale processes such as cumulus clouds, convection, updrafts and downdraft in storms are not well represented. These phenomena are linked to small-scale processes that cannot be simulated by the GCMs due to limitations in computing power or limited scientific understanding of the physical processes. They do a good job at simulating global and continental scale climate and provide a general overview of how the climate is changing. Long term averages of parameters such as temperature and precipitation along with less dynamic parameters like ocean temperatures, boundary currents and ice cover, are well represented by the GCMs. They are also adept at simulating aspects of regional climate variability, such as major monsoon systems and seasonal changes in temperature, often driven by these less dynamic parameters.

Detecting climate change signals at different scales

Detecting climate change signals is about the signal versus the natural variability (or signal to noise) ratio for the area of interest. The larger the area, the more the day-to-day variability is dampened down, so the more likely it is to reveal climate trends. Specific locations, especially in the extratropical parts of Australia on the boundary between the polar and tropical air masses, have high variability. A good example is somewhere like Melbourne. When looking at extreme heat days, 40°C days for example, and attempting to establish a climate change signal, it is difficult because the variability in temperature in Melbourne is very high. The summer range of daily maximum temperature is around 30°C, so a one degree climate change signal is going to have very little effect on how many 40°C days are experienced in Melbourne. When looking at Australia as a whole however, this day-to-day variability is lower because a hot day in Melbourne is often accompanied by a cool day in different parts of the continent, so the Australian average temperature is relatively stable. This means that if there's a heatwave, where Australia is for example three degrees warmer than the climatological mean, it's more likely that this event would have been impossible without climate change and that this event can be attributed to climate change. This is also true over shorter and longer timescales. The longer the timescale (e.g., annual vs decadal), the more variability (or noise) is averaged out and more of the signal is revealed.

Uncertainty in climate projections

There are three main sources of uncertainty in climate models, which become more/less dominant as the model-runs go further into the future. These are internal climate variability, model uncertainty and future emission scenario. The importance of each of these sources of uncertainty varies across different variables, the size of the area of interest and the length of time period.

Internal variability

Internal variability is due to the year-to-year changes in the weather which are independent of climate change. This timescale is difficult for the climate models to simulate as they are driven by mesoscale processes (that are often at smaller scales than the grid resolution). This uncertainty remains present throughout the model-runs but has less weighting as time goes on due to the other sources growing. The smaller the area of interest, the more this internal variability dominates the total uncertainty, however it is still significant at the global scale. This is linked to phenomena such as ENSO and other drivers of natural variability.

Model uncertainties

Model uncertainties are either due to different: representations of the same process within different model configurations (i.e., differing equations to solve the same problem); parameterisations due to differing model resolutions; poor understanding and simulation of processes within the model (i.e., the equations or parameterisation schemes are unable to represent the processes correctly). Many of these model uncertainties would be greatly improved with higher model resolution, however, there will always be model uncertainty because microscale processes are impossible to fully simulate. These uncertainties will always grow as a model run goes further into the future.

Emission scenarios

Uncertainty regarding emission scenarios are based on Representative Concentration Pathways (RCPs, discussed above). These are storylines of how humans act into the future and are represented by the resulting change in average global radiative forcing by 2100. The four RCPs are numbered according to the change in radiative forcing by 2100; +2.6, +4.5, +6.0 and +8.5 watts per square metre. The spread in these emission scenarios add uncertainty to GCM projections which always increase through time. Until 2050, all scenarios result in similar climate change impacts, so do not add much uncertainty to the future outcome. However, past 2050, they begin to diverge rapidly, eventually becoming the dominant source of uncertainty when estimating the future climate.

Importance of uncertainties with scales and parameters

When investigating global mean temperature, at first the internal variability is the main source of spread, with the different models and emission scenarios having less of an impact early on in the projections. From 2000 to 2020 the model uncertainties begin to dominate the overall uncertainty, whereas the emission scenario, still has little influence (although for some variables, such as global mean precipitation, model uncertainty is by far the largest contributor throughout). Past 2050 it is the uncertainty surrounding the emissions scenario, the socio-economic pathway the global community chooses to take, that drives uncertainty around global (and in turn local) temperatures.

How can uncertainty be dealt with when using projections?

Research into understanding why the uncertainties in the models exist and what can and can't be relied on is key to dealing with these uncertainties. The models produce plausible futures, rather than a single certain one, giving us an insight into what the future may look like. This means that we need to adapt to possible futures and be aware of the *worst case* scenarios. Using multi-model ensembles of simulations provides information covering all potential futures, allowing decision makers to apply a risk management approach with regards to imminent decisions being made today, while providing useful insights into what the longer term future may be to enhance the strategic decisions begin developed over the medium and longer terms.

The Coupled Model Intercomparison Project (CMIP)

The Coupled Model Intercomparison Project (CMIP) is a collaborative effort designed to improve our knowledge of climate change. CMIP provides an archive of outputs from a collection of global climate models contributed from the international climate modelling community. The CMIP archive facilitates the study of climate models in a standardised way, enabling a diverse community of scientists to better understand how the climate is represented by simulations; implement changes that improve simulations of the Earth's climate; and interpret the impact that differing plausible futures may have on humanity. This multi-model approach allows the global community to identify the most plausible impacts that will be realised following different socio-political pathways into the future. The range of Global Climate Models included in CMIP5 represent the most diverse range of independent climate models and projections of how the global climate will change.

The CMIP collaboration is now within its 6th phase (CMIP6), due to be completed in 2020. The atlas is based on CMIP5 model output. The CMIP5 series of global climate simulations were designed to test how various climate drivers impact upon the Earth's climate. Instead of the SRES emissions scenarios (e.g., A2, B1), which were used in previous CMIP archives, CMIP5 presented a series of experiments called the Representative Concentration Pathways (RCPs). These were designed to test the impact of different concentrations of heat-trapping gases (e.g., atmospheric CO_2 concentrations) over a range of time periods (see section below on RCP's). To further appreciate the depth and breadth of CMIP5 experiments scope, as well as develop an understanding of the value and implications realised by this internationally coordinated research effort, we recommend referring to:

> IPCC, 2014: Climate Change 2014: Synthesis Report. Contribution of Working Groups I, II and III to the Fifth Assessment Report of the Intergovernmental Panel on Climate Change [Core Writing Team, R.K. Pachauri and L.A. Meyer (eds.)]. IPCC, Geneva, Switzerland, 151 pp. (available here: `https://ar5-syr.ipcc.ch/topic_summary.php`)

Emissions scenarios

One of the main sources of uncertainty around climate change is what choices humans make regarding the amount of greenhouse gases we release in the future. Different emissions scenarios are used to describe a range of socio-economic pathways the global community may follow, and the resulting influence on the Earth's climate. Some scenarios are based on the *business as usual* future where humans continue to be dependent on fossil fuels. Other scenarios are based on how well humans deal with the problem, with a range from making small, deliberate actions to reduce emissions, to actively removing greenhouse gases from the atmosphere. The resulting range reflects the uncertainty inherent in quantifying human activities and their influence on climate. Scenarios are essentially a set of storylines based on population projections, demographics, international trade, flow of information and technology, and other social, technological, and economic characteristics of plausible future worlds.

To ensure that the projections of GCMs can be compared in a sensible way, various scenarios of future greenhouse gas emissions are applied consistently to all GCMs. The latest scenarios used by the climate modelling community are known as Representative Concentration Pathways (RCPs). These are not emission scenarios in the traditional sense but encompass all of the changes in the storyline leading to range in average global radiative forcing (change in temperature due to change in atmospheric composition) by 2100.

The RCPs include RCP2.6, RCP4.5, RCP6.0 and RCP8.5. The size of the number indicates more energy (in the form of heat, in units of Wm^{-2}) being trapped in the Earth system so that RCP8.5 leads to a significantly warmer future climate than RCP2.6. The highest is RCP8.5 which is the *business as usual* scenario (though by no means the upper limit), whereas RCP2.6 is ambitious in that it achieves net negative carbon dioxide emissions before the end of the century by including a policy option. The other scenarios have different pathways and represent different future worlds, which result in different levels of overall warming.

- RCP2.6 — following a low emissions, intense mitigation scenario where the heat trapping capacity of the Earth is 2.6 Wm^{-2}. This is the emission scenario that is closest to a <2°C, warming consistent with the Paris Agreement target. As of 2019, this scenario is only achievable with dramatic and rapid changes to our economic and social systems and arrangements that must be implemented by ~2030;
- RCP4.5 — following a late start to a low emissions, intense mitigation scenario where the heat trapping capacity of the Earth is 4.5 Wm^{-2}. As of 2019, this scenario is only achievable with dramatic and rapid changes to our economic and social systems and arrangements that must be implemented by ~2040;
- RCP6.0 — following a moderate emissions, less effective mitigation scenario where the heat trapping capacity of the Earth is 6.0 Wm^{-2}. This is the scenario that current international commitments to emissions reductions (as of 2019) could achieve if targets are met;
- RCP8.5 — following a high emissions, limited mitigation scenario where the heat trapping capacity of the Earth is 8.5 Wm^{-2}. This is also referred to as the *worst case* or *business as usual* scenario, as this is the trajectory we are currently following.

METHODS AND INTERPRETATION

Description of the regional climate modelling approach

General methods

Observations

Observed climate between 1997 and 2007 is summarised for each wine region, based on the Australian Gridded Climate Data products (AGCD). These are national gridded climate data at a resolution of 5km, based on interpolated weather station measurements. We use daily rainfall and daily maximum and minimum air temperature to calculate observed Growing Season Temperature and Rainfall, Aridity, Frost Risk Days and Excess Heat Factor. The AGCD were produced by the Australian Water Availability Project (AWAP), a collaborative effort of CSIRO and the Bureau of Meteorology (BoM).

Global Climate Models used in the atlas

Six Global Climate Models (GCMs) from the CMIP5 archive were downscaled for the atlas, These were CSIRO-BOM-ACCESS1-0, CNRM-CERFACS-CNRM-CM5, NOAA-GFDL-GFDL-ESM2M, MOHC-HadGEM2-CC, MIROC-MIROC5 and NCC-NorESM1-M. These models are based on the recommended GCMs for studying Australian climate change from the Climate Change in Australia web portal. The host GCMs for downscaling were selected to show a range of possible climate futures such as changes in the amount of warming and reductions in rainfall (see Table 1). Note that because we are selectively downscaling GCMs that show a range of possible futures, the downscaled simulations provide scenarios to explore the future climate, rather than an analysis of the most probable future climate, which lies within the range of downscaled climate.

Host GCM for downscaling	Relevance for downscaling regional climate
CSIRO-BOM-ACCESS1-0	A hot, dry model that is representative of the consensus of GCM projections, especially for south-eastern Australia. Warming exceeds 2.5°C across most of Australia, and >3.5°C in central Australia. Drying is projected over most areas. This model shows a high skill score with regard to historical climate.
CNRM-CERFACS-CNRM-CM5	A hot, wet model, consistent with the consensus of GCM projections in Southern Australia. It has a good representation of extreme El Niño in CMIP5 evaluations.
NOAA-GFDL-GFDL-ESM2M	A hot, very dry model, with warming in central regions exceeding 3.5°C. Drying is projected across most of the continent, with annual precipitation projected to decline more than 20% in many areas.
MOHC-HadGEM2-CC	A hot, dry model, with warming typically >2.5°C and >3.5°C in central regions. Annual precipitation is projected to increase in central Australia and decline elsewhere including the horticultural zone; Greatest reduction in wind. Maximum consensus for many regions.
MIROC-MIROC5	A low warming, wet model for Australia, especially the south-eastern region. Warming does not exceed 3°C, and slight changes in annual precipitation are projected with declines in north-east Queensland and south-west Australia.
NCC-NorESM1-M	Low warming, wetter model, representative of the wettest scenarios within the CMIP5 archive. Warming over most of Australia exceeding 2°C. Little change in annual precipitation is projected, particularly in the south-east, although there is drying in south-west WA.

Table 1: The six host GCMs used for dynamical downscaling and the reason for their selection

The high-resolution downscaled climate simulations available at the time of publication were only for the RCP8.5 scenario. This scenario is useful as at the time of publication, it is the scenario most representative of trajectory the Earth is following based on social, economic and political actions and achievements as of 2019. Moving forward, if action to mitigate the impacts of climate change are successful, such that the Earth follows a scenario more similar to RCP6.0 (or at best RCP4.5), the RCP8.5 scenario provides a *worst case* scenario for risk managers to test future strategies against, while also being inclusive of the projected impacts of lower emissions scenarios.

Description of the regional climate modelling approach

To develop high-resolution climate simulations for South East Australia, we used the Conformal Cubic Atmospheric Model (CCAM) developed at CSIRO (McGregor 2005 and McGregor and Dix 2008). Unlike most RCMs, CCAM is a global atmospheric model with a variable resolution grid that can be focused over an area of interest. In this way, CCAM can generate a higher resolution climate simulation, but is still coupled to the larger scale atmospheric circulation. Formally CCAM is a stretched grid global model, but we will refer to CCAM as an RCM in this atlas. CCAM includes several sub-models that are useful for simulating the Australian climate, including:

- direct and indirect aerosol feedbacks (Boucher et al., 2013)
- gravity wave drag (Chouinard et al., 1986)
- convection (McGregor, 2003)
- cloud microphysics (Lin et al., 1983; Rotstayn et al., 1997)
- radiation (Schwarzkopf and Ramaswamy, 1999; Freidenreich and Ramaswamy, 1999)
- aerosols (Rotstayn and Lohmann, 2002; Rotstayn et al., 2011; Horowitz et al. 2017)
- boundary layer turbulent mixing (McGregor, 1993)
- the Australian developed Community Atmospheric Biosphere Land Exchange (CABLE) land-surface and carbon cycle model (Kowalczyk, 2013),
- the Urban Climate and Energy Model (UCLEM) for Australian cities (Lipson, et al., 2018)

CCAM has been used for several regional climate simulations in Australia and South East Asia, including the *CORDEX intercomparison experiment*, the *National Resource Management (NRM) national projections for Australia*, the *Climate Futures for Tasmania*, *Climate projections for the Australian Alps* and *High-resolution projections for Queensland*.

The downscaling process used by CCAM for the high-resolution climate simulations involves two stages. The first stage involves taking the projected changes in the Sea Surface Temperatures (SSTs) from the GCMs, correcting the biases and variance on a month-by-month basis relative to the observed SSTs from 1980–2010 (Hoffman et al 2016). The CCAM model is then used to rebuild the atmosphere at a uniformly global 50km resolution consistent with the corrected SSTs. This removes the first order errors that are present in the GCM output and helps to simulate a more realistic present day climate. The second stage is to then downscale the 50km CCAM simulations to 5km resolution (centred over Victoria) using CCAM's stretched grid and scale-selective filters (Thatcher and McGregor 2009). Underlying model resolution is described in Figure **??**. This approach ensures that the regional 5km resolution simulation is consistent with the large-scale behaviour of the global 50km resolution simulation, but also allows CCAM to add additional information such as extreme events. It is important to note that the SST bias correction process retains the amount of warming represented in the SSTs but can allow CCAM to modify the projections of the GCMs in other respects (such as changes in mean sea level pressure or rainfall). When analysing the CCAM projections it can be useful to separate the regional-scale changes, the large-scale changes and the differences between the GCM projections so that the processes that explain the changes can be better understood.

The CFAP2019 ensemble were designed to balance competing needs of finer resolution, larger ensembles of downscaled host GCMs and additional emission scenarios. By simulating the climate at these scales, we can expect to better resolve mountains, coastlines and urban areas. We can also expect to better simulate extreme rainfall events that may lead to flooding. The running of new simulations is computationally intensive, so new fine-scale projections were only done for south eastern Australia and Tasmania, where the greatest added value would be achieved over the mountains and coastlines. For Western Australian regions (and South Burnett in Queensland), we investigated the usefulness of using dynamically downscaled simulations available from other archives, particularly those produced over the south west western Australia. We compared these archives for compatibility with the key archive we have used for the south-eastern Australian regions with regards to spatial resolution, available variables and both spatial and temporal domain (coverage). In order to be consistent with the rest of Australia, these alternative archives required continuous temporal coverage from the 1960s to 2100. Unfortunately alternative archives investigated were not continuous. This introduced confusion when visualising many of the outputs, and thus could not be used. An alternative approach was adopted that made use of the 50km resolution CFAP2019 ensemble outputs, as this model domain was global, which had coverage over all other Australian regions. However, this coarse resolution provided limited value when investigating the small wine regions. In order to transform the 50km outputs into more valuable forms, these were statistically downscaled to 5km resolution (using a quantile-quantile bias adjustment method Gudmundsson et al. 2013), based on the Australian Gridded Climate Data product. This produced far more useful, reasonable representations of the regions of interest to the project, providing the best continuous estimates currently available of climatic changes into the future.

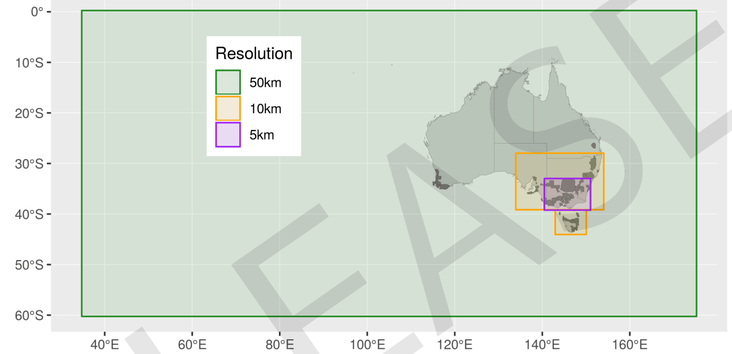

Figure 1: The domains of the CFAP2019 ensemble showing the different resolutions across Australia, ranging from 5km to 50km.

The CCAM model was configured for 35 vertical levels ranging from 20m to 40km in height, with more vertical levels concentrated in the lower portion of the atmosphere. Near surface variables (e.g., 2m air temperature or 10m winds) are calculated in the usual way based on Monin-Obukhov Similarity Theory (MOST). Essentially the near surface data is estimated from interpolating between the first atmospheric level and the surface, with the weighting of the interpolate dependent on the stability of the atmosphere near the surface (i.e., is air rising due to the surface being warmer than the air above it, causing mixing of the air). The CCAM downscaling process is divided into two stages. CCAM simulations are run from 1960 to 2100 for all six GCMs as well as downscaling ERA-Interim reanalyses. ERA-Interim reanalyses represent data sets where observations were assimilated into the atmospheric modelling. As a result, the ERA-Interim data corresponds to the observed weather from 1979 to 2015, although with the atmospheric simulation interpolating gaps in the observations. In this way, we can consider ERA-Interim is a useful reference experiment for downscaling the current climate that avoids errors that can arise in GCM simulations.

METHODS AND INTERPRETATION

Description of the regional climate modelling approach

Bias adjustment

Model biases introduce systematic errors which vary from place to place, as these errors are heavily dependent on the topography, altitude, latitude and distance from large water bodies. The biases are due to insufficient spatial resolution and the subsequent limited representation of meteorological processes (Rauscher et al. 2010). This is not a problem when investigating climate change as the interest is on the relative changes over time rather than the absolute values. However, when looking at climate impacts, the absolute values are needed, particularly when investigating temperature extremes. Therefore, in order to make the atlas more useful, there was a need to statistically bias adjusted the CCAM model outputs prior to climate impact assessment (Christensen et al., 2008).

Bias adjustment is a statistical method that adjusts the climate model output so that it matches the observations over the entire probability distribution. This adjustment is then applied to each quantile of the probability distribution into the future period, preserving any changes to the distribution projected by the climate models. The raw CFAP2019 ensemble outputs were bias-adjusted using the quantile statistical transformation, which has been widely used for adjusting modelled variables, especially temperature and rainfall (Gudmundsson et al., 2013). Temperature and rainfall were bias adjusted using the qmap package (Gudmundsson et al., 2013) within the R programming language. Specific parameter settings were: method = quant; qstep = 0.001 ; wet.day = FALSE for Temperature and TRUE for rainfall. Observation data inputs were from the Australian Gridded Climate Data product (Jones et al., 2009).

An example of the impact bias adjustment can have on the distribution of values is presented in Figure 2. The probability distribution of the model output has been adjusted such that it reflects the distribution of observed values.

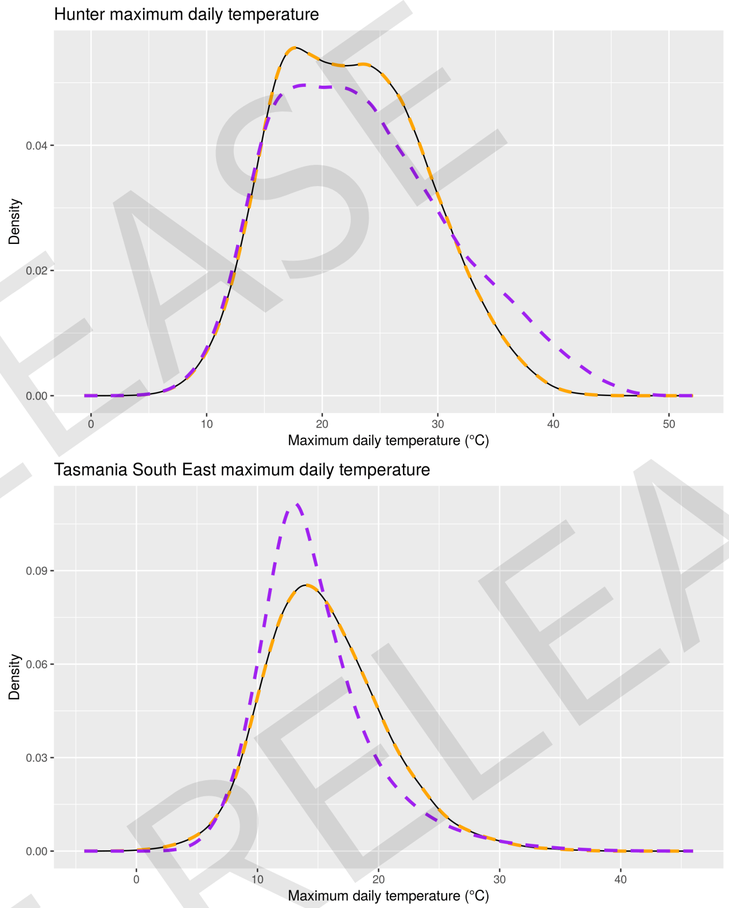

Figure 2: Probability distributions of maximum daily temperature at screen height (2m above the surface) for the period 1961-1990, for different data archives, displayed for the example wine regions *Hunter* and *Tasmania South East*. Observed data is sourced from AGCD. Only a single example ensemble member from CFAP2019 is displayed (CNRM-CERFACS-CNRM-CM5), similar impacts are observed when bias-adjusting the other ensemble members. The black solid thin lines are the observations. The purple dashed lines are the raw CFAP2019 output. The orange dashed lines are bias-adjusted CFAP2019 output. Note how the bias-adjusted CFAP2019 distributions (orange dashed lines) closely resemble the observed distributions (black thin solid line).

Time periods

Time periods were calculated based on Australian growing years, which are the period from July to June each annual cycle, winter to winter in the Southern Hemisphere. Growing years were labelled as the calendar year in which July fell. Time periods used within this atlas are defined as:

Time period	Start and end month
1961–1990	July 1961 to June 1991
1997–2017	July 1997 to June 2018
2001–2020	July 2001 to June 2021
2021–2040	July 2021 to June 2041
2041–2060	July 2041 to June 2061
2061–2080	July 2061 to June 2081
2081–2100	July 2081 to June 2100[1]

Table 2: Start and end months for each time period

Wine Regions / Geographic Indications (GIs)

The terms *Wine Regions* and *Geographic Indications* (or GIs) are used interchangeably throughout this atlas. They are determined, registered, managed and curated by Wine Australia (Wine Australia, 2019). Shapefiles of all wine regions were provided by Wine Australia.

[1] this period is 19 years (instead of 20 years like the others) due to an absence of available data past December 2100

Evaluation of the CFAP2019 ensemble

The following section evaluates the CFAP2019 ensemble for the period 1986–2005 by comparing the results to observations. In this section we use the Australian Gridded Climate Data products (AGCD), which were produced by the Australian Water Availability Project (AWAP), a collaborative effort of CSIRO and the Bureau of Meteorology (BoM). These are national gridded data sets at 5km resolution of observed daily rainfall and daily maximum and minimum air temperature at 2m. AGCD data is based on interpolated weather station measurements and hence there are some gaps where the station network is less densely populated (e.g., in the Victorian Alps). We also used ERA-Interim reanalyses for evaluating the larger-scale performance of the CFAP2019 ensemble such as mean sea level or winds at 850 hPa. The ERA-Interim reanalysis is a combination of model simulations and observations. As such, it is a reconstruction of the weather through time, providing information about surface conditions (e.g., temperature, precipitation, wind speed and direction, humidity, evaporation and soil moisture), information at pressure and model levels, and information on solar radiation and cloud cover. It provides a reasonably accurate representation of past weather over a number of years, so is valuable to validate the model output over the same time period. The Bureau of Meteorology Australian Regional Reanalysis for Australia (BARRA) was under development at the time of atlas development and publication, so was not yet available.

The region of Victoria was used to assess the capability of the model because it covers a large number of the Australian wine regions and has a range of climate zones (coastal, open plains, low elevation hills through to high elevation alpine mountains).

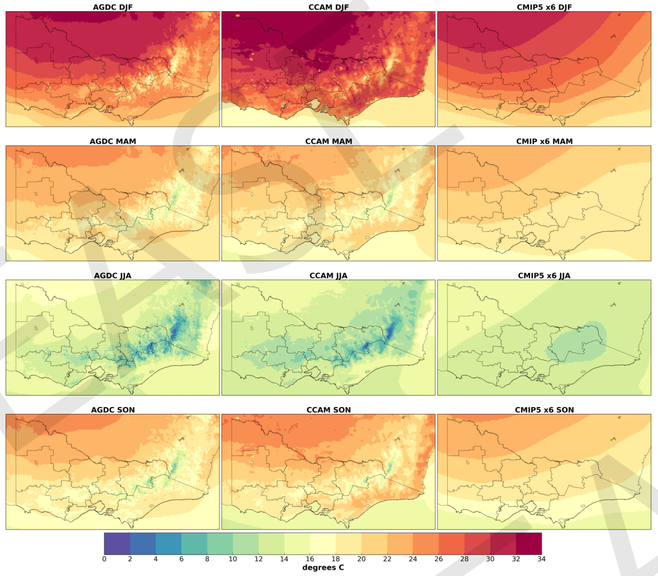

Figure 3: Comparison of average daily maximum 2m air temperature between 1986–2005 between AGCD interpolated observations (left column), CCAM 5km resolution simulation (middle column) and host GCM (right column). The CCAM and GCM results are averaged over the six GCMs used for downscaling. The rows from top to bottom correspond to December-January-February (DJF), March-April-May (MAM), June-July-August (JJA) and September-October-November (SON), respectively.

Temperature

The CFAP2019 ensemble variables average daily maximum and minimum air temperature (at 2m, i.e. screen temperatures) between 1986–2005 are compared to the AGCD interpolated observations and the host GCM models in Figures 3 and 4. The ensemble mean for CFAP2019 ensemble and six host GCMs are presented. The results indicate that CFAP2019 ensemble better represents the temperatures for mountain regions and coastlines than the GCMs when compared to AGCD. The CFAP2019 ensemble also show a significant improvement (compared to the host GCMs) in daily minimum temperature, as well as much better representation of colder daily minimum temperatures for alpine regions of Victoria. The host GCMs tend to show a warm bias in the daily minimum temperatures over Victoria that is not apparent in the CFAP2019 ensemble. However, for maximum temperatures there is a warm bias apparent in the CFAP2019 ensemble in summer, particularly for eastern Victoria. The spatial pattern of this warm bias is not apparent in the future projected change in daily maximum temperature, suggesting that the issue is related to the diagnoses of the 2m air temperature for tall vegetation (e.g., forests). Some caution is therefore advised in interpreting the projected changes in climate for daily maximum temperatures within or nearby forested regions.

Another example of how the CFAP2019 ensemble has improved the daily minimum temperature can be see by examining the Urban Heat Island (UHI) for Melbourne. Urban areas result in an increased daily minimum temperature compared to the surrounding natural vegetation of typically 1°to 2°C, depending on the density of the urban area and the amount of green space. Urban areas are generally poorly resolved in GCMs. However, regional models like CCAM include special parameterisations to account for the building materials, urban drainage, shadowing effects and changes to air circulation within the urban canyon. Figure 5 compares the difference in daily minimum temperature between an inner-city weather station (BoM Melbourne regional office) and three outer city locations (Laverton RAAF, Coldstream and Cranbourne Botanic Gardens) between 1986–2005. Weather stations show that average daily minimum temperatures at Laverton RAAF, Cranbourne Botanic Gardens and Coldstream are approximately 2°C, 2°C and 4°C, cooler than the inner-city site. Figure 5 shows that the CFAP2019 ensemble better represents this difference in daily minimum temperatures due to the UHI, correctly projecting a 2°C difference between the inner-city and Laverton and Cranbourne sites (although the CFAP2019 ensemble is still slightly too warm at the Coldstream site). In comparison, the GCM results do not simulate any change in daily minimum temperature between the inner-city and outer-city locations.

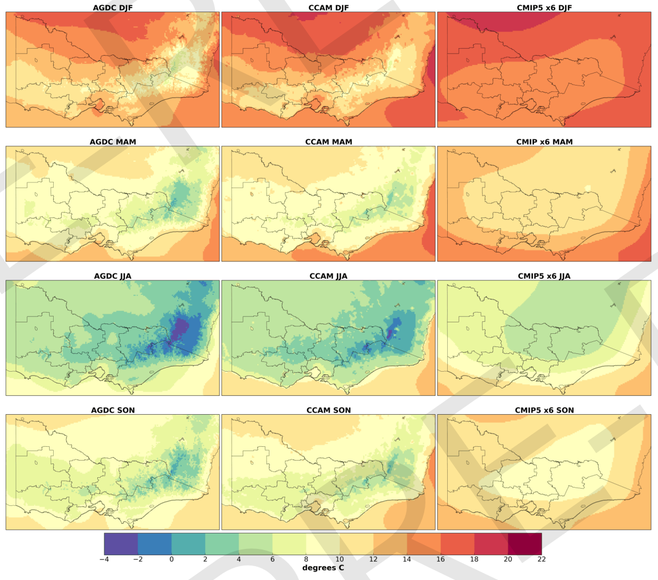

Figure 4: Comparison of the daily minimum 2m air temperature between 1986–2005 for AGCD (left column), CCAM averaged over the six downscaled simulations (middle column) and the average of the six host GCMs (right column). The rows from top to bottom correspond to December-January-February (DJF), March-April-May (MAM), June-July-August (JJA) and September-October-November (SON), respectively.

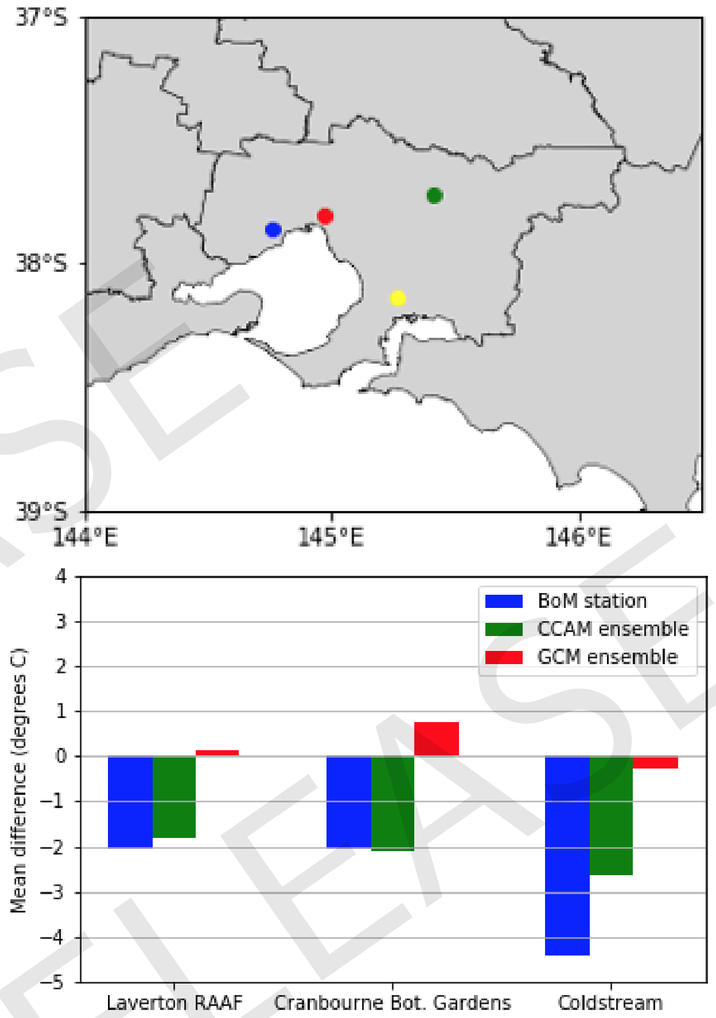

Figure 5: Comparison of the Urban Heat Island (UHI) measured as the difference in average daily minimum temperature over 1986–2005 between an inner-city weather station (BoM Melbourne Regional Office — Red dot) and three outer-city weather stations (Laverton RAAF — Blue dot, Coldstream - Green dot and Cranbourne Botanic Gardens — Yellow dot). Location of the weather stations are shown in the top plot and the observed and simulated difference in temperatures between the inner-city site and the three outer city sites is shown in the bottom plot.

METHODS AND INTERPRETATION

Mean Sea Level Pressure and 850 hPa winds

Rainfall

A comparison of the average rainfall simulated for different seasons from 1986–2005 by CCAM with AGCD interpolated observations and the host GCMs can be seen in Figure 6. The CCAM 5km resolution simulations better represent the average rainfall over the Victorian Alps than the GCMs where the mountains are poorly resolved. CCAM also represents increased rainfall along the southern coastline that was not represented by the GCM simulations. The simulated average rainfall from the CCAM 5km resolution simulations is higher than what is measured for the AGCD interpolated observations. However, the AGCD interpolated observations can also underestimate the rainfall in mountain regions due to a more sparse network of observing stations. The larger scale features in the CCAM simulated rainfall resemble some of the larger scale features in the GCM simulations (e.g., a slightly higher average rainfall in the north west of Victoria in summer and autumn), which reflects some similarities in how rainfall is parameterised in global and regional dynamical climate models. Nevertheless, downscaling does improve the distribution of simulated average rainfall, demonstrated in the CCAM 5km simulations.

Extreme rainfall

Another aspect where downscaling should improve the simulated climate is extreme rainfall. We used the 99th percentile of daily rainfall over the 1986–2005 period as an indicator of CCAM's ability to represent extreme rainfall. A comparison of the 99th percentile of daily rainfall between 1986–2005 for AGCD, CCAM and the GCMS is shown in Figure 7. The extreme rainfall is overestimated by CCAM when compared to AGCD interpolated observations, although CCAM significantly improves on the extreme rainfall from the GCMs which do not represent the high rainfall for the Alpine regions at all. As for average daily rainfall, the AGCD interpolated observations may underestimate the size of the extreme rainfall for mountain regions due to the sparse observing network, which is also suggested by comparing the results to BARRA (not shown). Nevertheless, CCAM is able to represent extreme rainfall that could not be captured in the GCM simulations.

Mean Sea Level Pressure and 850 hPa winds

Although the use of CCAM simulations is primarily for downscaling the regional climate, it is also important to consider the large-scale behaviour of the CCAM atmospheric simulation. This large-scale behaviour can influence the projections of the climate model simulations and is useful for interpreting the outputs of CCAM in the context of the ensemble of CMIP5 GCM projections. As discussed when describing CCAM, the use of bias corrected SSTs can allow CCAM to differ from the host GCM in some respects.

Figure 8 compares the simulated Mean Sea Level Pressure (MSLP) averaged between 1986–2005 from the six CCAM 50km global simulations with the ERA-Interim reanalyses and the average of the six host GCMs. When compared to ERA-Interim, the CCAM 50km simulations are somewhat biased towards eastwards flow in the MSLP compared to the host GCMs, most noticeable in autumn and winter. This can lead to winds too easterly as indicated with the 850 hPa winds shown in Figure 9. Figure 9 compares the average 850 hPa wind speed and direction for different seasons over 1986–2005 between the ERA-Interim reanalyses, the average of the six CCAM 50km global simulations and the average of the six host GCMs. The 850 hPa winds represent the winds at approximately 1 to 1.5km above the surface, where ERA-Interim is less influenced by smaller scale mountains. Although the CCAM simulations are a reasonably good representation of the 850 hPa winds, the wind speed is too strong and the wind direction is too zonal in autumn and winter. This result is consistent with the easterly bias within MSLP results for those seasons. The CCAM simulation results are still a reasonable representation of the global climate and the projected future changes in climate are physically reasonable. Nevertheless, we can expect some differences in the larger scale changes projected by the CCAM simulations compared to the host GCMs.

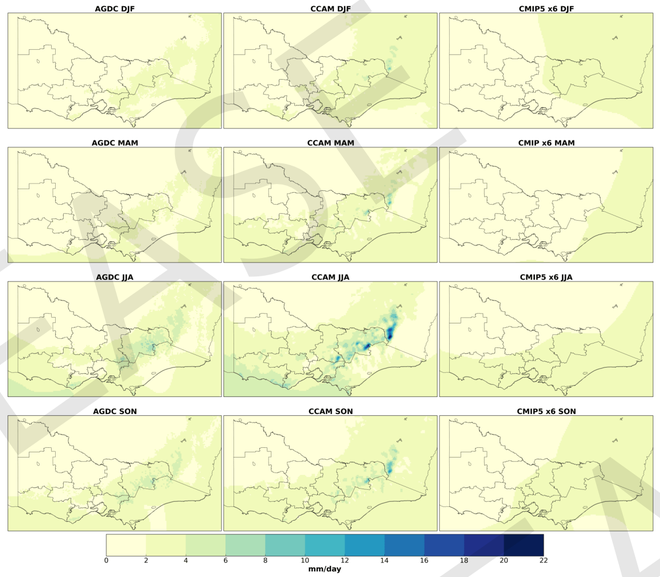

Figure 6: Comparison of daily average rainfall from 1986–2005 between AGCD interpolated observations (left column), the average of six CCAM 5km simulations (middle column) and the average of the six host GCMS (right column). The rows indicate different seasons with top to bottom showing December-January-February (DJF), March-April-May (MAM), June-July-August (JJA) and September-October-November (SON), respectively.

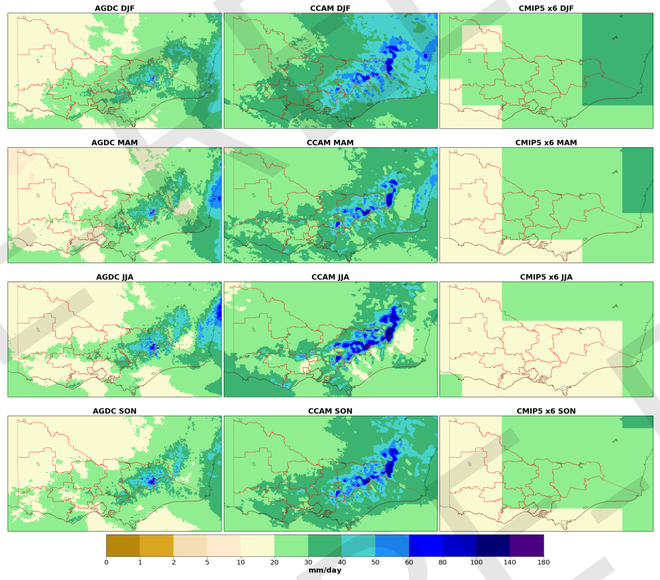

Figure 7: Comparison of the 99th percentile of daily rainfall between 1986 and 2005 from AGCD interpolated observations (left column), the average of six CCAM simulations (middle column) and the average of six GCMs (right column). The rows indicate different seasons with December-January-February (DJF), March-April-May (MAM), June-July-August (JJA) and September-October-November (SON).

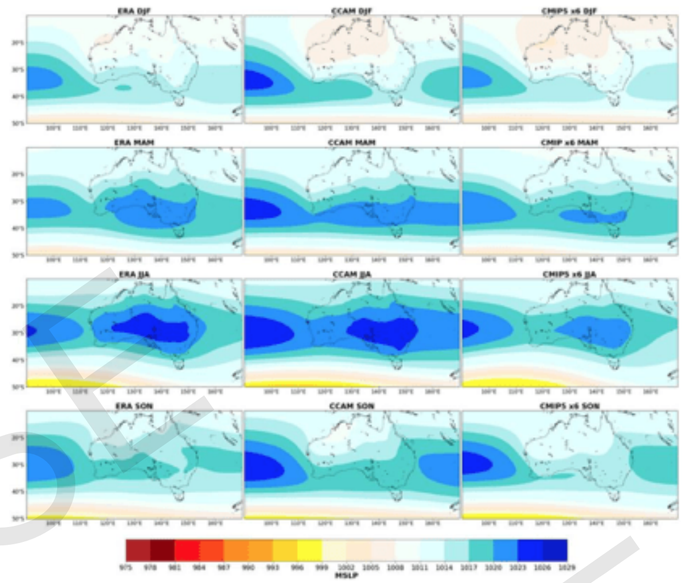

Figure 8: Comparison of Mean Sea Level Pressure averaged over 1986–2005 between ERA-Interim reanalyses (left column), the average of the six CCAM 50km global simulations (middle column) and the average of the six host GCMs (right column). The rows indicate different seasons with December-January-February (DJF), March-April-May (MAM), June-July-August (JJA) and September-October-November (SON).

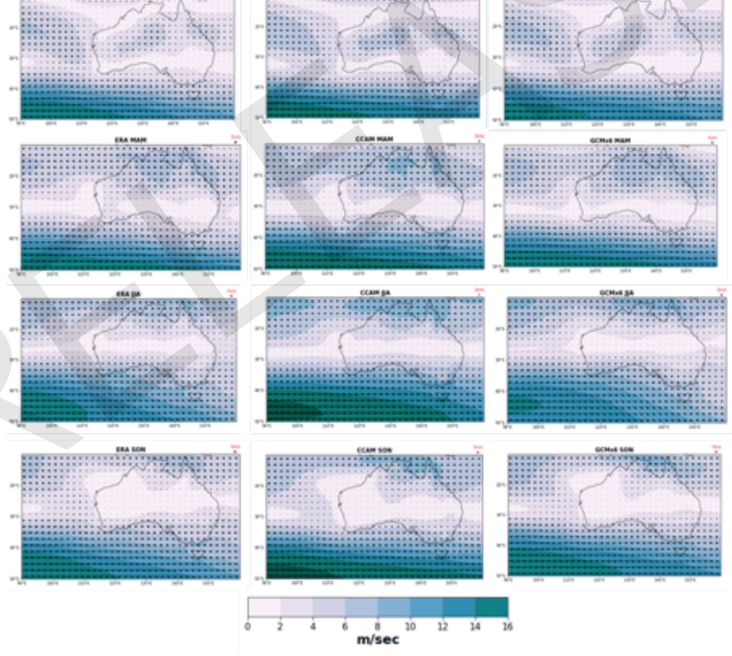

Figure 9: Comparison of average wind speed and direction at 850 hPa (approximately 1 to 1.5km above the surface) between 1986–2005. The ERA-Interim reanalysis is shown on the left column, the average of the six CCAM 50km simulations in the middle column and the average of the six GCMs on the right column. The rows indicate different seasons for December-January-February (DJF), March-April-May (MAM), June-July-August (JJA) and September-October-November (SON).

Methods and interpretation of figures

Infographic

Each regional section of the atlas starts with an infographic page that summarises the future changes in climate in general terms. This section describes the methods used to calculate each index.

Interpretation:

These infographics provide a snapshot of the projected climate across each region at different time periods. Values are summarised across space and time, so they give a good overall indication of change across the region, but may be less useful when interested in exact conditions at specific sites. These summaries enable easy and rapid comparisons between regions, or across time periods, in a broad, general sense.

Data sources

Values for the 1997–2017 (the *current period*) were calculated using the Australian Gridded Climate Data product (Jones et al., 2009).

Values for the time periods 2041–2060 and 2081–2100 were calculated from the Climate Futures Australasian Projections 2019 (CFAP2019), produced collaboratively by the CSIRO, the ACECRC and the University of Tasmania.

Mean values

Mean values are the spatial and temporal average of the target variable within a specific time-period, across all grid cells within each wine industry *Australian Geographical Indications* (Wine Australia, 2019). For example, the mean GST value for the period 2041–2060 for the Barossa Valley is an average of 260 input values (13 grid-cells x 20 annual timesteps), summarised into a single value.

Interpretation:

Values are presented for selected 20-year periods representing the:

- *current period* (1997–2017) — reflecting recent memory;
- the *mid-term future* (2041–2060) — the high-likelihood future expected by 2050 (before which RCP scenarios are similar and after which they begin to diverge), this period is most relevant to strategic decision making; and the
- *far future* (2081–2100) — providing a quantitative estimate of changes by the end of century (following the worst case scenario).

The three time periods indicate the rate of adaptation that may be required over the next 20 or 40 years while providing context to help guide planning over a longer time frame.

Temperature

Growing Season Temperature (GST) is defined as the mean atmospheric temperature at screen height (2m above the land surface) over the period from October to April of each annual cycle. This is calculated for every growing season year, for every grid-cell within the region. Annual values from all grid-cells and all annual timesteps are averaged.

Interpretation:

Growing Season Temperature (GST) increases into the future for every region across Australia. The rate of increase accelerates exponentially towards 2100. Values are summarised over space and time, so for regions with high topographic variability, average values are unlikely to reflect conditions at specific sites within the wine region, although they will give a reasonable indication of the direction and rate of change projected into the future.

Extreme Heat

Excess Heat Factor (EHF) is an index that describes the severity of short term, acute heat impacts on humans during heat waves. It accounts for how hot any three-day period is in relation to an annual temperature threshold at a particular location, as well as how hot the three-day period is with respect to the recent past (the previous 30 days). This reflects the fact that people acclimatise, to a certain extent, to their local climate but may not be prepared for a sudden rise in temperature above that of the recent past.

The calculation is described in Nairn and Fawcett (2015). Annual values from all grid-cells and all annual timesteps are averaged.

Interpretation:

Excess Heat Factor (EHF) represents the intensity of heatwaves within a region as experienced by humans, after accounting for any capacity to acclimatise to the typical conditions within a region. Increasing EHF rates indicate more intense heatwaves. As heatwaves are large synoptic scale features, regional variability is less influential than longer term climatic changes.

Aridity Index

The *Aridity Index* provides an indication of available water by considering the magnitude of precipitation compared to the magnitude of evaporation. This is calculated as annual precipitation / annual pan evaporation. The aridity index is independent of site specific characteristics (e.g., soil type, vine varietal) or changes in vineyard management (e.g., shading, row orientation, mulching), but captures elevation, aspect, humidity and the influence of wind. Annual values from all grid cells and all annual timesteps are averaged.

The annual cycle was defined as July to June, which is winter to winter in the southern hemisphere. Annual precipitation is the sum of all rainfall that has fallen within a single grid cell within the period July to June of each annual cycle. Annual pan evaporation is the sum of all evaporation that could occur if water was always present within a grid-cell over the period July to June of each annual cycle. This follows the approach from numerous published methods that have all devised similar (yet slightly different) methods of estimating aridity by dividing a measure of rainfall by a measure of evaporation (or similar variables such as evapotranspiration, potential evaporation, etc.) (Transeau, 1905; Vyssotsky, 1905; Oldekop, 1911; Thornthwaite, 1931; Ivanova, 1941; Kostin, 1952; Hargreaves, 1971; UNESCO, 1979; Sarker and Biwas, 1980).

Interpretation:

The *Aridity Index* (AI) reflects the difference between evaporation and rainfall over the year. High (low) values indicate more (less) rainfall than evaporation. In a rapidly warming climate, evaporation rates increase substantially, so in order to maintain similar AI values rainfall must increase sufficiently to offset evaporative losses. Temperature increases have high certainty, thus evaporation increases are also highly certain. There are few places (globally) where rainfall is projected to increase at a rate fast enough to maintain AI values at their current levels. Therefore AI is expected to decrease in all wine regions across Australia. Values are summarised over space and time, so for regions with high topographic variability, average values are unlikely to reflect conditions at specific sites within the wine region, although they will give a reasonable indication of the direction and rate of change projected into the future.

Extreme Cold

Mean *Growing Season Frost Risk Days* is the number of days within the period from October to April of each annual cycle where temperatures are <2°C. Annual values from all grid cells and all annual timesteps are averaged.

Interpretation:

Mean *Growing Season Frost Risk Days* are projected to decrease in all wine regions across Australia as temperatures continue to rise. Values are summarised over space and time. For regions with high elevations within the wine regions, average values will be higher (lower) than those expected in the lowlands (highlands).

Rainfall

Mean *Growing Season Rainfall* is the average sum of all precipitation that falls within the period from October to April of each annual cycle. Annual values from all grid cells and all annual timesteps are averaged.

Interpretation:

Rainfall is one of the most uncertain components within the climate system. However, even modest increases in annual rainfall can actually result in decreased moisture availability across a region within a warming climate, as rainfall rates are required to increase in order to offset evaporative (and other) losses (see Aridity Index sections). Confidence in temperature, the warming trend and evaporative demands is high. Thus, although confidence surrounding rainfall projections is low, very few simulations indicate increases in rainfall with sufficient magnitude to offset these projected losses. Rainfall should be viewed in concert with Aridity Index projections.

Heat

Interpretation:

We have high confidence in how temperature will change into the future (depending on the emissions scenario). The physical drivers of how it changes within the climate system are well understood, are valid across large spatial scales and are therefore straightforward to represent within climate models. This allows the models to achieve high levels of skill in the predictions (weather forecasts) and projections (climate projections) they produce.

There is strong agreement across the CFAP2019 ensemble members regarding the rate and magnitude of warming projected into the future. As such, there is high confidence regarding projected variables related to temperature.

Each ensemble member describes a possible future, with different timing and sequencing of broad global drivers (such as the Southern Annular Mode (SAM), the El Niño Southern Oscillation (ENSO) and the Indian Ocean Dipole (IOD)). As such, hot or cold years can be out of phase with each other. This is a strength of an ensemble mean as the highs and lows (expressions of the natural variability within the climate system) are smoothed out, revealing the general climate trend. For some regions, variability between the different ensemble members is lower than the variability that occurs spatially across a wine region. This is especially true for those regions with significant hills or mountains (e.g., Barossa Valley, Tasmania East Coast). For regions that are more uniform spatially (e.g., Riverland), the ensemble variability is more noticeable, expressed as clusters of points that escape the point cloud in some years. These high and low years are useful for understanding the likelihood of extremely hot or cold years over time. Often, the extremely hot years are indicative of the conditions to expect in the future. For example, the hot year (along with the associated extreme daily temperatures) observed in south east Australia during the 2015/2016 growing year is indicative of *typical projected conditions* in 2050. Similarly, cooler conditions (relative to the surrounding decades) can occur at any time (although even the coldest year by the end of century would be considered an average year today).

The trend lines highlight how typical conditions are projected to change over time — they are representative of the ensemble mean at warmer and cooler locations within the region. It is most interesting to determine when the cooler location becomes hotter than the warmer location (typically around 2030, depending on the region and the magnitude of spatial variability). It is important to note that interannual and decadal variability is present, but the trend is clearly warming, especially from 2020 onwards.

Figure 1: Observed mean Growing Season Temperature

Underlying data source: Australian Gridded Climate Data Product (Jones et al., 2009).

Daily average temperature is calculated as the mean of daily maximum and minimum temperatures each day. Growing Season Temperature (GST) was calculated as the average of all daily average temperature values for each day within the period from October to April of each growing season year. Mean Growing Season Temperature is the average of all annual GST values over the *current period* (1997–2017). Grid cells selected were those within (or intersecting with the boundary of) the polygon that defined each wine industry *Australian Geographical Indications* (Wine Australia, 2019). Values were calculated for each grid cell.

Interpretation:

Each tile represents the mean Growing Season Temperature during the period 1997–2017, (which is the period of recent memory). This map reflects the level of variability across the region as it is currently experienced. Tiles are the resolution of the underlying data. Lower values typically correspond to higher elevation regions. Towns and roads are included to help identify specific sites within the region. Tiles have an average elevation of the area they represent, so they best represent regions that have similar elevations (±200m) across 5–10km^2 scales. Typically, the highest peaks occur at smaller scales (~1km^2) and thus are poorly represented. This can influence the representation of some climatic features and should be considered when interpreting these figures.

Figure 2: Observed change in mean Growing Season Temperature

Underlying data source: Australian Gridded Climate Data Product (Jones et al., 2009).

Growing Season Temperature (GST) was calculated as the average of all minimum and maximum temperature values for each day within the period from October to April of each growing season year. Mean Growing Season Temperature is the average of all annual GST values over the *current period* (1997–2017), or the *baseline period* (1961–1990). The *baseline period* mean GST was then subtracted from the *current period* mean GST, resulting in the *observed change in mean GST*. Grid cells selected were those within (or intersecting with the boundary of) the polygon that defined each wine industry *Australian Geographical Indications* (Wine Australia, 2019). Values were calculated for each grid cell.

Interpretation:

Each tile represents how mean Growing Season Temperature during the current period (1997–2017) has changed when compared to mean Growing Season Temperature during the historical period (1961–1990). Climate change is a large scale feature, so the level of change observed is relatively similar when viewed at local scales. Towns and roads are included to help identify specific sites within the region. Tiles have an average elevation of the area they represent, so they best represent regions that have similar elevations (±200m) across 5–10km^2 scales. Typically, the highest peaks occur at smaller scales (~1km^2) and thus are poorly represented. This can influence the representation of some climatic features and should be considered when interpreting these figures.

Figure 3: Projected mean Growing Season Temperature

Underlying data source: Climate Futures Australasian Projections 2019 (CFAP2019).

Growing Season Temperature (GST) was calculated as the average of all minimum and maximum temperature values for each day within the period from October to April of each growing season year for each member within the *CCAM ensemble*. Grid cells selected were those within (or intersecting with the boundary of) the polygon that defined each wine industry *Australian Geographical Indications* (Wine Australia, 2019). Values were calculated for each grid cell. Mean Growing Season Temperature is the average of all annual GST values within each time period (2021–2040; 2041–2060; 2061–2080; 2081–2100). These were calculated for each ensemble member within the *CFAP2019*. The 6 ensemble member values (for each cell) are averaged generating the ensemble mean for each cell within the region.

Interpretation:

Each tile represents the mean Growing Season Temperature during each 20-year period of 2021–2040, 2041–2060, 2061–2080, 2081–2100 (following the RCP8.5 scenario). These reflect the level of variability across the region, and the rate of change projected into the future. Tiles are the resolution of the underlying data. Lower values typically correspond to higher elevation regions. Tiles have an average elevation of the area they represent, so they best represent regions that have similar elevations (±200m) across 5–10km^2 scales. Typically, the highest peaks occur at smaller scales (~1km^2) and thus are poorly represented. This can influence the representation of some climatic features and should be considered when interpreting these figures.

Figure 4: Projected annual Growing Season Temperature

Underlying data source: Climate Futures Australasian Projections 2019 (CFAP2019).

Blue points: Growing Season Temperature (GST) was calculated as the average of all minimum and maximum temperature values for each day within the period from October to April of each growing season year for each member within the *CCAM ensemble*. Grid cells selected were those within (or intersecting with the boundary of) the polygon that defined each wine industry *Australian Geographical Indications* (Wine Australia, 2019). Values were calculated for each grid cell.

Solid lines: The solid lines are annual time series of the ensemble mean for a single grid cell. Each solid line represents either a *warmer location* or a *cooler location* relative to the rest of the region. These locations were selected based on observed mean GST values, calculated from the Australian Gridded Climate Data product (Jones, et al., 2009) for the *current period* (1997–2017). The *warmer location* (*cooler location*) is a grid cell that represents the 80th (20th) percentile of all mean GST values across the region. The 20th and 80th percentile thresholds were selected so that typical subregions where highlighted, rather than high elevations, coastlines or particularly warm grid cells (or subregions in the larger wine regions).

Grey Bars: The grey bars represent the observed mean GST for the *current period* (1997–2017) from contrasting wine industry *Australian Geographical Indications* (Wine Australia, 2019). Values were averaged across space and time, calculated from the Australian Gridded Climate Data product (Jones, et al., 2009).

Coloured zones: The coloured zones indicate the time when *average global climate temperature* increases by 1°C, 2°C, 3°C or 4°C, following the Representative Concentration Pathway 8.5 scenario (RCP8.5, often referred to as the *business as usual* scenario). These estimates are the ensemble means as reported by the Intergovernmental Panel on Climate Change Fifth Assessment Report (IPCC-AR5), based on the World Climate Research Programme (WCRP) Coupled Model Intercomparison Project - phase 5 (CMIP5) global climate model archive (which has >100 ensemble members).

Interpretation:

Key elements:

- There is a strong warming trend, with a rate of change that increases towards the end of the century.
- All ensemble members agree so there is high confidence in the direction and magnitude of the projected future following the RCP8.5 scenario.
- Extremely hot years (representative of mean conditions in the future), can occur as much as 30 years earlier than projected by the mean trend.
- The pathways exhibited by different ensemble members (hotter vs warmer, which in some regions are obvious) are all plausible potential futures.
- Lines represent ensemble means (extreme years have been smoothed away), representing the average changes projected into the future.

Each point represents the annual Growing Season Temperature for individual grid cells within the region for each separate CFAP2019 ensemble member. For each year, the spread of points represents the spatial variability as well as the variability across the ensemble members. From 1961 to around 2000, interannual and decadal variability dominate the changes seen in climate trends.

(continued)

After 2000 the influence of climate change emerges, becoming clearly important by 2020. From 2020 to 2100 climate change becomes progressively more influential than natural variability.

Solid lines indicate the average direction of change for a single location into the future. These lines are the ensemble mean. These are intended to highlight that the cloud of points is created in part by the range of conditions across the region. Users are expected to know if they are within the warmer, average or cooler part of their region and thus can infer where they are likely to sit within the point cloud, allowing them to extract more detail from these figures. Because these lines are the ensemble mean (the average of 6 values), extreme years have been smoothed out. To get a feel for the influence of extreme events, the peaks and troughs indicated by the points are more helpful.

The grey bars are the regional average for contrasting GIs across Australia. They do not represent the regional variability within each of those GIs, but are intended to provide approximate climate analogues to aid interpretation.

The coloured zones are intended to be used independently of the *Growing Year (July to June)* axis, allowing decisions to be made based on the expected magnitude of global warming (such as those national governments are committed to within the *Paris Agreements*), rather than being based on the passage of time. This allows these plots to be useful regardless of the emissions scenario the world eventually follows.

Figure 5: Probability distribution of Growing Season Temperature

Underlying data source: Climate Futures Australasian Projections 2019 (CFAP2019).

Growing Season Temperature (GST) was calculated as the average of all minimum and maximum temperature values for each day within the period from October to April of each growing season year for each member within the *CCAM ensemble*. Values were calculated for each cell. Grid cells selected were those within (or intersecting with the boundary of) the polygon that defined each wine region's *Geographical Indications* (Wine Australia, 2019).

The curves represent the distribution of GST values from all grid cells and all ensemble members during each different 20-year period. Time periods were: 2001–2020; 2021–2040; 2041–2060; 2061–2080; 2081–2100.

The grey, filled curves represent the distribution of observed GST values for contrasting Australian regions for the *current period* (1997–2017).

Interpretation:

Probability distributions reflect the spread and potential likelihood of values within a particular population of values. High, narrow peaks indicate low variability with a high frequency of particular values occurring within the population. Low, broad peaks indicate high variability, with few values occurring frequently. The probability distributions displayed in the atlas incorporate all spatial grid cell values, across each 20-year time period, from six ensemble members (i.e., independent simulations). Variability across spatial and temporal scales as well as across the CFAP2019 ensemble is represented with each curve. This has the advantage of reflecting the diversity that is found within each wine region (cooler vs warmer subregions) and across different types of years (e.g., hot, average or cold). Different ensemble members capture different climate configurations (e.g., El Niño, neutral, or La Niña phases of ENSO), thus better estimate the range of possible extremes. Low likelihood years (extreme hot or cold) can be included, indicating what is possible, while simultaneously representing the expected or typical conditions for a particular region. Curves with multiple peaks indicate either strong, stable spatial differences (highland vs lowlands conditions), or a strong modal character of the regions climate (e.g., a region is either has very warm years, or very cold years but rarely is in between). The different coloured curves indicate how conditions are expected to change into the future. As the curves are all distinct and the direction of change across the five time-periods is consistent, this indicates all ensemble members agree on the rate and direction of warming into the future. The future curves are typically lower and broader as different simulations follow different trajectories, increasing the variability within the population of values.

METHODS AND INTERPRETATION

Heat

(continued)

The grey curves are the probability distribution for contrasting Australian wine regions, selected to present the range observed across Australia, and indicate the approximate analogues a region may become similar to into the future. These grey curves are calculated using the Australian Gridded Climate Data product from the period 1997–2017. The coloured curves are calculated using the bias-adjusted CFAP2019 ensemble during the period 2001–2020. As there are differences between these two archives, the 2001–2020 curves for these selected regions are slightly different to the grey curves. These differences are expected.

Growing Degree Days

Growing Degree Days calculations are not standardised across Australia. Growers within each GI often have their own adaptation either for their vineyard or across their region. As such, GDD means different things to different people and the values are not interchangeable. For this atlas, we selected a method to calculate GDD that was standardised, relevant and useful across Australia. The two main limitations of existing methods were: 1) limiting the period where heat is accumulated to after October — this does not account for the effect of warm winter/spring periods, increasingly important under a warming climate; 2) limiting the influence of heat to daily values >10°C — this does not account for physiological responses that clearly occur at far lower temperatures, especially during the winter/spring period.

In response to these limitations, we established a new method to use daily climate values as inputs, take into account the influence of heat across the entire growing year (July to June) and reflect the physiological demands of grape vines as they change throughout the year. The method is simple enough to implement (and adjust) at the vineyard scale where required (by users external to the atlas) and remains relevant into warmer future conditions. The approach captures the importance of increased heat accumulation prior to October as the climate warms, providing a better representation of the impacts expected to be seen into the future, while also improving the utility of the GDD metric as a measure of heat accumulation within cooler climates (or cooler seasons) as it better reflects the influence of low temperature days relevant to grape-vine phenology.

Method description

Growing Degree Day values for each day are calculated using this (standard) equation:

$$GDD = \max(\frac{T_{max} + T_{min}}{2} - T_{base}, 0)$$

Where: GDD = *Growing Degree Days*; T_{max} = Maximum daily temperature; T_{min} = Minimum daily temperature; T_{base} = the temperature threshold above which heat is considered of value to the vines.

The value of T_{base} is altered for three different phenological stages: *dormancy to budbreak*, *budbreak to leaf appearance*, *leaf appearance to harvest (or end of season)*, reflecting the physiological requirements of grape vines during these different periods of growth. We used the values determined by Moncur et al. (1989) and account for the most significant varieties cultivated in Australia, T_{base} for each phenological stage is set as: $T_{base} = 4°C$ from July 1st until *budbreak*; $T_{base} = 7°C$ from *budbreak* until *leaf appearance*; $T_{base} = 10°C$ from *leaf appearance* until June 30th.

The value of this adaptation is the additional information it provides earlier in the season, especially the influence of colder days, which are particularly important within cooler climate regions. However, in order to implement this approach, accumulated GDD values that indicate when each threshold has been reached are required such that the timing of these trigger points within each year can be estimated. Given that cool climate varietals are more likely to be sensitive to this method than those suited to warmer climates, the thresholds were estimated using data presented by Moncur et al. (1989). Thus, the above transition points for T_{base} as defined by accumulated GDD thresholds were: *budbreak* = 350 GDD; *leaf appearance* = 1000 GDD. In order to provide a useful translation of different GDD approaches, lookup tables are presented comparing the method used within this atlas (which we have called the $GDD_{Adjusted}$ method) and a range of methods used from across Australia. These are presented for four contrasting regions:

		GDD										
		July–June					October–April					Adjusted
Month	T_{base}	10°C	7°C	4°C	2°C	0°C	10°C	7°C	4°C	2°C	0°C	4-7-10°C
Jul		0	70	163	225	287	—	—	—	—	—	163
Aug		4	157	343	467	591	—	—	—	—	—	343
Sep		50	292	568	752	936	—	—	—	—	—	484
Oct		135	471	840	1086	1332	85	178	271	333	395	663
Nov		271	697	1156	1462	1768	221	404	587	709	831	889
Dec		464	983	1535	1903	2271	414	690	966	1150	1334	1121
Jan		702	1313	1958	2388	2818	652	1021	1390	1636	1882	1358
Feb		910	1605	2334	2820	3306	860	1313	1766	2068	2370	1566
Mar		1104	1893	2715	3263	3811	1054	1600	2146	2510	2874	1761
Apr		1222	2100	3012	3620	4228	1172	1808	2444	2868	3292	1878
May		1274	2246	3251	3921	4591	1172	1808	2444	2868	3292	1931
Jun		1278	2330	3425	4155	4885	1172	1808	2444	2868	3292	1935

Table 3: Mean cumulative monthly GDD for example location in Tasmania East Coast for the current period (1997–2017)

		GDD										
		July–June					October–April					Adjusted
Month	T_{base}	10°C	7°C	4°C	2°C	0°C	10°C	7°C	4°C	2°C	0°C	4-7-10°C
Jul		0	70	163	225	287	—	—	—	—	—	163
Aug		9	167	353	477	601	—	—	—	—	—	353
Sep		63	311	587	771	955	—	—	—	—	—	497
Oct		177	518	887	1133	1379	114	207	300	362	424	704
Nov		368	799	1258	1564	1870	305	488	671	793	915	985
Dec		623	1148	1700	2068	2436	560	836	1112	1296	1480	1247
Jan		947	1565	2210	2640	3070	884	1253	1622	1868	2114	1571
Feb		1240	1942	2671	3157	3643	1177	1630	2083	2385	2687	1864
Mar		1484	2278	3100	3648	4196	1421	1967	2513	2877	3241	2107
Apr		1628	2512	3424	4032	4640	1565	2201	2837	3261	3685	2251
May		1695	2672	3677	4347	5017	1565	2201	2837	3261	3685	2318
Jun		1696	2751	3846	4576	5306	1565	2201	2837	3261	3685	2320

Table 4: Mean cumulative monthly GDD for example location in Coonawarra for the current period (1997–2017)

		GDD										
		July–June					October–April					Adjusted
Month	T_{base}	10°C	7°C	4°C	2°C	0°C	10°C	7°C	4°C	2°C	0°C	4-7-10°C
Jul		87	180	273	335	397	—	—	—	—	—	273
Aug		186	372	558	682	806	—	—	—	—	—	492
Sep		306	582	858	1042	1226	—	—	—	—	—	702
Oct		493	862	1231	1477	1723	187	280	373	435	497	982
Nov		761	1220	1679	1985	2291	454	637	820	942	1064	1256
Dec		1105	1657	2209	2577	2945	798	1074	1350	1534	1718	1600
Jan		1513	2158	2803	3233	3663	1206	1575	1944	2190	2436	2008
Feb		1889	2618	3347	3833	4319	1583	2036	2489	2791	3093	2384
Mar		2257	3079	3901	4449	4997	1951	2497	3043	3407	3771	2752
Apr		2520	3432	4344	4952	5560	2213	2849	3485	3909	4333	3015
May		2710	3715	4720	5390	6060	2213	2849	3485	3909	4333	3205
Jun		2823	3918	5013	5743	6473	2213	2849	3485	3909	4333	3318

Table 5: Mean cumulative monthly GDD for example location in Geographe for the current period (1997–2017)

		GDD										
		July–June					October–April					Adjusted
Month	T_{base}	10°C	7°C	4°C	2°C	0°C	10°C	7°C	4°C	2°C	0°C	4-7-10°C
Jul		99	192	285	347	409	—	—	—	—	—	285
Aug		218	404	590	714	838	—	—	—	—	—	518
Sep		364	640	916	1100	1284	—	—	—	—	—	754
Oct		589	958	1327	1573	1819	224	317	410	472	534	1054
Nov		909	1368	1827	2133	2439	544	727	910	1032	1154	1374
Dec		1311	1863	2415	2783	3151	946	1222	1498	1682	1866	1776
Jan		1784	2429	3074	3504	3934	1420	1789	2158	2404	2650	2249
Feb		2220	2949	3678	4164	4650	1855	2308	2761	3063	3365	2685
Mar		2643	3465	4287	4835	5383	2279	2825	3371	3735	4099	3108
Apr		2949	3861	4773	5381	5989	2585	3221	3857	4281	4705	3414
May		3153	4158	5163	5833	6503	2585	3221	3857	4281	4705	3618
Jun		3275	4370	5465	6195	6925	2585	3221	3857	4281	4705	3740

Table 6: Mean cumulative monthly GDD for example location in Swan District for the current period (1997–2017)

Figure 6: Probability distribution of Growing Degree Days

Underlying data source: Climate Futures Australasian Projections 2019 (CFAP2019).

Annual Maximum Growing Degree Days is the sum of all daily GDD values (calculated as described above) over the period from July 1st to June 30th for each growing season year for each member within the *CCAM ensemble*. Grid cells selected were those within (or intersecting with the boundary of) the polygon that defined each wine industry *Australian Geographical Indications* (Wine Australia, 2019). Values were calculated for each grid cell.

The coloured curves represent the probability distribution of *Annual Maximum GDD* values from all grid cells and all ensemble members during each different 20-year period. Time periods were: 2001–2020; 2021–2040; 2041–2060; 2061–2080; 2081–2100.

The grey, filled curves represent the distribution of observed *Annual Maximum GDD* values within the *current period* (1997–2017) for contrasting wine industry *Australian Geographical Indications* (Wine Australia, 2019).

Interpretation:

Probability distributions reflect the spread and potential likelihood of values within a particular population of values. High, narrow peaks indicate low variability with a high frequency of particular values occurring within the population. Low, broad peaks indicate high variability, with few values occurring frequently. The probability distributions displayed in the atlas incorporate all spatial grid cell values, across each 20-year time period, from six ensemble members (i.e., independent simulations). Variability across spatial, temporal scales and across the CFAP2019 ensemble is represented with each curve. This has the advantage of reflecting the diversity that is found within each wine region (cooler vs warmer subregions) and across different types of years (e.g., hot, average or cold). Different ensemble members capture different climate configurations (e.g., El Niño, neutral, or La Niña phases of ENSO), thus better estimate the range of possible extremes. Low likelihood years (extreme hot or cold) can be included, indicating the possible, while simultaneously representing the expected or typical conditions for a particular region. Curves with multiple peaks indicate either strong, stable spatial differences (highland vs lowlands conditions), or strong modal character of the regions climate (e.g., a region is either has very warm years, or very cold years but rarely is in between). The different coloured curves indicate how conditions are expected to change into the future. As the curves are all distinct and the direction of change across the five time-periods is consistent, this indicates all ensemble members agree on the rate and direction of warming into the future. The future curves are typically lower and broader as different simulations follow different trajectories, increasing the variability within the population of values.

The grey curves are the probability distribution for contrasting Australian wine regions, selected to present the range observed across Australia, and indicate the approximate analogues a region may become similar to into the future. These grey curves are calculated using the Australian Gridded Climate Data product from the period 1997–2017. The coloured curves are calculated using the bias-adjusted CFAP2019 ensemble during the period 2001–2020. As there are differences between these two archives, the 2001–2020 curves for these selected regions are slightly different to the grey curves. These differences are expected.

Figure 7: Projected annual cumulative Growing Degree Days

Underlying data source: Climate Futures Australasian Projections 2019 (CFAP2019).

Annual Cumulative Growing Degree Days is the cumulative sum of all daily GDD values (calculated as described above) over the period from July 1st to June 30th for each growing season year for each member within the *CCAM ensemble*. Grid cells selected were those within (or intersecting with the boundary of) the polygon that defined each wine industry *Australian Geographical Indications* (Wine Australia, 2019). Values were calculated for each grid cell. Each curve represents the annual accumulation of heat for a single grid cell for each ensemble member. Time periods were: 2001–2020; 2021–2040; 2041–2060; 2061–2080; 2081–2100.

Dashed horizontal lines are indicative thresholds for important phenological stages across Australia (selected depending on the varietal, style or regional standards). For cooler regions they may represent only the harvest period, for warmer regions they may be approximately representative of flowering, veraison and harvest periods (for some varietals). The selection of these thresholds is broadly consistent with the heat accumulation hours represented within Moncur et al. (1989).

Interpretation:

Growing Degree Days curves reflect how the heat a region is exposed to accumulates across each growing year. Curves are allocated colours based on the time period within which they occur, demonstrating the projected interannual variability to be expected. Notably, the CFAP2019 ensemble has relatively similar projected futures (a narrow range), increasing the certainty of projected conditions. The shape of the GDD accumulation curves indicate how accumulation rates will change, where by 2081–2100, heat has accumulated in the system such that compared to 2001–2020, typical GDD values in: August occur 2 weeks earlier; October occur 4 weeks earlier; December occur 6 weeks earlier; and February occurs 8 weeks. Maximum values reached by the end of the growing year increase accordingly, with values never before experienced projected to become a regular expectation every few years.

The Growing Degree Days equation used within the atlas uses a novel method, designed to better represent the physiological requirements of grape vines during the entire growing year. In the context of climate change it is particularly important to accumulate heat from July (not October) as the influence of increased heat units at the beginning of the season are important to the potential timing of key phenological stages (for example, in 2017 many growers had already observed budbreak and flowering was occurring earlier in the season, often prior to October). Across most regions, the GDD units accumulated by October during the 2001–2020 period, are reached about 4–5 weeks earlier within the 2081–2100 period. Such substantial changes (and the potential impact on phenology) would not be represented using the typical October to April configuration of the GDD equation. In a similar way, using a T_{base} of 10°C (0°C) underestimates (overestimates) useful daily heat units in cooler (warmer) regions, thus the implementation of the staged T_{base} as described in the methods. It is recommended that users refer to the methods section (on page 55), where the translation of the GDD values presented within the atlas (i.e. $GDD_{Adjusted}$) are converted to other GDD configurations (e.g., $GDD_{T_{base10},Oct-Apr}$).

Figure 8: Probability distribution of date when Growing Degree Days reaches threshold

Underlying data source: Climate Futures Australasian Projections 2019 (CFAP2019).

Date when cumulative Growing Degree Days reaches threshold was calculated by determining the date within each year (for each member within the *CCAM ensemble*) when each cumulative Growing Degree Days threshold (1000, 1500, 2000, 2500) was exceeded. Values were calculated for each cell. Grid cells selected were those within (or intersecting with the boundary of) the polygon that defined each wine region's *Geographical Indications* (Wine Australia, 2019).

The coloured curves represent the probability distribution of *Date when cumulative Growing Degree Days reaches threshold* values from all grid cells and all ensemble members during each different 20-year period, displayed separately for each threshold. Time periods were: 2001–2020; 2021–2040; 2041–2060; 2061–2080; 2081–2100. Curves with <60 underlying values were excluded.

Interpretation:

Probability distributions reflect the spread and potential likelihood of values within a particular population of values. High, narrow peaks indicate low variability with a high frequency of particular values occurring within the population. Low, broad peaks indicate high variability, with few values occurring frequently. The probability distributions displayed in the atlas incorporate all spatial grid cell values, across each 20-year time period, from six ensemble members (i.e., independent simulations). Variability across spatial, temporal scales and across the CFAP2019 ensemble is represented with each curve. This has the advantage of reflecting the diversity that is found within each wine region (cooler vs warmer subregions) and across different types of years (e.g., hot, average or cold).

(continued)

Different ensemble members capture different climate configurations (e.g., El Niño, neutral, or La Niña phases of ENSO), thus better estimate the range of possible extremes. Low likelihood years (extreme hot or cold) can be included, indicating the possible, while simultaneously representing the expected or typical conditions for a particular region. Curves with multiple peaks indicate either strong, stable spatial differences (highland vs lowlands conditions), or strong modal character of the regions climate (e.g., a region is either has very warm years, or very cold years but rarely is in between).

The different coloured curves indicate how conditions are expected to change into the future. As the curves are all distinct and the direction of change across the five time-periods is consistent, this indicates all ensemble members agree on the rate and direction of warming into the future. The future curves are typically lower and broader as different simulations follow different trajectories, increasing the variability within the population of values.

For some wine regions, higher *Growing Degree Days* thresholds are not reached, or are reached irregularly. In these cases the curves have inconsistent, irregular shapes (due to a lack of underlying data, please note, curves with <60 underlying values were excluded). Irregular shapes should not be over-interpreted, they just indicate an emerging trend to reach these higher GDD thresholds. As these curves transition towards more *normal distributions*, there is higher confidence in the information they provide and they become more useful.

Moisture

Interpretation:

Rainfall projections from the bias adjusted CFAP2019 ensemble are the highest accuracy, highest precision rainfall projections currently available for Australia. Rainfall is a well understood weather and climate variable, controlled by the ocean, atmosphere and landform dynamics at large, medium and small scales across space and time. Large and medium scale processes are well resolved within the CFAP2019 ensemble, resulting in reasonable representation of the distribution of rainfall across Australia. This is exemplified with the representation of wet and dry subregions within some wine regions. However, it is those processes that occur at small spatial scales which are sometimes poorly resolved leading to inaccuracies or poor precision. As such, there is greater inaccuracy and precision within the projections of rainfall than there are for temperature. This means there is reduced levels of confidence (i.e greater uncertainty) surrounding projections of this variable.

There is often greater variability across the ensemble than there is spatially across a region, reflecting the large differences between wet and dry years across most regions. Each ensemble member describes a possible future, with different timing and sequencing of broad global drivers (such as the Southern Annular Mode (SAM), the El Niño Southern Oscillation (ENSO) and the Indian Ocean Dipole (IOD)). This results in the timing of wet or dry years being out of phase with each other, resulting in dramatically different projections of any one year (sometimes seen as disconnected clusters of points). Because of this, 10-year or 20-year averages (or distributions) are far more useful for characterising the rainfall typical for a wine region. Annualised values are useful for identifying the possible extremes, especially the potential timing of their occurrence (for example, is it more likely to have a wet year now, or by 2100?).

Figure 1: Observed mean Growing Season Rainfall

Underlying data source: Australian Gridded Climate Data Product (Jones et al., 2009).

Growing Season Rainfall (GSR) was calculated as the sum of all daily rainfall values within the period from October to April of each growing season year. Mean Growing Season Rainfall is the average of all annual GSR values over the *current period* (1997–2017). Grid cells selected were those within (or intersecting with the boundary of) the polygon that defined each wine industry *Australian Geographical Indications* (Wine Australia, 2019). Values were calculated for each grid cell.

Interpretation:

Each tile represents the mean Growing Season Rainfall during the period 1997–2017, (which is the period of recent memory). This map reflects the level of variability across the region as it is currently experienced, indicating subregions with higher or lower rainfall. Tiles are the resolution of the underlying data. Towns and roads are included to help identify specific sites within the region. Rain shadows are often visible, although the exact boundaries should be interpreted with caution, especially in small regions where grid cells may be large compared to the controlling topographic features.

Figure 2: Observed change in mean Growing Season Rainfall

Underlying data source: Australian Gridded Climate Data Product (Jones et al., 2009).

Growing Season Rainfall (GSR) was calculated as the sum of all daily rainfall values within the period from October to April of each growing season year. Mean Growing Season Rainfall is the average of all annual GSR values over the *current period* (1997–2017), or the *baseline period* (1961–1990). The *baseline period* mean GSR was then subtracted from the *current period* mean GSR, resulting in the *observed change in mean GSR*. Grid cells selected were those within (or intersecting with the boundary of) the polygon that defined each wine industry *Australian Geographical Indications* (Wine Australia, 2019). Values were calculated for each grid cell.

Interpretation:

Each tile represents how mean Growing Season Rainfall during the current period (1997–2017) has changed when compared to mean Growing Season Rainfall during the historical period (1961–1990). Change is presented in millimetres. Towns and roads are included to help identify specific sites within the region. Rain shadows are often visible, although the exact boundaries should be interpreted with caution, especially in small regions where grid cells may be large compared to the influential topographic features.

Figure 3: Projected mean Growing Season Rainfall

Underlying data source: Climate Futures Australasian Projections 2019 (CFAP2019).

Growing Season Rainfall (GSR) was calculated as the sum of all daily rainfall values within the period from October to April of each growing season year for each member within the *CFAP2019*. Grid cells selected were those within (or intersecting with the boundary of) the polygon that defined each wine industry *Australian Geographical Indications* (Wine Australia, 2019). Values were calculated for each grid cell. Mean Growing Season Rainfall is the average of all annual GSR values within each time period (2021–2040; 2041–2060; 2061–2080; 2081–2100). These were calculated for each ensemble member within the *CFAP2019*. The 6 ensemble member values (for each cell) are averaged generating the ensemble mean for each cell within the region.

Interpretation:

Each tile represents the mean Growing Season Rainfall during each 20-year period of 2021–2040, 2041–2060, 2061–2080, 2081–2100 (following the RCP8.5 scenario). These reflect the level of variability across the region, indicating subregions with higher or lower rainfall and how these are projected to change into the future. Tiles are the resolution of the underlying data. Towns and roads are included to help identify specific sites within the region. Rain shadows are often visible, although the exact boundaries should be interpreted with caution, especially in small regions where grid cells may be large compared to the influential topographic features.

Figure 4: Projected annual Growing Season Rainfall (October to April)

Underlying data source: Climate Futures Australasian Projections 2019 (CFAP2019).

Blue points: Growing Season Rainfall (GSR) was calculated as the sum of all daily rainfall values within the period from October to April of each growing season year for each member within the *CFAP2019*. Grid cells selected were those within (or intersecting with the boundary of) the polygon that defined each wine industry *Australian Geographical Indications* (Wine Australia, 2019). Values were calculated for each grid cell.

Grey Bars: The grey bars represent the observed mean GSR for the *current period* (1997–2017) from contrasting wine industry *Australian Geographical Indications* (Wine Australia, 2019). Values were averaged across space and time, calculated from the Australian Gridded Climate Data product (Jones, et al., 2009).

Coloured zones: The coloured zones indicate the ensemble mean time when *average global climate temperature* increases by 1°C, 2°C, 3°C or 4°C, following the Representative Concentration Pathway 8.5 scenario (RCP8.5, often referred to as the *business as usual* scenario). These estimates were taken from the Intergovernmental Panel on Climate Change Fifth Assessment Report (IPCC-AR5), which are based on the World Climate Research Programme (WCRP) Coupled Model Intercomparison Project - phase 5 (CMIP5) global climate model archive.

Interpretation:

Key elements:

- Natural variability of Growing Season Rainfall is very high over the entire 140 year period for most regions, with dramatic differences between wet and dry years. Regional variability in any one year is exhibited by large regions.
- For most regions, Growing Season Rainfall exhibits minimal influence of climate change, with natural variability dominating the signal out to 2100.

(continued)

- Ensemble members do not always agree in the direction or magnitude of the projected changes following the RCP8.5 scenario. When they disagree, there is reduced confidence in projected changes to Growing Season Rainfall. Decreasing rainfall trends are common across the CFAP2019 ensemble, however, for some regions rainfall is not projected to change substantially (i.e., the trends are neutral). Increasing rainfall trends are rare across all the wine regions, with only a single ensemble member indicating this direction in those cases. This reduces the certainty, as it indicates divergent possibilities for the future of those regions.
- Extremely wet years can occur at any time over the 140 period.

Each point represents the annual Growing Season Rainfall for individual grid cells within the region for each separate CFAP2019 ensemble member. For each year, the spread of points represents the spatial variability as well as the variability across the ensemble members. From 1961 to 2100, interannual and decadal variability dominate the projected future, with no obvious influence of climate change across most regions.

The grey bars are the regional average for contrasting GIs across Australia. They do not represent the regional variability within each of those GIs, but are intended to provide approximate climate analogues to aid interpretation.

The coloured zones are intended to be used independently of the *Growing Year (July to June)* axis, allowing decisions to be made based on the expected magnitude of global warming (such as those national governments are committed to within the *Paris Agreements*), rather than being based on the passage of time. This allows these plots to be useful regardless of the emissions scenario the world eventually follows.

Figure 5: Projected annual Non-Growing Season Rainfall (May to September)

Underlying data source: Climate Futures Australasian Projections 2019 (CFAP2019).

Non-Growing Season Rainfall is the sum of all daily rainfall values within the period from May to September of each calendar year (i.e., the May to September prior to the growing season year) for each member within the *CFAP2019*. Grid cells selected were those within (or intersecting with the boundary of) the polygon that defined each wine industry *Australian Geographical Indications* (Wine Australia, 2019). Values were calculated for each grid cell.

Grey Bars: The grey bars represent the observed mean Non-Growing Season Rainfall for the *current period* (1997–2017) from contrasting wine industry *Australian Geographical Indications* (Wine Australia, 2019). Values were averaged across space and time, calculated from the Australian Gridded Climate Data product (Jones, et al., 2009).

Coloured zones: The coloured zones indicate the ensemble mean time when *average global climate temperature* increases by 1°C, 2°C, 3°C or 4°C, following the Representative Concentration Pathway 8.5 scenario (RCP8.5, often referred to as the *business as usual* scenario). These estimates were taken from the Intergovernmental Panel on Climate Change Fifth Assessment Report (IPCC-AR5), which are based on the World Climate Research Programme (WCRP) Coupled Model Intercomparison Project - phase 5 (CMIP5) global climate model archive.

Interpretation:

Key elements:

- Natural variability of Non-Growing Season Rainfall is very high over the entire 140 year period for most regions, with dramatic differences between wet and dry years. Regional variability in any one year is exhibited by large regions.
- For Non-Growing Season Rainfall the influence of climate change is observable from around the 2000s onwards for most regions, although for some the influence appears to have been since the 1980s and for others there is no obvious climate change signal at all.
- Although ensemble members do not always agree on the magnitude of the projected changes, following the RCP8.5 scenario most regions exhibit a drying trend during the non-growing season into the future. Where this trend is occurring, model agreement in the direction provides improved confidence, however the rate and magnitude is far less certain.

(continued)

- Where the drying trend is clear, extremely wet years become far less common into the future. Where there is no obvious change, wet years are equally likely across the 140 year period.

Each point represents the annual Non-Growing Season Rainfall for individual grid cells within the region for each separate CFAP2019 ensemble member. For each year, the spread of points represents the spatial variability as well as the variability across the ensemble members. In most cases, ensemble member variability (an ensemble member either has a wet, average or dry year) is larger than regional variability (an entire region typically has a wet, average or dry year, rather than a subregion being wet while the rest is dry).

The grey bars are the regional average for contrasting GIs across Australia. They do not represent the regional variability within each of those GIs, but are intended to provide approximate climate analogues to aid interpretation.

The coloured zones are intended to be used independently of the *Growing Year (July to June)* axis, allowing decisions to be made based on the expected magnitude of global warming (such as those national governments are committed to within the *Paris Agreements*), rather than being based on the passage of time. This allows these plots to be useful regardless of the emissions scenario the world eventually follows.

Figure 6: Projected monthly rainfall

Underlying data source: Climate Futures Australasian Projections 2019 (CFAP2019).

Monthly Rainfall was calculated as the sum of all daily rainfall values within each month, for each year and each ensemble member within the *CFAP2019*. Grid cells selected were those within (or intersecting with the boundary of) the polygon that defined each wine industry *Australian Geographical Indications* (Wine Australia, 2019). Values were calculated for each grid cell.

Violin plots represent 20-years of values for each month within each time period (2021–2040; 2041–2060; 2061–2080; 2081–2100). All individual spatial and ensemble member values are included, no spatial or ensemble averaging is performed.

Interpretation:

Violin plots are a combination of box-and-whisker plots and probability distribution curves. Like a box-and-whisker plot, the shape is defined by the values within that population. The *violin* is created by mirroring the probability distribution of the values, plotted in the vertical direction, describing the frequency and spread of values in the y-axis space. Where there is a concentration of values, the *violin* is broad. Where there are few values the *violin* is narrow (possibly only a single line). As the probability distribution is continuous, where extreme outlier values occur, narrow lines can be drawn between the main body and the outlier (typical of high rainfall areas that may receive extremely high rainfall events in some years). Where very low values are common, *violins* can look odd, with very wide bases and narrow tops (typical of low rainfall areas, that may typically receive almost no rainfall in some months, but then rarely receive comparatively high rainfall events in some years).

Differences between the months, or time periods is expressed as changes to the shape of each *violin*. The 2001–2020 *violin* for each month is shadowed underneath future time periods, so that changes in future periods can be more easily determined.

Figure 7: Probability distribution of seasonal rainfall

Underlying data source: Climate Futures Australasian Projections 2019 (CFAP2019).

Seasonal Rainfall is the sum of all daily rainfall values within each calendar season (Winter, Spring, Summer, Autumn), for each growing season year for each ensemble member within the *CFAP2019*. Grid cells selected were those within (or intersecting with the boundary of) the polygon that defined each wine industry *Australian Geographical Indications* (Wine Australia, 2019). Values were calculated for each grid cell. All individual spatial and ensemble member values are included, no spatial or ensemble averaging is performed.

The coloured curves represent the probability distribution of *seasonal rainfall* values from all grid cells and all ensemble members during each different 20-year period. Time periods were: 2001–2020; 2021–2040; 2041–2060; 2061–2080; 2081–2100.

The grey, filled curves represent the distribution of observed *seasonal rainfall* values within the *current period* (1997–2017) for contrasting wine industry *Australian Geographical Indications* (Wine Australia, 2019).

Interpretation:

Probability distributions reflect the spread and potential likelihood of values within a particular population of values. High, narrow peaks indicate low variability with a high frequency of particular values occurring within the population. Low, broad peaks indicate high variability, with few values occurring frequently. The probability distributions displayed in the atlas incorporate all spatial grid cell values, across each 20-year time period, from six ensemble members (i.e., independent simulations). Variability across spatial and temporal scales as well as across the CFAP2019 ensemble is represented with each curve. This has the advantage of reflecting the diversity that is found within each wine region (wetter vs drier subregions) and across different types of years (e.g., wet, average or dry). Different ensemble members capture different climate configurations (e.g., El Niño, neutral, or La Niña phases of ENSO), thus better estimate the range of possible extremes. Low likelihood years (extreme wet or dry) can be included, indicating what is possible, while simultaneously representing the expected or typical conditions for a particular region. Curves with multiple peaks indicate either strong, stable spatial differences (e.g., desert adjacent to alpine), or a strong modal character of the regions climate (e.g., a region either has wet years, or dry years but rarely average years). The different coloured curves indicate how conditions are expected to change into the future. The future curves are typically lower and broader as different simulations follow different trajectories, increasing the variability within the population of values.

When curves for each time period are all distinct and the direction of change across the five time-periods is consistent, this indicates all ensemble members agree broadly on the rate and direction of warming into the future. In such cases there is increased certainty surrounding the projected future.

When the curves from all time periods are overlapping, natural variability dominates the climate change trend, with the future conditions projected to be much the same as at present.

When the direction of change is confused between time periods, or the spread of the curve is significantly broadened (but the average conditions are more or less the same), ensemble variability is high, there is significant uncertainty regarding the projections of the future.

The grey curves are the probability distribution for contrasting Australian wine regions, selected to present the range observed across Australia, and indicate the approximate analogues a region may become similar to into the future. These grey curves are calculated using the Australian Gridded Climate Data product from the period 1997–2017. The coloured curves are calculated using the bias-adjusted CFAP2019 ensemble during the period 2001–2020. As there are differences between these two archives, the 2001–2020 curves for these selected regions are slightly different to the grey curves. These differences are expected.

Figure 8: Probability distribution of number of rainy days during harvest

Underlying data source: Climate Futures Australasian Projections 2019 (CFAP2019).

Harvest date was determined as the date within each year when each cumulative Growing Degree Days threshold (1000, 1500, 2000, 2500) was exceeded. The *harvest period* was determined as the 15-day period, starting 7 days before the *harvest date* and ending 7 days after the *harvest date*. Thus, there were 4 potential *harvest periods*, to account for different regional, varietal or style preferences of different users of the atlas. The *number of rainy days during harvest* was calculated by counting the number of days with rainfall >10mm during the *harvest period*. Values were calculated for each cell and for each ensemble member within *CFAP2019*. Grid cells selected were those within (or intersecting with the boundary of) the polygon that defined each wine region's *Geographical Indications* (Wine Australia, 2019).

The coloured curves represent the probability distribution of *number of rainy days during harvest* values from all grid cells and all ensemble members during each different 20-year period. Time periods were: 2001–2020; 2021–2040; 2041–2060; 2061–2080; 2081–2100. These are displayed separately for each GDD threshold (1000, 1500, 2000, 2500). Higher thresholds were often not reached in some regions. Only curves that represented >60 individual values were displayed (otherwise they were excluded, as they would only represent outliers).

Interpretation:

Probability distributions reflect the spread and potential likelihood of values within a particular population of values. High, narrow peaks indicate low variability with a high frequency of particular values occurring within the population. Low, broad peaks indicate high variability, with few values occurring frequently. The probability distributions displayed in the atlas incorporate all spatial grid cell values, across each 20-year time period, from six ensemble members (i.e., independent simulations). Variability across spatial and temporal scales as well as across the CFAP2019 ensemble is represented with each curve. This has the advantage of reflecting the diversity that is found within each wine region (wetter vs drier subregions) and across different types of years (e.g., wet, average or dry). Different ensemble members capture different climate configurations (e.g., El Niño, neutral, or La Niña phases of ENSO), thus better estimate the range of possible extremes. Low likelihood years (extreme wet or dry) can be included, indicating what is possible, while simultaneously representing the expected or typical conditions for a particular region. Curves with multiple peaks indicate either strong, stable spatial differences (e.g., desert adjacent to alpine zones), or a strong modal character of the regions climate (e.g., a region either has wet years, or dry years but rarely average years). The different coloured curves indicate how conditions are expected to change into the future. The future curves are typically lower and broader as different simulations follow different trajectories, increasing the variability within the population of values.

When curves for each time period are all distinct and the direction of change across the five time-periods is consistent, this indicates all ensemble members agree broadly on the rate and direction of warming into the future. In such cases there is increased certainty surrounding the projected future.

When the curves from all time periods are overlapping, natural variability dominates the climate change trend, with the future conditions projected to be much the same as at present.

When the direction of change is confused between time periods and the spread of the curve is significantly broadened (but the average conditions are more or less the same), ensemble variability is high, there is significant uncertainty regarding the projections of the future.

Aridity

Figure 1: Observed mean annual aridity index

Underlying data source: Australian Gridded Climate Data Product (Jones et al., 2009).

Annual Aridity Index was calculated as P/E where: P = the sum of daily rainfall during the period from July to June each annual cycle; and E = the sum of daily evaporation during the period from July to June each annual cycle. Aridity Index values below 0.05 and above 2 offer limited meaningful information, so values >0.05 were rounded up to 0.05 and values >2 were rounded down to 2. Mean Annual Aridity Index is the average of all Annual Aridity Index values over the *current period* (1997–2017). Grid cells selected were those within (or intersecting with the boundary of) the polygon that defined each wine industry *Australian Geographical Indications* (Wine Australia, 2019). Values were calculated for each grid cell.

Interpretation:

Each tile represents the mean annual Aridity Index during the period 1997–2017, (which is the period of recent memory). This map reflects the level of variability across the region as it is currently experienced, indicating drier/wetter Aridity Index subregions (if they exist). Tiles are the resolution of the underlying data. Towns and roads are included to help identify specific sites within the region. Rain shadows or regions more exposed to evaporation are often visible, although the exact boundaries should be interpreted with caution, especially in small regions where grid cells may be large compared to the controlling topographic features.

Figure 2: Observed change in mean annual aridity index

Underlying data source: Australian Gridded Climate Data Product (Jones et al., 2009).

Annual Aridity Index was calculated as P/E where: P = the sum of daily rainfall during the period from July to June each annual cycle; and E = the sum of daily evaporation during the period from July to June each annual cycle. Mean Annual Aridity Index is the average of all Annual Aridity Index values over the *current period* (1997–2017), or the *baseline period* (1961–1990). The *baseline period* mean Annual Aridity Index was then subtracted from the *current period* mean Annual Aridity Index, resulting in the *observed change in mean Annual Aridity Index* (as an absolute value). This was divided by the *baseline period* mean Annual Aridity Index and multiplied by 100 to produce the *observed change in mean Annual Aridity Index* as a percentage), which was considered more useful than the logarithmic scale of the aridity index. Grid cells selected were those within (or intersecting with the boundary of) the polygon that defined each wine industry *Australian Geographical Indications* (Wine Australia, 2019). Values were calculated for each grid cell.

Interpretation:

Each tile represents how mean annual Aridity Index during the current period (1997–2017) has changed when compared to mean annual Aridity Index during the historical period (1961–1990). Change is presented as a percentage, to allow regions with high variability to understand the rate of change within their subregion. Towns and roads are included to help identify specific sites within the region. Rain shadows or regions more exposed to evaporation are often visible, although the exact boundaries should be interpreted with caution, especially in small regions where grid cells may be large compared to the controlling topographic features.

Figure 3: Projected mean annual aridity index

Underlying data source: Climate Futures Australasian Projections 2019 (CFAP2019).

Annual Aridity Index was calculated as P/E where: P = the sum of daily rainfall during the period from July to June each annual cycle; and E = the sum of daily evaporation during the period from July to June each annual cycle. Grid cells selected were those within (or intersecting with the boundary of) the polygon that defined each wine industry *Australian Geographical Indications* (Wine Australia, 2019). Values were calculated for each grid cell. Mean Annual Aridity Index is the average of all Annual Aridity Index values within each time period (2021–2040; 2041–2060; 2061–2080; 2081–2100). These were calculated for each ensemble member within the *CFAP2019*. The 6 ensemble member values (for each cell) are averaged to produce the ensemble mean for each cell within the region.

Interpretation:

Each tile represents the mean annual Aridity Index during each 20-year period of 2021–2040, 2041–2060, 2061–2080, 2081–2100 (following the RCP8.5 scenario). These reflect the level of variability across the region, indicating drier/wetter subregions (if they exist) and how these are projected to change into the future. Tiles are the resolution of the underlying data. Towns and roads are included to help identify specific sites within the region. Rain shadows or regions more exposed to evaporation are often visible, although the exact boundaries should be interpreted with caution, especially in small regions where grid cells may be large compared to the controlling topographic features.

All Australian wine regions exhibit annual Aridity Index values that are decreasing into the future, indicating a drier, moisture constrained future.

Figure 4: Projected annual aridity index

Underlying data source: Climate Futures Australasian Projections 2019 (CFAP2019).

Blue points: Annual Aridity Index was calculated as P/E where: P = the sum of daily rainfall during the period from July to June each annual cycle; and E = the sum of daily evaporation during the period from July to June each annual cycle. Grid cells selected were those within (or intersecting with the boundary of) the polygon that defined each wine industry *Australian Geographical Indications* (Wine Australia, 2019). Values were calculated for each grid cell.

Grey Bars: The grey bars represent the observed mean Annual Aridity Index for the *current period* (1997–2017) from contrasting wine industry *Australian Geographical Indications* (Wine Australia, 2019). Values were averaged across space and time, calculated from the Australian Gridded Climate Data product (Jones, et al., 2009).

Coloured zones: The coloured zones indicate the ensemble mean time when *average global climate temperature* increases by 1°C, 2°C, 3°C or 4°C, following the Representative Concentration Pathway 8.5 scenario (RCP8.5, often referred to as the *business as usual* scenario). These estimates were taken from the Intergovernmental Panel on Climate Change Fifth Assessment Report (IPCC-AR5), which are based on the World Climate Research Programme (WCRP) Coupled Model Intercomparison Project - phase 5 (CMIP5) global climate model archive.

Interpretation:

Key elements:

- Ensemble members broadly agree on the magnitude and direction of the projected changes. Following the RCP8.5 scenario most regions exhibit a drying trend.
- Extremely wet years become far less common in the future.
- For annual Aridity Index, the influence of climate change is obvious from around 2020 onwards for most regions, although for some regions the influence appears to have been since about the 1980s.
- Values are limited to between 0.05 and 2 (outside of this range values become meaningless). As such, in some cases, values cluster at these boundaries. Divergence away from these clusters (say from 2 to 1.5) indicates a significant, strong drying trend.
- Data is presented on a log scale, as the differences across regions (e.g., the difference between the Riverland and the Barossa Valley) are difficult to see on a standard scale.
- Due to the log scale, decreasing trends are amplified (so they look steeper than they are), however, this is a good representation of how these rapid changes in moisture availability will be experienced on the ground (a small change in the Aridity Index has a big impact).

(continued)

Each point represents the annual Aridity Index for each grid cell within the region for each separate CFAP2019 ensemble member. For each year, the spread of points represents the spatial variability as well as the variability across the ensemble members. In most cases, ensemble member variability (an ensemble member either has a wet, average or dry year) is larger than regional variability (an entire region typically has a wet, average or dry year, rather than a subregion being wet while the rest is dry).

The grey bars are the regional average for contrasting GIs across Australia. They do not represent the regional variability within each of those GIs, but are intended to provide approximate climate analogues to aid interpretation.

The coloured zones are intended to be used independently of the *Growing Year (July to June)* axis, allowing decisions to be made based on the expected magnitude of global warming (such as those national governments are committed to within the *Paris Agreements*), rather than being based on the passage of time. This allows these plots to be useful regardless of the emissions scenario the world eventually follows.

Figure 5: Projected monthly aridity index

Underlying data source: Climate Futures Australasian Projections 2019 (CFAP2019).

Monthly aridity index was calculated as P/E where: P = the sum of rainfall within each month (per year); and E = the sum of evaporation within each month. Values were calculated for each month, within each year, for each ensemble member within the *CFAP2019*. Grid cells selected were those within (or intersecting with the boundary of) the polygon that defined each wine industry *Australian Geographical Indications* (Wine Australia, 2019). Values were calculated for each grid cell.

Violin plots represent 20-years of values for each month within each time period (2021–2040; 2041–2060; 2061–2080; 2081–2100). All individual spatial and ensemble member values are included, no spatial or ensemble averaging is performed.

Interpretation:

Violin plots are a combination of box-and-whisker plots and probability distribution curves. Like a box-and-whisker plot, the shape is defined by the values within that population. The *violin* is created by mirroring the probability distribution of the values, plotted in the vertical direction, describing the frequency and spread of values in the y-axis space. Where there is a concentration of values, the *violin* is broad. Where there are few values the *violin* is narrow (possibly only a single line). As the probability distribution is continuous, where extreme outlier values occur, narrow lines can be drawn between the main body and the outlier (typical of high rainfall areas/months that may be particularly dry in some years).

Differences between the months, or time periods is expressed as changes to the shape of each *violin*. The 2001–2020 *violin* for each month is shadowed underneath future time periods, so that changes in future periods can be more easily determined.

Figure 6: Probability distribution seasonal aridity index

Underlying data source: Climate Futures Australasian Projections 2019 (CFAP2019).

Seasonal Aridity Index is calculated as P/E where: P = the sum of rainfall within each calendar season (Winter, Spring, Summer, Autumn); and E = the sum of evaporation within each calendar season (Winter, Spring, Summer, Autumn). This is calculated for each growing season year and for each ensemble member within the *CFAP2019*. Grid cells selected were those within (or intersecting with the boundary of) the polygon that defined each wine industry *Australian Geographical Indications* (Wine Australia, 2019). Values were calculated for each grid cell. All individual spatial and ensemble member values are included, no spatial or ensemble averaging is performed.

The coloured curves represent the probability distribution of *Seasonal Aridity Index* values from all grid cells, all ensemble members and all years during each 20-year period. Time periods are: 2001–2020; 2021–2040; 2041–2060; 2061–2080; 2081–2100.

The grey, filled curves represent the distribution of observed *Seasonal Aridity Index* values within the *current period* (1997–2017) for contrasting wine industry *Australian Geographical Indications* (Wine Australia, 2019).

Interpretation:

Probability distributions reflect the spread and potential likelihood of values within a particular population of values. High, narrow peaks indicate low variability with a high frequency of particular values occurring within the population. Short, broad peaks indicate high variability, with few values occurring frequently. The probability distributions displayed in the atlas incorporate all spatial grid cell values, across each 20-year time period, from six ensemble members (i.e., independent simulations). Variability across spatial and temporal scales as well as across the CFAP2019 ensemble is represented with each curve. This has the advantage of reflecting the diversity that is found within each wine region (wetter vs drier subregions) and across different types of years (e.g., wet, average or dry). Different ensemble members capture different climate configurations (e.g., El Niño, neutral, or La Niña phases of ENSO), thus better estimate the range of possible extremes. Low likelihood years (extreme wet or dry) can be included, indicating what is possible, while simultaneously representing the expected or typical conditions for a particular region. Curves with multiple peaks indicate either strong, stable spatial differences (e.g., desert adjacent to alpine), or a strong modal character of the regions climate (e.g., a region either has wet years, or dry years but rarely average years). The different curves indicate how conditions are expected to change into the future. The future curves are typically shorter and broader as different simulations follow different trajectories, increasing the variability within the population of values.

When curves for each time period are all distinct and the direction of change across the five time-periods is consistent, this indicates all ensemble members agree broadly on the rate and direction of warming into the future. In such cases there is increased certainty surrounding the projected future.

When the curves from all time periods are overlapping, natural variability dominates the climate change trend, with the future conditions projected to be much the same as at present.

When the direction of change is confused between time periods, or the spread of the curve is significantly broadened (but the average conditions are more or less the same), ensemble variability is high, there is significant uncertainty regarding the projections of the future.

The grey curves are the probability distribution for contrasting Australian wine regions, selected to present the range observed across Australia, and indicate the approximate analogues a region may become similar to into the future. These grey curves are calculated using the Australian Gridded Climate Data product from the period 1997–2017. The coloured curves are calculated using the bias-adjusted CFAP2019 ensemble during the period 2001–2020. As there are differences between these two archives, the 2001–2020 curves for these selected regions are slightly different to the grey curves. These differences are expected.

Figure 7: Probability distribution of mean aridity index from season start until harvest

Underlying data source: Climate Futures Australasian Projections 2019 (CFAP2019).

Harvest date was determined as the date within each year when each cumulative Growing Degree Days threshold (1000, 1500, 2000, 2500) was exceeded. Thus, there were 4 potential *harvest dates*, to account for different regional, varietal or style preferences of different users of the atlas. The *aridity index from season start until harvest* was calculated as P/E, where: P = the sum of rainfall from July 1st to *harvest date*; and E = the sum of evaporation from July 1st to *harvest date*. Values were calculated for each cell and for each ensemble member within *CFAP2019*. Grid cells selected were those within (or intersecting with the boundary of) the polygon that defined each wine region's *Geographical Indications* (Wine Australia, 2019).

The coloured curves represent the probability distribution of *aridity index from season start until harvest* values for all grid cells and all ensemble members for all years during each different 20-year period, displayed separately for each GDD threshold. Time periods were: 2001–2020; 2021–2040; 2041–2060; 2061–2080; 2081–2100.

Interpretation:

Probability distributions reflect the spread and potential likelihood of values within a particular population of values. High, narrow peaks indicate low variability with a high frequency of particular values occurring within the population. Short, broad peaks indicate high variability, with few values occurring frequently. The probability distributions displayed in the atlas incorporate all spatial grid cell values, across each 20-year time period, from six ensemble members (i.e., independent simulations). Variability across spatial and temporal scales as well as across the CFAP2019 ensemble is represented with each curve. This has the advantage of reflecting the diversity that is found within each wine region (wetter vs drier subregions) and across different types of years (e.g., wet, average or dry). Different ensemble members capture different climate configurations (e.g., El Niño, neutral, or La Niña phases of ENSO), thus better estimate the range of possible extremes. Low likelihood years (extreme wet or dry) can be included, indicating what is possible, while simultaneously representing the expected or typical conditions for a particular region. Curves with multiple peaks indicate either strong, stable spatial differences (e.g., desert adjacent to alpine zones), or a strong modal character of the regions climate (e.g., a region either has wet years, or dry years but rarely average years). The different curves indicate how conditions are expected to change into the future. The future curves are typically shorter and broader as different simulations follow different trajectories, increasing the variability within the population of values.

When curves for each time period are all distinct and the direction of change across the five time-periods is consistent, this indicates all ensemble members agree broadly on the rate and direction of warming into the future. In such cases there is increased certainty surrounding the projected future.

When the curves from all time periods are overlapping, natural variability dominates the climate change trend, with the future conditions projected to be much the same as at present.

When the direction of change is confused between time periods and the spread of the curve is significantly broadened (but the average conditions are more or less the same), ensemble variability is high, there is significant uncertainty regarding the projections of the future.

Extreme Heat

Figure 1: Observed mean excess heat factor

Underlying data source: Australian Gridded Climate Data Product (Jones et al., 2009).

Excess Heat Factor (EHF) is an index that describes the severity of short term, acute heat impacts on humans during heat waves. It accounts for how hot a period of three days or more is in relation to an annual temperature threshold at a particular location, as well as how hot the period is with respect to the recent past (the previous 30 days). This reflects the fact that people acclimatise to a certain extent to their local climate but may not be prepared for a sudden rise in temperature above that of the recent past. The calculation is described in Nairn and Fawcett (2015). In order to apply this assessment into the future, the *baseline period* used to calculate the *typical annual temperatures* needed to be applied on a rolling basis, to take into account acclimatisation. The baseline period was always calculated as the previous 30 years (rounded to the nearest 5 years, so for example: the baseline period for the year 2019 was 1985–2014; the baseline period for the year 2020 was 1990–2019). Grid cells selected were those within (or intersecting with the boundary of) the polygon that defined each wine industry *Australian Geographical Indications* (Wine Australia, 2019). Values were calculated for each grid cell. Heatwave days were identified as those days when EHF is positive for 3 consecutive days or more. Mean EHF is the average of all observed EHF values during heatwave days within the *current period* (1997–2017).

Interpretation:

Each tile represents the mean Excess Heat Factor (EHF) during the period 1997–2017, (which is the period of recent memory). Higher (lower) EHF values indicate more (less) intense heatwaves. For more information refer to Nairn and Fawcett (2015). This map reflects the level of variability across the region as it is currently experienced. Lower values tend to be in regions exposed to large water bodies (typically oceans) that can provide relief, particularly overnight. Tiles are the resolution of the underlying data. Towns and roads are included to help identify specific sites within the region.

Figure 2: Observed change in excess heat factor

Underlying data source: Australian Gridded Climate Data Product (Jones et al., 2009).

Excess Heat Factor (EHF) is an index that describes the severity of short term, acute heat impacts on humans during heat waves. It accounts for how hot a period of three days or more is in relation to an annual temperature threshold at a particular location, as well as how hot the period is with respect to the recent past (the previous 30 days). This reflects the fact that people acclimatise to a certain extent to their local climate but may not be prepared for a sudden rise in temperature above that of the recent past. The calculation is described in Nairn and Fawcett (2015). In order to apply this assessment into the future, the *baseline period* used to calculate the *typical annual temperatures* needed to be applied on a rolling basis, to take into account acclimatisation. The baseline period was always calculated as the previous 30 years (rounded to the nearest 5 years, so for example: the baseline period for the year 2019 was 1985–2014; the baseline period for the year 2020 was 1990–2019). Grid cells selected were those within (or intersecting with the boundary of) the polygon that defined each wine industry *Australian Geographical Indications* (Wine Australia, 2019). Values were calculated for each grid cell. Heatwave days were identified as those days when EHF is positive for 3 consecutive days or more. Mean EHF is the average of all observed EHF values during heatwave days within the *current period* (1997–2017), or the *baseline period* (1961–1990). The *baseline period* mean EHF was then subtracted from the *current period* mean EHF, resulting in the *observed change in mean EHF*.

Interpretation:

Each tile represents how mean EHF during the current period (1997–2017) has changed when compared to mean EHF during the historical period (1961–1990). Climate change is a large scale feature, so the level of change observed is relatively similar when viewed at local scales. Higher (lower) EHF values indicate more (less) intense heatwaves. For more information refer to Nairn and Fawcett (2015).

(continued)

This map reflects the level of variability across the region as it is currently experienced. Lower values tend to be in regions exposed to features (typically oceans or higher elevations) that can provide relief, particularly overnight. Tiles are the resolution of the underlying data. Towns and roads are included to help identify specific sites within the region.

Figure 3: Projected mean excess heat factor

Underlying data source: Climate Futures Australasian Projections 2019 (CFAP2019).

Excess Heat Factor (EHF) is an index that describes the severity of short term, acute heat impacts on humans during heat waves. It accounts for how hot a period of three days or more is in relation to an annual temperature threshold at a particular location, as well as how hot the period is with respect to the recent past (the previous 30 days). This reflects the fact that people acclimatise to a certain extent to their local climate but may not be prepared for a sudden rise in temperature above that of the recent past. The calculation is described in Nairn and Fawcett (2015). In order to apply this assessment into the future, the *baseline period* used to calculate the *typical annual temperatures* needed to be applied on a rolling basis, to take into account acclimatisation. The baseline period was always calculated as the previous 30 years (rounded to the nearest 5 years, so for example: the baseline period for the year 2019 was 1985–2014; the baseline period for the year 2020 was 1990–2019). Grid cells selected were those within (or intersecting with the boundary of) the polygon that defined each wine industry *Australian Geographical Indications* (Wine Australia, 2019). Values were calculated for each grid cell.

Heatwave days were identified as those days when EHF is positive for 3 consecutive days or more.

Mean EHF is the average of all EHF values during heatwave days within each time period (2001–2020, 2021–2040; 2041–2060; 2061–2080; 2081–2100). These were calculated for each ensemble member within the *CFAP2019*. The 6 ensemble member values (for each cell) are averaged, generating the ensemble mean for each cell within the region.

Interpretation:

Each tile represents the mean EHF during each 20-year period of 2021–2040, 2041–2060, 2061–2080, 2081–2100 (following the RCP8.5 scenario). These reflect the level of variability across the region, and the rate of change projected into the future. In many regions, heatwave intensity is relatively stable, as EHF assumes communities will acclimatise to more extreme conditions and this index does not account for hard physiological limits. Higher (lower) EHF values indicate more (less) intense heatwaves. Tiles are the resolution of the underlying data.

Figure 4: Projected mean number of extreme heat days

Underlying data source: Climate Futures Australasian Projections 2019 (CFAP2019).

The annual number of days where daily maximum temperature exceeded either 30°C, 35°C, 40°C or 45 °C was calculated for each cell and ensemble member within *CFAP2019*. Grid cells selected were those within (or intersecting with the boundary of) the polygon that defined each wine industry *Australian Geographical Indications* (Wine Australia, 2019). Values were calculated for each grid cell. These values were then averaged into a regional ensemble mean for each year (i.e., a summary single value for each year from all inputs).

Interpretation:

The mean number of extreme heat days (based on various thresholds) is projected to increase into the future. In many regions, extreme temperatures that are rare will become common. Extreme temperatures that have never before been experienced will emerge as new challenges to manage. Natural variability is high, with high frequency extreme heat day years projected to occur regularly, interspersed by years where hot days are far less frequent. There is a strong, general trend towards greater frequencies of high temperature days into the future.

Figure 5: Projected number of days with severe risk to humans working outside

Underlying data source: Climate Futures Australasian Projections 2019 (CFAP2019).

Humans have physical limitations within which they can safely operate without adaptive technology or behaviours, with humidity contributing to heat stress. When temperatures are >30°C and humidity is >60%, conditions are classified as being a *Severe risk of heat stress* for humans. Days when both these conditions were met were classified as *high human heat stress days* and the annual count calculated. Grid cells selected were those within (or intersecting with the boundary of) the polygon that defined each wine industry *Australian Geographical Indications* (Wine Australia, 2019). Values were calculated for each grid cell. All individual spatial and ensemble member values are included, no spatial or ensemble averaging is performed.

Interpretation:

The number of days identified as exhibiting conditions that expose humans working outside to severe risk of heat stress (>30°C and >60% humidity) is projected to increase in many regions. Those regions at greatest risk are those where moisture availability remains high enough to support high humidity days.

In most regions, increases are projected to increase exponentially, diverging from historical levels from around 2020 onwards. For some regions, projections indicate 40–60 days at risk (i.e., most of summer) by the end of the century (following RCP8.5).

Figure 6: Projected range of hot summer days

Underlying data source: Climate Futures Australasian Projections 2019 (CFAP2019).

The annual 90th, 95th and 99th percentile values were calculated to characterise *Hot summer days* within each time period. Values were calculated for each year for each ensemble member within the *CFAP2019*. Grid cells selected were those within (or intersecting with the boundary of) the polygon that defined each wine industry *Australian Geographical Indications* (Wine Australia, 2019). Values were calculated for each grid cell.

Violin plots represent 20-years of values within each time period (2001–2020, 2021–2040; 2041–2060; 2061–2080; 2081–2100). All individual spatial and ensemble member values are included, no spatial or ensemble averaging is performed.

Interpretation:

Violin plots are a combination of box-and-whisker plots and probability distribution curves. Like a box-and-whisker plot, the shape is defined by the values within that population. The *violin* is created by mirroring the probability distribution of the values, plotted in the vertical direction, describing the frequency and spread of values in the y-axis space. Where there is a concentration of values, the *violin* is broad. Where there are few values the *violin* is narrow (possibly only a single line). As the probability distribution is continuous, where extreme outlier values occur, narrow lines can be drawn between the main body and the outlier.

Percentile values can be used to describe how the distribution of values changes. The 90th percentile represents the threshold above which are the ~35 hottest days of the year. The 95th percentile represents ~17 hottest days of the year. The 99th percentile represents ~4 hottest days of the year. By assessing these percentiles within each 20-year period, we can get an indication of how the *hot summer days* are changing. In most regions, by 2081–2100, the 90th percentile is projected to be hotter than the 2001–2020 95th percentile.

Differences between percentiles or time periods is expressed as changes to the shape of each *violin*.

Figure 7: Probability distribution of daily minimum and maximum temperature during a heatwave

Underlying data source: Climate Futures Australasian Projections 2019 (CFAP2019).

Excess Heat Factor (EHF) is an index that describes the severity of short term, acute heat impacts on humans during heat waves. The calculation is described in Nairn and Fawcett (2015). Heatwave days were identified as those days when EHF is positive for 3 consecutive days or more.

Date of Heatwave Days was determined as the date within each year a heatwave occurred. For multi-day events, all days were included and daily minimum and maximum temperature values of those days were extracted. Values were extracted for each cell and for each ensemble member within *CFAP2019*. Grid cells selected were those within (or intersecting with the boundary of) the polygon that defined each wine region's *Geographical Indications* (Wine Australia, 2019).

The coloured curves represent the probability distribution of *daily minimum temperature* and *daily maximum temperature* during a heatwave. Values are for all grid cells, all ensemble members, for all years during each 20-year period. Time periods were: 2001–2020; 2021–2040; 2041–2060; 2061–2080; 2081–2100. All individual spatial and ensemble member values are included, no spatial or ensemble averaging is performed.

Interpretation:

Probability distributions reflect the spread and potential likelihood of values within a particular population of values. High, narrow peaks indicate low variability with a high frequency of particular values occurring within the population. Short, broad peaks indicate high variability, with few values occurring frequently. The probability distributions displayed in the atlas incorporate all spatial grid cell values, across each 20-year time period, from six ensemble members (i.e., independent simulations). Variability across spatial and temporal scales as well as across the CFAP2019 ensemble is represented with each curve. This has the advantage of reflecting the diversity that is found within each wine region (wetter vs drier subregions) and across different types of years (e.g., wet, average or dry). Different ensemble members capture different climate configurations (e.g., El Niño, neutral, or La Niña phases of ENSO), thus better estimate the range of possible extremes. Low likelihood years (extreme wet or dry) can be included, indicating what is possible, while simultaneously representing the expected or typical conditions for a particular region. Curves with multiple peaks indicate either strong, stable spatial differences (e.g., desert adjacent to alpine), or a strong modal character of the regions climate (e.g., a region either has wet years, or dry years but rarely average years). The different curves indicate how conditions are expected to change into the future. The future curves are typically shorter and broader as different simulations follow different trajectories, increasing the variability within the population of values.

When curves for each time period are all distinct and the direction of change across the five time-periods is consistent, this indicates all ensemble members agree broadly on the rate and direction of warming into the future. In such cases there is increased certainty surrounding the projected future.

When the curves from all time periods are overlapping, natural variability dominates the climate change trend, with the future conditions projected to be much the same as at present.

When the direction of change is confused between time periods, or the spread of the curve is significantly broadened (but the average conditions are more or less the same), ensemble variability is high, there is significant uncertainty regarding the projections of the future.

Figure 8: Probability distribution of date of heatwave days

Underlying data source: Climate Futures Australasian Projections 2019 (CFAP2019).

Excess Heat Factor (EHF) is an index that describes the severity of short term, acute heat impacts on humans during heat waves. A definition of how it is calculated is described in Nairn and Fawcett (2015). Heatwave days were identified as those days when EHF was positive.

Date of Heatwave Days was determined as date within each year a heatwave occurred. For multi-day events, all values were included. Values were calculated for each cell and for each ensemble member within *CFAP2019*. Grid cells selected were those within (or intersecting with the boundary of) the polygon that defined each wine region's *Geographical Indications* (Wine Australia, 2019).

The coloured curves represent the probability distribution of *Date of Heatwave Days* values for all grid cells and all ensemble members for all years during each 20-year period. Time periods were: 2001–2020; 2021–2040; 2041–2060; 2061–2080; 2081–2100. All individual spatial and ensemble member values are included, no spatial or ensemble averaging is performed.

Interpretation:

Probability distributions reflect the spread and potential likelihood of values within a particular population of values. High, narrow peaks indicate low variability with a high frequency of particular values occurring within the population. Short, broad peaks indicate high variability, with few values occurring frequently. The probability distributions displayed in the atlas incorporate all spatial grid cell values, across each 20-year time period, from six ensemble members (i.e., independent simulations). Variability across spatial and temporal scales as well as across the CFAP2019 ensemble is represented with each curve. This has the advantage of reflecting the diversity that is found within each wine region (wetter vs drier subregions) and across different types of years (e.g., wet, average or dry). Different ensemble members capture different climate configurations (e.g., El Niño, neutral, or La Niña phases of ENSO), thus better estimate the range of possible extremes. Low likelihood years (extreme wet or dry) can be included, indicating what is possible, while simultaneously representing the expected or typical conditions for a particular region. Curves with multiple peaks indicate either strong, stable spatial differences (e.g., desert adjacent to alpine), or a strong modal character of the regions climate (e.g., a region either has wet years, or dry years but rarely average years). The different curves indicate how conditions are expected to change into the future. The future curves are typically shorter and broader as different simulations follow different trajectories, increasing the variability within the population of values.

When curves for each time period are all distinct and the direction of change across the five time-periods is consistent, this indicates all ensemble members agree broadly on the rate and direction of warming into the future. In such cases there is increased certainty surrounding the projected future.

When the curves from all time periods are overlapping, natural variability dominates the climate change trend, with the future conditions projected to be much the same as at present.

When the direction of change is confused between time periods, or the spread of the curve is significantly broadened (but the average conditions are more or less the same), ensemble variability is high, there is significant uncertainty regarding the projections of the future.

Heatwaves are a specifically characterised event. The date of heatwave days for most regions does not change significantly. Heatwaves are calculated relative to a *30-year baseline* period. However, within a climate change context, the 30-year baseline needs follow behind the *target year* (to account for acclimatisation of organisms within the region as the climate warms). This *rolling 30-year baseline period* warms with climate change. This ensures that the *hottest days* threshold typically occurs at the peak of summer (with a normally distributed spread surrounding this mean). The absolute temperatures of heatwaves are much hotter and in many regions the EHF values increase, indicating an increase in heatwave intensity, however, the chance of a heatwave in any month of the year is projected to remain relatively constant into the future.

Extreme Cold

Figure 1: Observed mean frost risk days

Underlying data source: Australian Gridded Climate Data Product (Jones et al., 2009).

A *frost risk day* was defined as any day when daily minimum temperature was <2°C.

Annual frost risk days is the number of individual *frost risk day* events that occur during the period from October to April each annual cycle.

Mean frost risk days is the average of all *annual frost risk days* within the *current period* (1997–2017).

Grid cells selected were those within (or intersecting with the boundary of) the polygon that defined each wine industry *Australian Geographical Indications* (Wine Australia, 2019). Values were calculated for each grid cell.

Interpretation:

Each tile represents the mean frost risk days during the period 1997–2017, (which is the period of recent memory). Higher (lower) frost risk values indicate more (less) days where minimum temperatures were <2°C. For many regions, frost risk is very low (often less than 1 day per year). This map reflects the level of variability across the region as it is currently experienced. Tiles are the resolution of the underlying data. Higher values typically correspond to higher elevation regions. Tiles have an average elevation of the area they represent, so they best represent regions that have similar elevations (±200m) across 5–10km^2 scales. Typically, the highest peaks occur at smaller scales (~1km^2) and thus are poorly represented. This can influence the representation of some climatic features and should be considered when interpreting these figures. Towns and roads are included to help identify specific sites within the region.

Figure 2: Observed change in mean frost risk days

Underlying data source: Australian Gridded Climate Data Product (Jones et al., 2009).

A *frost risk day* was defined as any day when daily minimum temperature was <2°C.

Annual frost risk days is the number of individual *frost risk day* events that occur during the period from October to April each annual cycle.

Mean frost risk days is the average of all *annual frost risk days* within the *current period* (1997–2017), or the *baseline period* (1961–1990).

The *baseline period* mean *frost risk days* was then subtracted from the *current period* mean *frost risk days*, resulting in the *observed change in mean frost risk days*.

Grid cells selected were those within (or intersecting with the boundary of) the polygon that defined each wine industry *Australian Geographical Indications* (Wine Australia, 2019). Values were calculated for each grid cell.

Interpretation:

Each tile represents how mean frost risk days during the current period (1997–2017) has changed when compared to mean frost risk days during the historical period (1961–1990). Higher (lower) frost risk values indicate more (less) days where minimum temperatures were <2°C. This map reflects the level of variability across the region as it is currently experienced and for many regions frost risk is very low, often less than 1 day per year (so these figures have few features). Tiles are the resolution of the underlying data. Higher values typically correspond to higher elevation regions. Tiles have an average elevation of the area they represent, so they best represent regions that have similar elevations (±200m) across 5–10km^2 scales. Typically, the highest peaks occur at smaller scales (~1km^2) and thus are poorly represented. This can influence the representation of some climatic features and should be considered when interpreting these figures. Towns and roads are included to help identify specific sites within the region.

Figure 3: Projected mean frost risk days

Underlying data source: Climate Futures Australasian Projections 2019 (CFAP2019).

A *frost risk day* was defined as any day when daily minimum temperature was <2°C.

Annual frost risk days is the number of individual *frost risk day* events that occur during the period from October to April each annual cycle.

Mean frost risk days is the average of all *annual frost risk days* within each time period (2001–2020, 2021–2040; 2041–2060; 2061–2080; 2081–2100). These were calculated for each ensemble member within the *CFAP2019*. The 6 ensemble member values (for each cell) are averaged, generating the ensemble mean for each cell within the region.

Grid cells selected were those within (or intersecting with the boundary of) the polygon that defined each wine industry *Australian Geographical Indications* (Wine Australia, 2019). Values were calculated for each grid cell.

Interpretation:

Each tile represents the mean frost risk days during each 20-year period of 2021–2040, 2041–2060, 2061–2080, 2081–2100 (following the RCP8.5 scenario). Higher (lower) frost risk values indicate more (less) days where minimum temperatures were <2°C. This map reflects the level of variability across the region as it is currently experienced and for many regions frost risk is very low, often less than 1 day per year (so these figures have few features). Tiles are the resolution of the underlying data. Higher values typically correspond to higher elevation regions. Tiles have an average elevation of the area they represent, so they best represent regions that have similar elevations (±200m) across 5–10km^2 scales. Typically, the highest peaks occur at smaller scales (~1km^2) and thus are poorly represented. This can influence the representation of some climatic features and should be considered when interpreting these figures. Towns and roads are included to help identify specific sites within the region.

Figure 4: Projected monthly minimum temperature

Underlying data source: Climate Futures Australasian Projections 2019 (CFAP2019).

Monthly minimum temperatures were extracted directly from the CFAP2019.

Violin plots represent 20-years of values for each month within each time period (2021–2040; 2041–2060; 2061–2080; 2081–2100). All individual spatial and ensemble member values are included, no spatial or ensemble averaging is performed. Grid cells selected were those within (or intersecting with the boundary of) the polygon that defined each wine industry *Australian Geographical Indications* (Wine Australia, 2019).

Interpretation:

Violin plots are a combination of box-and-whisker plots and probability distribution curves. Like a box-and-whisker plot, the shape is defined by the values within that population. The *violin* is created by mirroring the probability distribution of the values, plotted in the vertical direction, describing the frequency and spread of values in the y-axis space. Where there is a concentration of values, the *violin* is broad. Where there are few values the *violin* is narrow (possibly only a single line). As the probability distribution is continuous, where extreme outlier values occur, narrow lines can be drawn between the main body and the outlier (typical of high rainfall areas/months that may be particularly dry in some years).

Differences between the months, or time periods is expressed as changes to the shape of each *violin*. The 2001–2020 *violin* for each month is shadowed underneath future time periods, so that changes in future periods can be more easily determined.

In all wine regions across Australia, minimum daily temperatures are projected to increase rapidly from 2020 onwards.

Figure 5: Projected monthly frost risk days

Underlying data source: Climate Futures Australasian Projections 2019 (CFAP2019).

Frost risk days were defined as days when daily minimum temperature was <2°C. The monthly count of *frost risk days* was calculated for each month, within each year for each ensemble member within *CFAP2019*. Grid cells selected were those within (or intersecting with the boundary of) the polygon that defined each wine industry *Australian Geographical Indications* (Wine Australia, 2019). Values were calculated for each grid cell and then averaged into a regional ensemble mean for each 20-year time period (i.e., a single summary value for each time period from all inputs across the region). Time periods were: 2001–2020; 2021–2040; 2041–2060; 2061–2080; 2081–2100.

Interpretation:

Average monthly frost risk days for each 20-year period of 2021–2040, 2041–2060, 2061–2080, 2081–2100 (following the RCP8.5 scenario). Differences between the months, or time periods is expressed as changes to the height of each column. The 2001–2020 column for each month is shadowed underneath future time periods, so that changes in future periods can be more easily determined.

Figure 6: Projected accumulated frost intensity

Underlying data source: Climate Futures Australasian Projections 2019 (CFAP2019).

Frost risk days were defined as days when daily minimum temperature was <2°C. The *daily frost intensity* was calculated as the absolute value of temperature less than <2°C (e.g., a daily minimum temperature of 0.5°C has a *daily frost intensity* of 1.5°C). The annual *accumulated frost intensity* was calculated as the sum of *daily frost intensity* over the period from July 1st to June 30th each annual cycle. This was calculated for each ensemble member within *CFAP2019*. Grid cells selected were those within (or intersecting with the boundary of) the polygon that defined each wine industry *Australian Geographical Indications* (Wine Australia, 2019). Values were calculated for each grid cell. All individual spatial and ensemble member values are included, no spatial or ensemble averaging is performed.

Interpretation:

For all Australian wine regions, accumulated frost intensity is projected to decrease into the future. As temperatures rise, days that are <2°C are projected to warm, decreasing the chill or frost intensity of these days. In many regions, these values are dominated by high elevation regions, rather than the true growing areas. However, they provide a strong indication of the direction and rate of change projected into the future. The decreasing trend appears to have been occurring since the 1960s (although it is possible it started earlier).

Figure 7: Projected mean number of extreme cold days

Underlying data source: Climate Futures Australasian Projections 2019 (CFAP2019).

The annual number of days where daily minimum temperature fell below either -2°C, 0°C, or 2 °C was calculated for each cell and ensemble member within *CFAP2019*. Grid cells selected were those within (or intersecting with the boundary of) the polygon that defined each wine industry *Australian Geographical Indications* (Wine Australia, 2019). Values were calculated for each grid cell. These values were then averaged into a regional ensemble mean for each year (i.e., a single summary value for each year from all inputs across the region).

Interpretation:

The number of days colder than selected thresholds (<2, <0, <-2) is projected to dramatically decrease into the future. The decreasing trend appears to have been occurring since the 1960s (although it is possible it started earlier). Interannual variability is high in most regions, but climate change is clearly the dominant influence over the long timescales.

References

Boucher, O., D. Randall, P. Artaxo, C. Bretherton, G. Feingold, P. Forster, V.-M. Kerminen, Y. Kondo, H. Liao, U. Lohmann, P. Rasch, S.K. Satheesh, S. Sherwood, B. Stevens and X.Y. Zhang, 2013: Clouds and Aerosols. In: Climate Change 2013: The Physical Science Basis. Contribution of Working Group I to the Fifth Assessment Report of the Intergovernmental Panel on Climate Change [Stocker, T.F., D. Qin, G.-K. Plattner, M. Tignor, S.K. Allen, J. Boschung, A. Nauels, Y. Xia, V. Bex and P.M. Midgley (eds.)]. Cambridge University Press, Cambridge, United Kingdom and New York, NY, USA.

Christensen, J. H., Boberg, F., Christensen, O. B., and Lucas-Picher, P.: On the need for bias correction of regional climate change projections of temperature and precipitation, Geophys. Res. Lett., 35, L20709, doi:10.1029/2008GL035694, 2008

Chouinard, C., M. B6land and N. McFarlane, 1986: A simple gravity wave drag parameterization for use in medium-range weather forecast models. Atmns. Ocean, 24, 9l-tto.

Freidenreich S.M. and Ramaswamy V. (1999) A new multiple-band solar radiative parameterization for general circulation models. Journal of Geophysical Research 104 D24 31389–31409.

Gudmundsson, L., Bremnes, J.B., Haugen, J.E. and Engen-Skaugen, T., 2013. Downscaling RCM precipitation to the station scale using statistical transformations—a comparison of methods. Hydrology and Earth System Sciences, 16(9), pp.3383–3390.

Hoffmann, P., Katzfey, J.J., McGregor, J.L. and Thatcher, M., 2016. Bias and variance correction of sea surface temperatures used for dynamical downscaling. Journal of Geophysical Research: Atmospheres, 121(21).

Horowitz HM, Garland RM, Thatcher M, Landman WA, Dedekind Z, van der Merwe J, Engelbrecht FA (2017) Evaluation of climate model aerosol seasonal and spatial variability over Africa using AERONET. Atmos. Chem. Phys. 17 13999–14023.

IPCC, 2014: Climate Change 2014: Synthesis Report. Contribution of Working Groups I, II and III to the Fifth Assessment Report of the Intergovernmental Panel on Climate Change [Core Writing Team, R.K. Pachauri and L.A. Meyer (eds.)]. IPCC, Geneva, Switzerland, 151 pp.

Jones, D.A., Wang, W. and Fawcett, R., 2009. High-quality spatial climate data-sets for Australia. Australian Meteorological and Oceanographic Journal, 58(4), p.233.

Kowalczyk E.A., Stevens L., Law R.M., Dix M., Wang Y.P., Harman, I.N., Haynes K., Srbinovsky J., Pak B. and Ziehn T. (2013) The land surface model component of ACCESS: description and impact on the simulated surface climatology. Australian Meteorological and Oceanographic Journal 63 65–82.

Lin Y-L, Farley RD and Orville HD (1983) Bulk parameterization of the snow field in a cloud model. Journal of climate and applied meteorology. 22 1065–1092.

Lipson, M, Thatcher, M, Hart, M and Pitman, A. (2018). A building energy demand and urban land surface model. Quarterly Journal of the Royal Meteorological Society. 144. 1–19.

McGregor, J.L., H.B. Gordon, I.G. Watterson, M.R. Dix and L.D. Rotstayn, 1993: The CSIRO 9-level atmospheric general circulation model. CSIRO Division of Atmospheric Research technical paper No. 26. 89 pp.

McGregor JL (2003) A new convection scheme using a simple closure. Bureau of Meteorology Research Centre Research Report 93:33–36

McGregor 2005: C-CAM: Geometric aspects and dynamical formulation. CSIRO Oceans and Atmosphere Research Technical Paper, 70, 43 pp.

McGregor, J. L. and M. R. Dix, 2008: An updated description of the conformal-cubic atmospheric model. High Resolution Simulation of the Atmosphere and Ocean, Hamilton, K. and W. Ohfuchi, Eds., Springer, 51–76.

Moncur, M.W., Rattigan, K., Mackenzie, D.H. and Mcintyre, G.N., 1989, Base Temperatures for Budbreak and Leaf Appearance of Grapevines. American Journal of Enology and Viticulture, 40(1).

Nairn, J.R. and Fawcett, R.J.B., The Excess Heat Factor: A Metric for Heatwave Intensity and Its Use in Classifying Heatwave Severity. International Journal of Environmental Research and Public Health, 2015, 12, 227–253; doi:10.3390/ijerph120100227

Rotstayn LD (1997) A physically based scheme for the treatment of stratiform cloud and precipitation in large-scale models. I: Description and evaluation of the microphysical processes. Q.J.R. Meteorol. Soc 123 pp 1227–1282

Rotstayn LD and Lohmann U (2002) Simulation of the tropospheric sulfur cycle in a global model with a physically based cloud scheme. Journal of Geophysical Research 107 D21 4592

Rotstayn LD, Collier MA, Mitchell RM, Qin Y, Campbell SK and Dravitzki SM (2011) Simulated enhancement of ENSO-related rainfall variability due to Australian dust. Atmos. Chem. Phys. 11, 6575–6592

Schwarzkopf MD and Ramaswamy V (1999) Radiative effects of CH4, N2O, halocarbons and the foreign-broadened H2O continuum: A GCM experiment. Journal of Geophysical Research 104 D8 9467–9448.

Thatcher, M. and Hurley, P. (2012) Simulating Australian urban climate in a mesoscale atmospheric numerical model. Boundary-Layer Meteorology, 142(1), 149–175.

Thatcher M and McGregor J (2009) Using a scale-selective filter for dynamical downscaling with the conformal cubic atmospheric model. Monthly Weather Review 137, 1742–1752.

Wine Australia, 2019, Register of Protected GIs and Other Terms (this is a living document, last accessed in January 2019), `https://www.wineaustralia.com/labelling/register-of-protected-gis-and-other-terms/geographical-indications`